UNIVERSIDADE FEDERAL DO PARANÁ E *LE MANS UNIVERSITÉ*

JOÃO PEDRO ELIAS MACHADO

EXPLORING THE MICROSTRUCTURE OF WATER IN WATER EMULSIONS WITH PROTEIN PARTICLES: THE EFFECT OF CHANGING THE pH, THE TEMPERATURE, AND ADDING POLYSACCHARIDES

CURITIBA/ LE MANS

2022

JOÃO PEDRO ELIAS MACHADO

EXPLORING THE MICROSTRUCTURE OF WATER IN WATER EMULSIONS WITH PROTEIN PARTICLES: THE EFFECT OF CHANGING THE pH, THE TEMPERATURE, AND ADDING POLYSACCHARIDES

Tese apresentada ao Programa de Pós-Graduação em Química, no setor de Ciências Exatas, na Universidade Federal do Paraná, como requisito parcial à obtenção do título de doutor em química em um acordo de cotutela entre a Universidade Federal do Paraná e a *Le Mans Université*.

Orientadores: Prof. Dr. Rilton Alves de Freitas
e Dr. Taco Nicolai

CURITIBA/ LE MANS
2022

DADOS INTERNACIONAIS DE CATALOGAÇÃO NA PUBLICAÇÃO (CIP)
UNIVERSIDADE FEDERAL DO PARANÁ
SISTEMA DE BIBLIOTECAS – BIBLIOTECA DE CIÊNCIA E TECNOLOGIA

Machado, João Pedro Elias
Exploring the microstructure of water in water emulsions with protein particles: the effect of changing the pH, the temperature, and adding polysaccharides / João Pedro Elias Machado. – Curitiba, 2022.
1 recurso on-line : PDF.

Tese (Doutorado) - Universidade Federal do Paraná, Setor de Ciências Exatas, Programa de Pós-Graduação em Química.

Orientador: Rilton Alves de Freitas
Coorientador: Taco Nicolai

1. Emulsões. 2. Misturas (Química). 3. Soluções poliméricas. 4. Microestrutura. 5. Proteínas. 6. Polissacarídeos. 7. Géis tipo cold-set. I. Universidade Federal do Paraná. II. Programa de Pós-Graduação em Química. III. Freitas, Rilton Alves de. IV. Nicolai, Taco. V. Título.

Bibliotecário: Elias Barbosa da Silva CRB-9/1894

MINISTÉRIO DA EDUCAÇÃO
SETOR DE CIÊNCIAS EXATAS
UNIVERSIDADE FEDERAL DO PARANÁ
PRÓ-REITORIA DE PESQUISA E PÓS-GRADUAÇÃO
PROGRAMA DE PÓS-GRADUAÇÃO QUÍMICA - 40001016026P2

TERMO DE APROVAÇÃO

Os membros da Banca Examinadora designada pelo Colegiado do Programa de Pós-Graduação QUÍMICA da Universidade Federal do Paraná foram convocados para realizar a arguição da tese de Doutorado de **JOÃO PEDRO ELIAS MACHADO** intitulada: **EXPLORING THE MICROSTRUCTURE OF WATER IN WATER EMULSIONS WITH PROTEIN PARTICLES: THE EFFECT OF CHANGING THE pH, THE TEMPERATURE, AND ADDING POLYSACCHARIDES**, sob orientação do Prof. Dr. RILTON ALVES DE FREITAS, que após terem inquirido o aluno e realizada a avaliação do trabalho, são de parecer pela sua APROVAÇÃO no rito de defesa.

A outorga do título de doutor está sujeita à homologação pelo colegiado, ao atendimento de todas as indicações e correções solicitadas pela banca e ao pleno atendimento das demandas regimentais do Programa de Pós-Graduação.

CURITIBA, 26 de Agosto de 2022.

Assinatura Eletrônica
15/09/2022 20:10:36.0
IZABEL CRISTINA RIEGEL VIDOTTI MIYATA
Presidente da Banca Examinadora

Assinatura Eletrônica
15/09/2022 15:45:03.0
RILTON ALVES DE FREITAS
Avaliador Interno (UNIVERSIDADE FEDERAL DO PARANÁ)

Assinatura Eletrônica
15/09/2022 15:26:58.0
VALÉRIE RAVAINE
Avaliador Externo (UNIVERSITé DE BORDEAUX)

Assinatura Eletrônica
22/09/2022 15:37:20.0
TACO NICOLAI
Avaliador Externo (LE MANS UNIVERSITÉ)

Assinatura Eletrônica
15/09/2022 08:19:45.0
WATSON LOH
Avaliador Externo (UNIVERSIDADE ESTADUAL DE CAMPINAS)

Assinatura Eletrônica
21/09/2022 06:18:29.0
ISABELLE CAPRON
Avaliador Externo (INRAE NANTES)

Leia tudo, leia o mundo.
Um dia tudo fará sentido
Eliane de F. Elias

ACKNOWLEDGMENTS

To my supervisors Rilton A. de Freitas and Taco Nicolai. You two provided me support and gave me the opportunity to work alongside two great scientists.

To my parents, which gave me solid foundation to rely on so I could develop scientifically and personally.

To Lazhar Benyahia, Isabelle Capron and Christophe Chassinieux for the scientific discussions and the friendship created throughout those approximately 2 years.

To my family, for the unmeasurable examples of how the education is fundamental for the development.

To Gabriela Parchen, who was incredibly able to make herself present even 8625 km away. I would also thank Croissant for keeping me awake whenever I should be sleeping.

To Universidade Federal do Paraná and Le Mans Université, for opening their doors and conceding facilities to work. Also, I would like to thank the colleagues and friends from both laboratories I've worked, PCI and BioPol.

RESUMO

As emulsões formadas pela mistura de soluções poliméricas aquosas são chamadas de emulsões água-em-água (a/a). Devido à composição majoritariamente aquosa, a tensão interfacial (γ_{ab}) é consideravelmente baixa (cerca de 10 – 100 μN m^{-1} e 0 no ponto crítico) e a interface é mais espessa do que a interface entre óleo e água. Portanto, essas características inibem o uso de surfactantes contra a coalescência das gotículas. No entanto, essas inconveniências podem ser superadas pela adição de partículas sólidas ou alguns polímeros lineares que residam na interface e promovem estabilização estérea. Para ocupar a interface uma partícula deve ser molhada por ambos os líquidos, ou seja, γ_{ab} deve ser mais elevada do que a tensão interfacial entre a partícula e cada um dos líquidos. Vários métodos já foram propostos para controlar o posicionamento de partículas em emulsões, como modificações na superfície ou na morfologia da partícula ou mudança do pH ou força iônica do meio em que ela está inserida. Um parâmetro ainda não investigado é o efeito causado pela adição de um terceiro polissacarídeo que não interage diretamente com os componentes. Assim, o objetivo desse trabalho foi estudar do ponto de vista fundamental e experimental emulsões formadas por dois ou mais polímeros aquosos. Em seguida, uma emulsão a/a formada por pululana e amilopectina foi escolhida para ser investigada mais minuciosamente. Nela, foi explorado o efeito causado pela adição de um polissacarídeo na partição de microgéis de proteína. Depois, o efeito causado pela variação do pH e da temperatura foi brevemente investigado. Finalmente, dois métodos para se induzir a formação de géis do tipo *cold-set* foram comparados. As emulsões foram analisadas por microscopia confocal de varredura à laser e macroscopicamente. Observou-se que através da associação das gotículas em sistemas aquosos de múltiplas fases foi possível determinar tensões interfaciais relativas. Em alguns casos, as emulsões de múltiplas fases formadas foram estabilizadas por partículas proteicas através da formação de redes alternadas de gotículas. Na emulsão de amilopectina e pululana, a adição de um terceiro polissacarídeo forneceu a possibilidade de se controlar a posição dos microgéis de proteína, os quais foram quantificados por espectroscopia na região do ultravioleta-visível. Notou-se que a partição das partículas dependia da concentração do polissacarídeo adicionado na fase de pululana. O controle do posicionamento da partícula se mostrou como um comportamento geral em emulsões a/a. Diferenças marcantes foram observadas entre as duas maneiras estudadas de se formar géis do tipo *cold-set* com relação à estabilidade. Em alguns casos, os géis formados na interface resistiram à diluição, aumento do pH ou cisalhamento.

Palavras-chave: emulsões água-em-água; microgéis de proteína; microestrutura; géis tipo *cold-set.*

ABSTRACT

Emulsions formed by the mixture of incompatible aqueous polymer solutions are referred as water-in-water (w/w) emulsions. Due to the major aqueous composition, the interfacial tension (γ_{ab}) is considerably low (around 10 – 100 μN m^{-1} and 0 at the critical point) and the interface is wider than that between oil and water. Thus, these characteristics inhibit the use of surfactants as stabilizers against droplets coalescence. However, these inconveniences can be solved by adding solid particles or some linear polymers that reside at the interface and procure steric stabilization. In the case of a particle, to adhere at the interface it should be wetted by both liquids. Several methods have been suggested to control the positioning of the particle in emulsions such as modifying the surface or the morphology of the particle or changing the pH or the ionic strength of the media in which it is insert. A not-yet investigated parameter is the effect caused by the addition of a polysaccharide that does not interact directly with the components. The objective of this work was to study emulsions formed by two or more aqueous polymers from the fundamental and experimental point of view. One w/w emulsion of amylopectin and pullulan was chosen to be studied more thoroughly. For this emulsion, it was explored the influence of adding a polysaccharide on the partition of protein microgels. Then, the impact of changing the pH and the temperature was briefly investigated. Finally, two methods to induce cold gelation of protein particles were compared. The emulsions were analyzed by confocal laser scanning microscopy and macroscopically. It was observed the possibility to determine relative interfacial tensions by the association of droplets in aqueous multiple phase systems (AMPS). In some cases, AMPS formed could be stabilized by networks formed by alternating droplets covered with protein particles. The addition of a third polysaccharide in the amylopectin-pullulan emulsion allowed the control of particle partition, which was quantified by UV-Vis spectroscopy. It was noticed that the partition depended on the third polysaccharide concentration within the pullulan phase. Apparently, the particle positioning control showed to be a general feature in w/w emulsions. Remarkable differences regarding the droplets' stability were observed between the two methods to form cold-set gels. In some cases, the interfacial gels formed resisted the dilution, the pH increment or shear.

Keywords: water-in-water emulsions; protein microgels; microstructure; cold-set gels.

RÉSUMÉ LONG EN LANGUE FRANÇAISE

(comme requis par la Convention Internacionale de Thèse en Cotutelle)

Beaucoup des produits alimentaires contiennent des polysaccharides et des protéines. La microstructure formée par ces composants dans la formulation est responsable pour donner des propriétés sensorielles, texturées et nutritionnelles à la nourriture. Les polysaccharides sont généralement utilisés pour augmenter la viscosité tandis que les protéines stabilisent les formulations pour former des émulsions et des mousses. Parmi les protéines utilisées par l'industrie alimentaire, celles qui viennent du lait sont beaucoup utilisées. L'isolat de lactosérum (whey protein isolate) est composé majoritairement de la β-lactoglobuline (β-lg) et la α-lactalbumine (α-la). Le point isoélectrique (PIE) de la protéine du lactosérum est 5,1. À ce pH, la densité de charge de la protéine est nulle. À des températures plus élevées que 60 °C, les protéines dénaturent et s'agrègent pour former des particules avec une morphologie qui dépend du pH. Cela permet d'obtenir différentes structures comme des sphères à pH 5,8, des bâtonnets rigides à pH 2,0 ou des fibrilles à pH 7,0, comme le montre la figure R1.

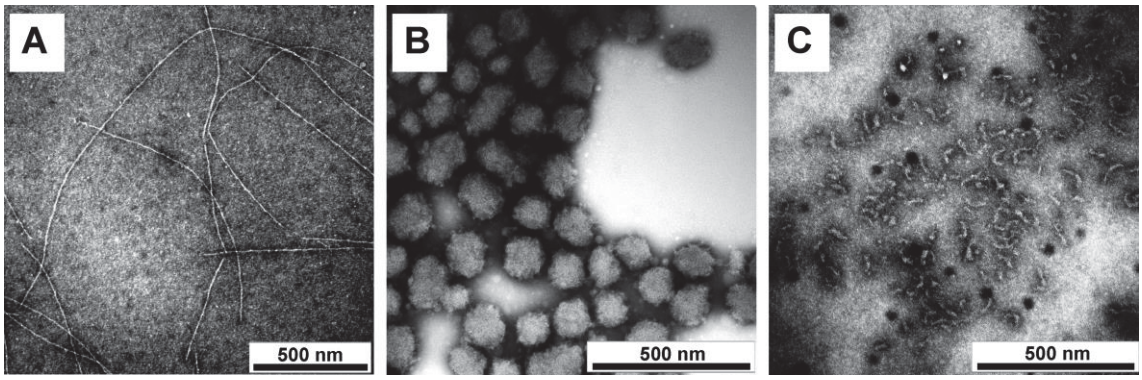

Figure R1 : les formes possibles des particules de protéine du lactosérum obtenues par chauffage aux pH 2,0 (A), 5,8 (B) et 7,0 (C).

Les émulsions contiennent une phase liquide dispersée en forme des gouttes dans une autre phase continue. Le beurre (émulsion eau dans huile) ou la crème hollandaise (émulsion huile dans l'eau) sont deux exemples courants d'émulsions agroalimentaires. La demande pour des produits sans huile ou sans matière graisse *(fret fat)*, suscite un intérêt croissant pour des émulsions formées par deux phases aqueuses, dites émulsions eau dans l'eau (E/E). Les émulsions E/E ont été visualisées la première fois au début des années 1990 pour un mélange de gélatine et d'amidon dans l'eau. Ces émulsions sont formées quand on mélange deux solutions aqueuses de polymères qui sont thermodynamiquement incompatibles et tendent vers

une séparation de phase macroscopique inéluctable en l'absence de stabilisant. La figure R2 montre le diagramme de phase d'un mélange gélatine/maltodextrine.

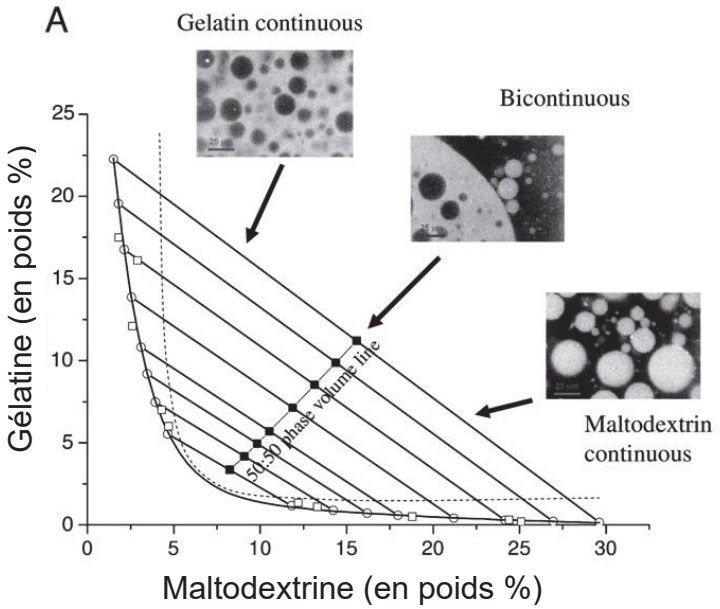

Figure R2 : Diagramme de phase typique d'un mélange de deux polymères incompatibles en solution aqueuse : gélatine et maltodextrine.

Pour stabiliser une émulsion E/E, il faut impérativement substituer les tensioactifs par des particules solides ou certains polymères linéaires, en raison de l'épaisseur de l'interface que est plus large que celle entre huile et eau et en raison de la très faible tension interfaciale. Dans ce contexte, l'utilisation de particules de protéines, mentionnées en haut, est très intéressante parce qu'elles sont biocompatibles, facilement formées et avec des tailles qui peuvent être contrôlées. Pour se localiser à l'interface, la particule doit être mouillée par les deux phases. Il est donc impératif que la particule présente une certaine compatibilité ou affinité avec les deux phases même si elle présente une affinité plus importante pour l'une des phases. Ceci peut générer une partition différentielle entre les deux phases. Pour moduler ou changer cette partition, on peut aussi modifier chimiquement la surface de la particule. Par ailleurs, le pH, la force ionique et la température peuvent être utilisés comme des stimuli physico-chimiques pour changer la localisation de la particule dans une émulsion. Une fois à l'interface, l'énergie d'adsorption des particules est suffisante pour éviter la désorption par énergie thermique (mouvement brownien). Néanmoins, malgré la localisation des particules à l'interface, les émulsions E/E stabilisées par effet Pickering ne sont pas forcément stables et les goutes peuvent finir par coalescer.

Dans cette thèse, des émulsions E/E ont été étudiées d'un point de vue fondamental, mais en visant une application potentielle de l'industrie agroalimentaire. Dans un premier temps, des mélanges binaires aqueux de nombreux polymères (amylopectine, pullulane, xyloglucane, dextran, poly (ethylene oxide), pectine, alginate, κ-carraghénane, caséinate, hydroxypropyl méthylcellulose, protéines sériques et gélatine) ont été investigués et la formation de systèmes aqueux multiphasiques identifiée et discutée. Par la suite, une méthode permettant de contrôler la partition des particules entre les phases d'émulsion E/E a été développée. Le mélange amylopectine/pullulane à pH 7,0 a été choisi pour étudier la partition de particules de microgels de protéine sérique en fonction de la concentration d'un polysaccharide non ionique (xyloglucane) ou anionique (pectine, alginate ou κ-carraghénane). L'étude a été généralisée en utilisant une particule de nature chimique et de morphologie différentes (nanocristaux de cellulose) et un autre couple de polymère (dextran/amylopectine) pour former l'émulsion E/E. De plus, deux méthodes de gélification des microgels à froid (*cold-set gels*), permettant de figer l'interface et de former des capsules permanentes, ont été comparées. Finalement, une investigation brève sur l'effet de la température sur la partition des microgels et leur localisation à l'interface des émulsions E/E a été conduite.

Les solutions des polymères ont été dissoutes dans l'eau ultra-pure et le pH a été ajusté en ajoutant HCl ou NaOH à 0,1 ou 1 $mol.L^{-1}$. Les polymères ont été analysés par chromatographie d'exclusion stérique pour obtenir leur masse molaire moyenne en poids : dextran $4{,}10 \times 10^5$ g/mol, alginate $7{,}90 \times 10^4$ g/mol, κ-carraghénane $8{,}77 \times 10^4$ g/mol, pectine $3{,}72 \times 10^6$ g/mol, pullulane $2{,}98 \times 10^5$ g/mol, xyloglucane $1{,}04 \times 10^6$ g/mol, hydroxypropyl méthylcellulose $2{,}91 \times 10^5$ g/mol, et amylopectine $1{,}64 \times 10^8$ g mol^{-1}.

Des microgels de protéine ont été produits en chauffant une solution de protéine sérique dans l'eau à 10 % à 85 °C pendant 15 h. Des mélanges de particules de protéine et polysaccharides anioniques ont été faits à pH 5,0 à différents rapports de massique pour étudier la formation éventuelle des complexes.

La conversion des protéines en microgels a été déterminée par la mesure de la concentration des protéines résiduelles dans le surnageant après avoir sédimenté les microgels par centrifugation. La concentration des protéines a été mesurée par spectroscopie UV-Vis (Jasco PAC-743). La taille des particules a été déterminée par diffusion de la lumière statique et dynamique sur an appareil commercial (ALV-CGS3). Les émulsions ont été étudiées visuellement et par microscopie confocale (Zeiss LSM 800) après avoir ajouté un fluorophore, la rhodamine B à 5 mg L^{-1}, pour marquer sourtout les particules tandis que l'excès de fluorophore a marqué les différentes phases. La pectine a été fonctionnalisée par la fluorescéine

isothiocyanate (FITC). Pour baisser le pH des émulsions, la glucono-δ-lactone (GDL) et une solution de HCl ont été utilisées. Les observations à des températures non ambiantes par microscopie confocale ont été réalisées à l'aide d'un appareil commercial (RheOptiCAD).

La conversion de protéines en microgels a été d'environ 70 %. La fraction restante est sous forme de petits agrégats qui n'ont pas des propriétés interfaciales pour les émulsions E/E. Les microgels avaient un rayon hydrodynamique de 38 nm et une masse molaire moyenne de $3{,}3 \times 10^8$ g mol^{-1}. Parmi tous les polysaccharides étudiés, l'amylopectine est le biopolymère qui présente la plus forte incompatibilité car beaucoup des mélanges binaires faits avec ce polymère présentent une séparation de phase. Par ailleurs, la gélatine est la protéine qui présente la plus forte incompatibilité. Voir les tableaux R1 et R2. Pour certains mélanges, des diagrammes de phases plus précis et plus complets ont été déterminés.

Tableau R1. Résumé des mélanges binaires aqueux entre polysaccharides qui rendent deux phases.

XG	**DX**	**AMP**	**ALG**	**HPMC**	**PEC**	**KC**	**PUL**	**PEO**
DX	XG	XG	CAS	DX	CAS	AMP	DX	XG
GEL	GEL	DX		GEL		CAS	GEL	DX
AMP	AMP	GEL		AMP			AMP	GEL
WPI	HPMC	HPMC		PUL			HPMC	AMP
PEO	PUL	KC					PEO	PUL
	PEO	PUL						WPI
		WPI						
		PEO						

Tableau R2. Résumé des mélanges binaires aqueux entre protéines et polysaccharides qui conduisent à une séparation de phase.

GEL	CAS	WPI
XG	ALG	XG
DX	PEC	AMP
AMP	KC	HPMC
HPMC		PEO
PUL		
PEO		

De manière originale et inédite pour ces systèmes tout aqueux, nous avons étudié des mélanges à trois ou plus polymères incompatibles. Des systèmes aqueux multiphasiques (SAMP) se forment où des gouttes dispersées de différentes phases s'associent avec des angles de contact déterminés, voire figure R3. Nous avons démontré que la mesure de l'angle de contact entre les gouttes permet de calculer la tension interfaciale relative. De cette façon, il a été possible de déterminer la tension interfaciale entre multiples couples de biopolymères en comparaison avec le mélange dextran/POE, voir figure R4. Nous avons également mis en évidence que l'ajout des microgels aux SAMP ne change pas les angles de contact entre les phases, voire figure R3.

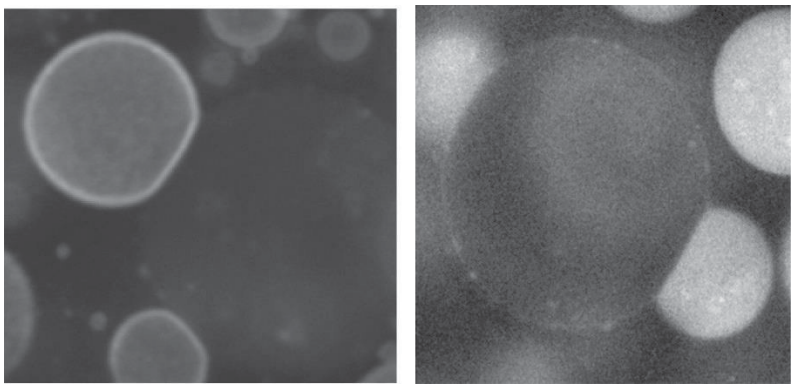

Figure R3. Émulsion entre amylopectine et poly (oxyde d'éthylène) dispersée dans pullulane. À gauche l'émulsion avec des microgels de protéine et à droite sans les microgels.

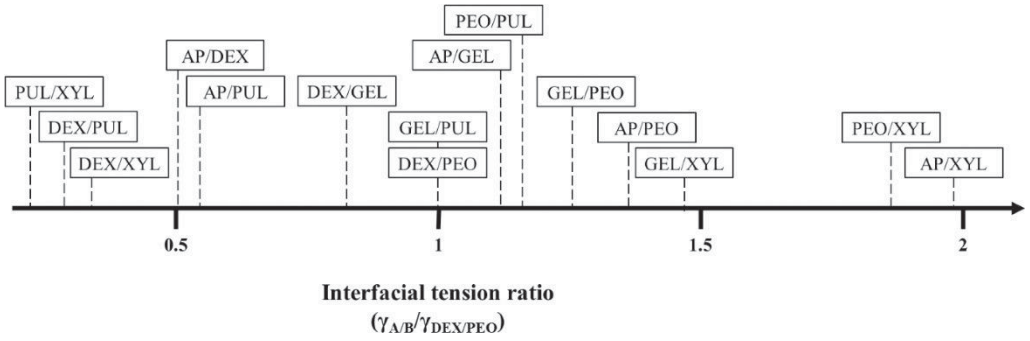

Figure R4. Schéma qui montre le rapport entre la tension interfaciale de différents mélanges binaires comparée à la tension interfaciale entre poly (oxyde d'éthylène) et dextran.

La complexation entre microgels et polysaccharides anioniques a été observée à pH 5,0, mais dans tous les cas les complexes se dissocient quand le pH remonte à 7,0.

L'émulsion à base d'amylopectine et pullulane a été la plus étudiée et le diagramme de phase est montré dans la figure R5.

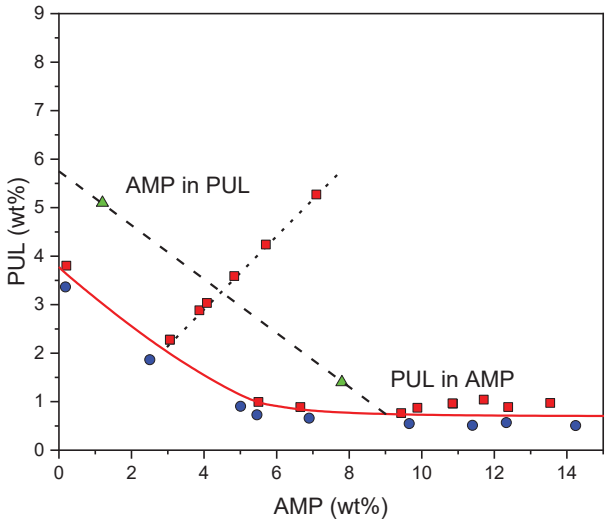

Figure R5. Diagramme de phase du mélange amylopectine/pullulane.

À pH 7,0, les microgels se partitionnent préférentiellement dans la phase pullulane sans que la coalescence des gouttelettes soit inhabitée. En revanche, nous avons observé que l'ajout progressif d'un polysaccharide anionique ou neutre conduit les particules à migrer vers la phase d'amylopectine, voir la figure R6. Il faut noter qu'il en faut moins de pectine pour changer la partition quand la fraction volumique de la phase pullulane est plus petite ce qui montre que la partition dépend de la concentration du polysaccharide dans la phase pullulane.

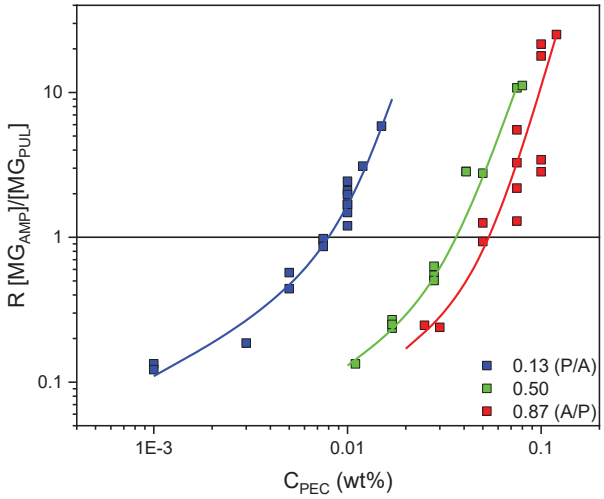

Figure R6. Rapport de concentration des microgels dans la phase d'amylopectine et de pullulane en fonction de la concentration de pectine à différentes fractions volumiques de la phase pullulane.

Théoriquement l'adsorption des particules à l'interface est plus importante pour R = 1, quand la concentration des particules est la même dans les deux phases. En effet, dans ce cas il s'avère que les microgels restent adsorbés à l'interface même très proche de la binodale tandis que sans l'ajout de pectine, les microgels ne sont adsorbés que loin de la binodale.

En changeant la nature des particules, en utilisant des nanocristaux de cellulose, ou le mélange de base, en prenant dextran/amylopectine, le comportement reste qualitativement le même. Ce résultat implique que le fait d'ajouter un polysaccharide pour contrôler la partition et l'adsorption des particules dans les émulsions E/E est plus générique et universelle.

À pH 3,5 les microgels préfèrent l'amylopectine même sans ajout de polysaccharide. À pH 5,0, dans une émulsion où la phase amylopectine est dispersée dans la phase pullulane (A/P), les microgels gélifient irréversiblement à l'interface. Sous l'effet de la gravité, les gouttes finissent par se déformer, mais restent même après une semaine. Cependant, dans une émulsion de pullulane dans l'amylopectine (P/A), les microgels gélifient dans la phase continue et emprisonnent les gouttelettes nues de la phase pullulane.

À l'aide d'un polysaccharide anionique, l'agrégation des microgels peut être évitée et reste donc bien dispersés tout en migrant à l'interface en stabilisant l'émulsion à pH 5,0. Néanmoins, il y a une concentration minimale pour éviter l'agrégation irréversible des microgels qui dépend légèrement du polysaccharide utilisé. Les résultats avec l'alginate sont montrés en figure R8 et R9.

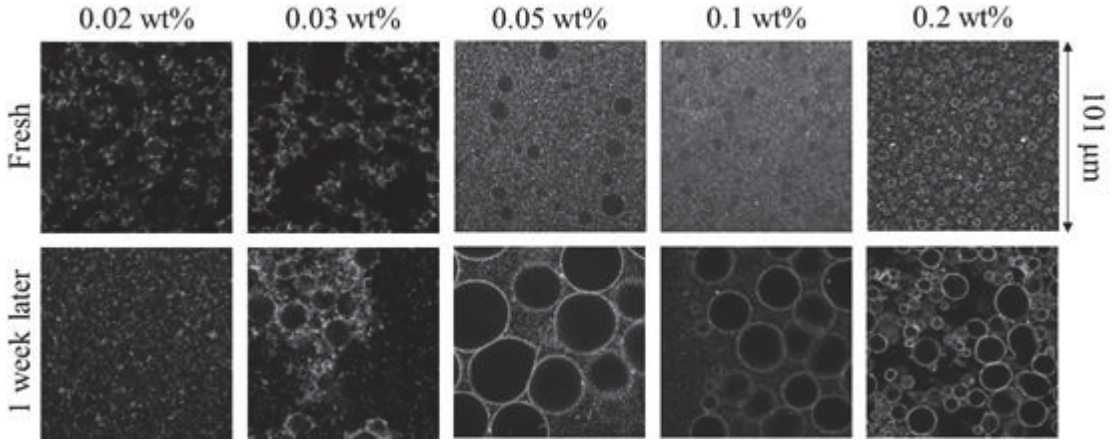

Figure R8. Images de microscopie confocale des émulsions d'amylopectine dans pullulane avec des microgels de protéine et différentes concentrations d'alginate à pH 5.

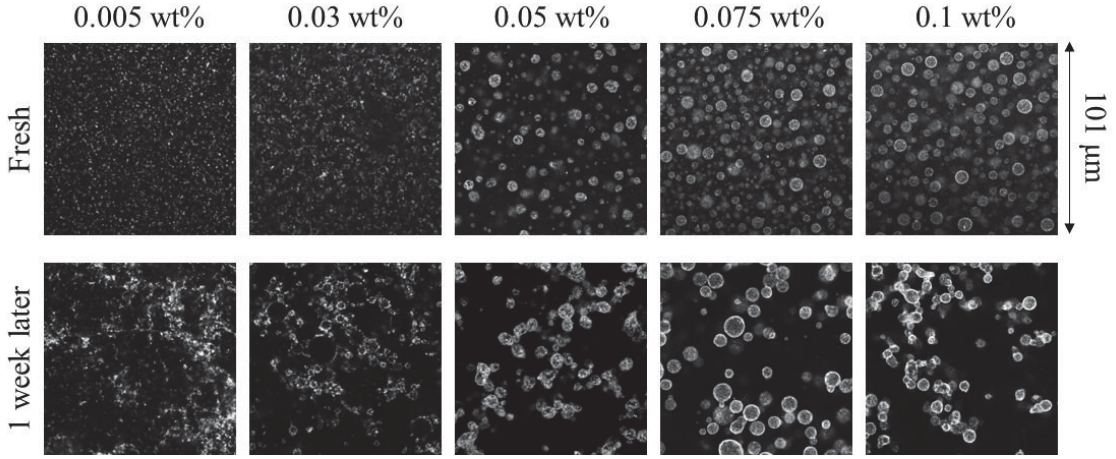

Figure R9. Images de microscopie confocale des émulsions de pullulane dans amylopectine avec des microgels de protéine et différentes concentrations d'alginate à pH 5.

Si on change la méthode d'acidification par l'ajoute de GDL au lieu de HCl, il est possible de gélifier l'interface même sans l'aide d'un polysaccharide anionique. En ajoutant le GDL, le pH diminue progressivement, tandis qu'avec le HCl le pH diminue pendant le mélange. Il faut souligner que les interfaces gélifiées en présence des polysaccharides anioniques présentaient en certaine résistance mécanique même sous un vortex, et une stabilité appréciable en augmentant du pH ou suite à une forte dilution, voire figure R10.

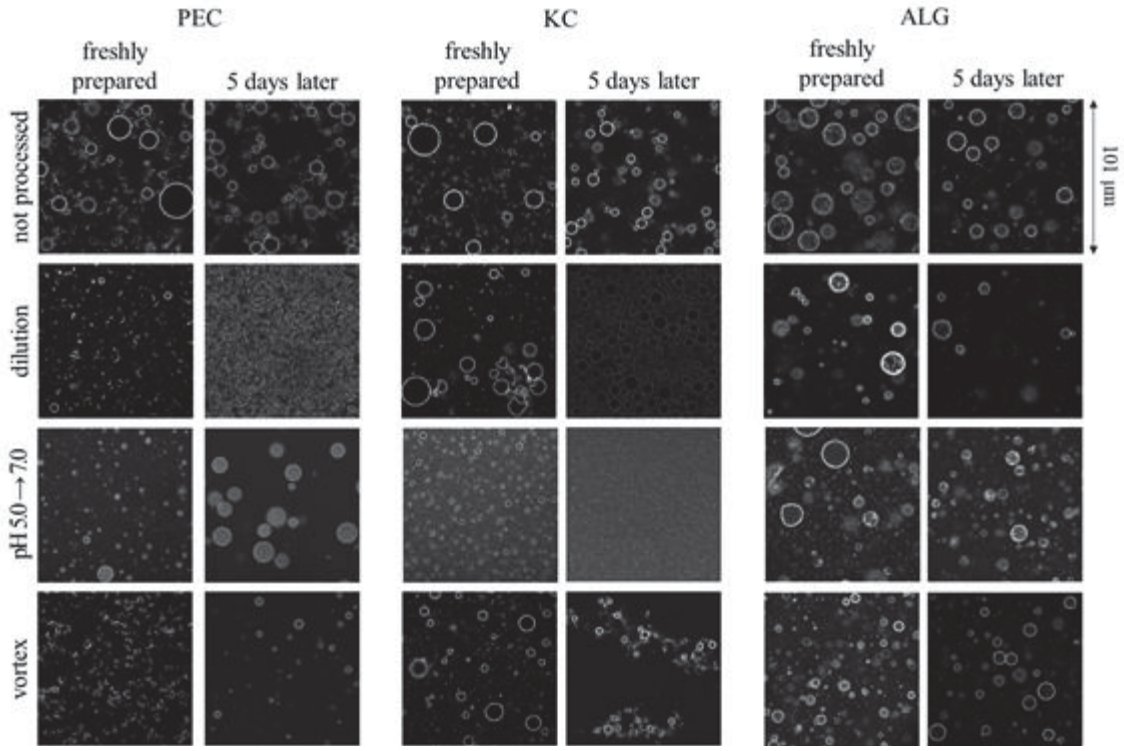

Figure R10. Images de microscopie confocale d'émulsions de pullulane dans l'amylopectine stabilisées par des microgels et en présence de plusieurs polysaccharides. Le GDL a été utilisé pour acidifier le milieu. Différentes procédures ont été testées avec les émulsions formées comme indiqué sur la figure.

La température peut aussi influencer la partition des microgels, mais également leur adsorption à l'interface. À 20 °C les microgels à pH 7,0 préfèrent le pullulane. En revanche, à 50 °C ils préfèrent l'amylopectine indépendamment de la fraction volumique des phases, voire figures R11 et R12. Cependant, cet effet a lieu seulement si on ajoute des polysaccharides, voire la figure R13.

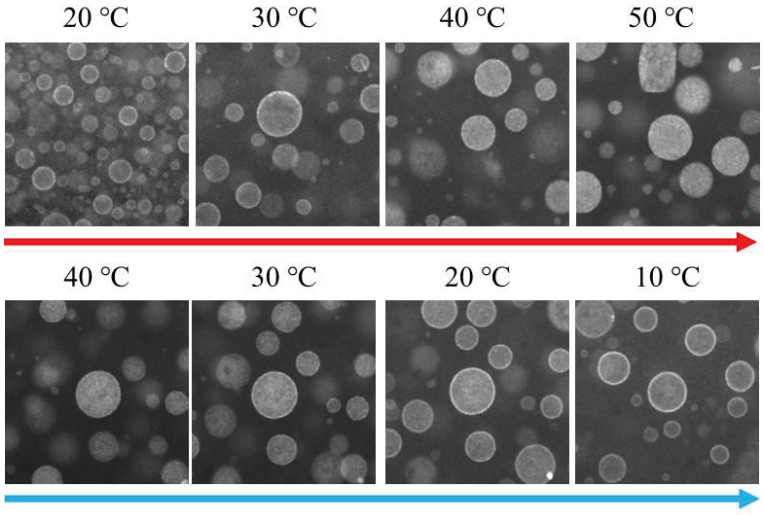

Figure R11. Images de microscopie confocale d'émulsions d'amylopectine dans pullulane stabilisées par des microgels de protéine en présence alginate et à différentes températures.

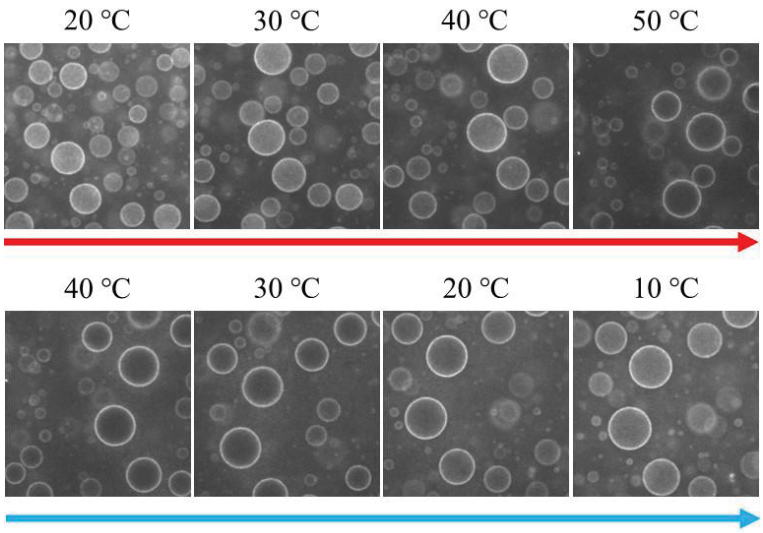

Figure R12. Images de microscopie confocale d'émulsions de pullulane dans amylopectine stabilisées par des microgels de protéine en présence d'alginate et à différentes températures.

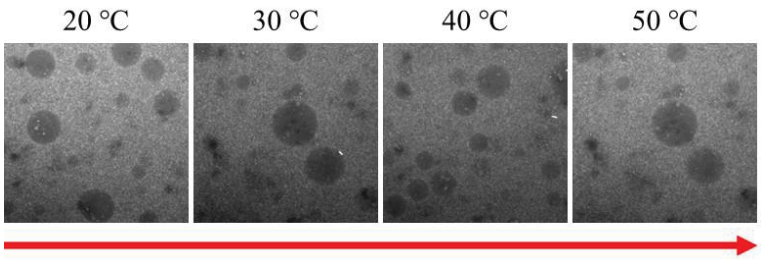

Figure R13. Images de microscopie confocale d'émulsions d'amylopectine dans pullulane stabilisées par des microgels de protéine sans l'ajoute de polysaccharide et à différentes températures.

LIST OF ABBREVIATIONS

3D	Three dimensional
A/P	Emulsions where the dispersed and the continuous phases are amylopectin and pullulan, respectively
ALG	Alginate
AMP	Amylopectin
AMPS	Aqueous multi-phase systems
CAS	Sodium caseinate
CLSM	Confocal laser scanning microscopy
CNC	cellulose nanocrystals
DLS	Dynamic light scattering
DMSO	Dimethyl sulphoxide
DX	Dextran
FITC	fluorescein isothiocyanate
GDL	Glucono-δ-lactone
GEL	Cold water fish skin gelatin
HPMC	Hydroxypropyl methylcellulose
IEP	Isoelectric point
KC	κ-carrageenan
MG	Microgels
MG-ALG	Complex of microgels with alginate
MG-KC	Complex of microgels with κ-carrageenan
MG-PEC	Complex of microgels with pectin
NB	Nile blue
P/A	Emulsions where the continuous and the dispersed phase are pullulan and amylopectin, respectively
PEC	Lemon peel pectin
PEC-FITC	Pectin covalently bonded to fluorescein isothiocyanate
PEO	Poly(ethylene oxide)
PUL	Pullulan
RodB	Rhodamine B
SEC	Size-exclusion chromatography

SLS	Static light scattering
TLL	Tie-line length
w/w	Water-in-water
WPI	Whey protein isolate
XG	Xyloglucan
α-la	α-Lactoalbumin
β-lg	β-Lactoglubulin

LIST OF SYMBOLS

$\partial n/\partial C$	Refractive index increment
C	Concentration of the solute in the solution for light scattering
C_{AMP}	Concentration of amylopectin
C_{DX}	Concentration of dextran
C_{PEC}	Concentration of pectin
C_{PEO}	Concentration of poly(ethylene oxide)
D	Diffusion coefficient
d_{bc}	distance between the centers of circles B and C
g	Acceleration due to gravity
H^+	Hydronium
HCl	Hydrochloric acid
I	Intensity of scattered light from the solution
I_S	Intensity of scattered light from the solvent
I_{tol}	Intensity of scattered light from the toluene
K	Optical constant
M_w	Weigth-average molar mass
n	Refractive index of the solvent
N_A	Avogadro's number
NaCl	Sodium chloride
NaOH	Sodium hydroxide
q	Scattering vector
R	Rayleigth ratio
$R_{[MG]}$	Concentration ratio of microgels in the pullulan phase and amylopectin phase
r_A	radius of circle A
r_B	radius of circle B
r_C	Radius of circle C
R_g	Radius of gyration
R_h	Hydrodynamic radius
R_{part}	Particle radius
R_{tol}	Rayleigth ratio for Toluene
S(q)	Structure factor

T	Absolute temperature
γ	Interfacial tension
$\Delta_{des}G$	Free energy of dessorption
$\Delta_{mix}G$	Free energy of mixing
$\Delta_{mix}H$	Enthalpy of mixing
$\Delta_{mix}S$	Entropy of mixing
ε	Extinction coefficient
η	Viscosity of the solvent
θ	Three-phasic contact angle
τ	Relaxation time
Φ_{PUL}	Volume fraction of pullulan

SUMMARY

1 INTRODUCTION

Food products have textural, sensorial, and nutritional properties that strongly depend on the components' internal microstructure, consisting mainly of polysaccharides and proteins. Polysaccharides are made of linked sugar units, which can be linear or branched, and formed exclusively by one type of sugar (homopolysaccharides) or more than one type (heteropolysaccharides). They are widely used as thickeners because they can impart viscosity to the solutions depending on its concentration, shape, and size. Polysaccharide chains can stabilize foams and emulsions by preventing the mobility of oil droplets and/or air bubbles, thus increasing the shelf-life of the products (STEPHEN; PHILIPS; WILLIAMS, 2006).

Proteins are well known for their emulsifying properties. Commercially, they are used as stabilizers of foams and emulsions. It is well known that proteins can reside at the water-air or at the water-oil interface and decrease the interfacial tension (γ) between the two fluids (KINSELLA, 1978, 1981). Proteins provide complementary properties to foods. The amount and composition of amino acids, net charge, size, and shape are the most significant variables that can be changed depending on the application (MCCLEMENTS, 2007). β-lactoglobulin (β-lg) and α-lactoalbumin (α-la) are the main globular proteins founded in whey protein isolate (WPI) from bovine milk. β-lg has approximately 18.2 kg mol^{-1}, correspondig to 60 % of the total protein content in WPI, whereas α-la comes in seccond place in quantity in WPI (20 %), and has a molar mass of 14.2 kg mol^{-1} (NICOLAI; BRITTEN; SCHMITT, 2011). In aqueous solutions, the isoelectric point (IEP) of WPI is mostly determined by the IEP of the β-lg, which is found to be approximately 5.1. In such condition, the protein acquire a net charge density of 0 and aggregation is seen at room temperature. The rate of aggregation is increased as the temperature or the concentration increase, leading to precipitation (MEHALEBI; NICOLAI; DURAND, 2008; SCHMITT et al., 2009). At temperatures above 60 °C the morphology of the aggregates formed depends strongly on the pH. At pH 2.0 elongated rod-like aggregates are formed, whereas worm-like aggregates with a hydrodynamic radius of about 14 nm are obtained at pH 7.0. In a narrow pH range close to 5.8, stable particles of around 120 nm are formed by heat-denatured whey proteins are obtained, as long as the concentration is below a critical value (MEHALEBI; NICOLAI; DURAND, 2008; SCHMITT et al., 2007, 2010a). Through the analysis of these particles obtained at pH 5.8 by a wide group of scattering techniques, it is possible to assure that the structure that best describes the aggregates is a densily-packed hard sphere with a

sharp interface with the solvent, which are denser than those structures formed at more distant pH values, see Figure 1.

FIGURE 1. TRANSMISSION ELECTRON MICROSCOPY IMAGES OF HEAT-DENATURED WHEY PROTEIN AGGREGATES FORMED AT 1 WT% AT pH 2.0 (A), pH 5.8 (B), AND pH 7.0 (C).

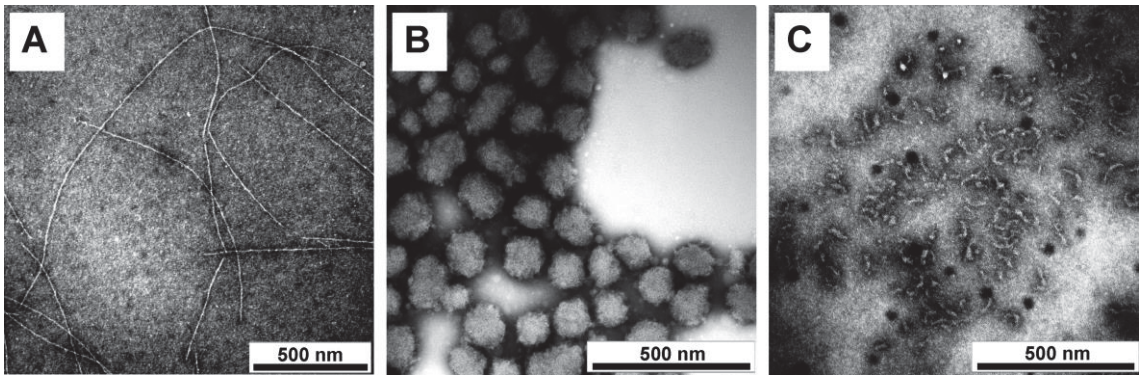

Source: extracted from JUNG et al., 2008.

The functionality of spherical WPI microgels have been explored mainly in foods, due to its biocompatibility. Several food products are formed of emulsions, consisting of a mixture of two immiscible liquids, one found as homogenized droplets (dispersed phase) into the other (continuous phase). To break down one liquid into small droplets, energy is required, and the droplets will coalesce through different mechanisms until macroscopic phase separation unless a third component is added. This third component - known as a stabilizer - provides kinetic stabilization to the droplets by residing at the interface and protecting against the contact between the dispersed droplets, maintaining the emulsion, thermodynamically, in a metastable state. A stabilizer is usually a surface-active molecule or a particle. However, recently, considerable attention has been devoted to the latter due to the irreversibly attachment to oil-water interfaces (FIROOZMAND; MURRAY; DICKINSON, 2009; GONZALEZ ORTIZ et al., 2020; SARKAR; DICKINSON, 2020; YANG et al., 2017).

Particles stabilized emulsions are known for a long time. The first reports date to the late years of the XIX century when independent researchers observed that solid particles were able to stabilize oil-water mixtures(PICKERING, 1907; RAMSDEN, 1903). Since then, emulsions stabilized by solid particles are referred to as Pickering emulsions, and the effect of interfacial particle accumulation is known as the Pickering effect. The reason why solid particles adhere at the liquid-liquid interface is known and it will be discussed below, however the mechanism of droplets' stabilization in Pickering emulsions is still far from being complete understood.

Usually, the particles cover the droplets fully so that the particle layer is responsible to avoid the contact between the bare surface of two droplets, thus preventing the coalescence. Also, when the surface of the droplets are sufficiently covered (above 60% of coverage) the lateral displacement of the particles plays an important role in the stabilization against coalescence (TAMBE; SHARMA, 1994).

Solid particle-stabilized emulsions are of fundamental importance for another type of emulsions formed by two immiscible aqueous phases, namely water-in-water emulsions (w/w) (ASENJO; ANDREWS, 2012; ESQUENA, 2016; HAZT et al., 2020; IQBAL et al., 2016; NICOLAI; MURRAY, 2017; VIS; ERNÉ; TROMP, 2016). Contrary to conventional oil-water interfaces, in aqueous mixtures of two incompatible polymers, γ between the two polymers solutions is remarkably low (10 - 100 $\mu N\ m^{-1}$ and 0 $\mu N\ m^{-1}$ at the critical point, whereas $\sim$ 40 $mN\ m^{-1}$ is typically found for oil-water interfaces), and the resulting macroscopic phases are rich in one polymer, resulting in a slight difference in densities. The low γ values along with the small density difference inhibit the use of conventional methods, such as tensiometry to calculate the interfacial tension between the two phases.

The origin of phase separation in w/w emulsions depends basically on the free energy of mixing ($\Delta_{mix}G$). If $\Delta_{mix}G < 0$, the mixing of the two solutes is thermodynamically favorable, and if $\Delta_{mix}G > 0$, then the two solutes tend to phase separate. $\Delta_{mix}G$ therefore is expressed as:

$$\Delta_{mix}G = \Delta_{mix}H - T\Delta_{mix}S \qquad 1$$

where $\Delta_{mix}H$ is the variation of enthalpy of mixing, T is the absolute temperature, and $\Delta_{mix}S$ is the variation of entropy of mixing.

If one considers mixtures with no net interaction energy between the components, the so-called ideal mixtures, the free energy of mixing depends only on $\Delta_{mix}S$. For two low molar mass entities - low enough compared to macromolecules -, the free energy of mixing will always be negative due to the magnitude and positive sign of $\Delta_{mix}S$. When small molecules are substituted by high molar mass solutes (macromolecules), the contribution of $\Delta_{mix}S$ to the free energy of mixing, although still positive, is extremely small according to the Flory-Huggins lattice theory (FLORY, 1954). Mixtures of neutral polymers and polyelectrolytes are remarkably different from those where both polymers are neutral. The insertion of only a small quantity of charged groups in one polymer considerably favors its miscibility with the neutral polymer, owing to the increase in the entropic term, $\Delta_{mix}S$

(PICULELL; BERGFELDT; NILSSON, 1995). That means, it becomes more difficult to separate both the polyelectrolyte chains and their numerous anions from the neutral polymer. Upon increasing the ionic strength, however, this effect becomes suppressed, thus favoring the phase separation.

A common example of phase separation seen in the literature is found between aqueous solutions of maltodextrin and gelatin (FIGURE 2). In this case, the contrast seen in confocal laser scanning microscopy is due to the preference of a fluorophore by one of the two phases. In this example, the solid line that separates the graph in two regions is called binodal and it shows us the region where phase separation occurs, so that outside this limit, the system behaves as a homogeneous mixture formed of two polymers. The dotted line close to the binodal is called spinodal and it delimits the region above which phase separation will occur by spinodal decomposition. In the small area between the spinodal and binodal, the phase separation will occur via nucleation and growth, which may take a much longer time to be seen macroscopically. The straight solid lines that connect opposite points of graph are denominated tie-lines and the mixtures prepared along these lines will have the same interfacial tension, the same polymer concentration within each separate compartment but will differ in the volume fraction of each phase. The perpendicular line that crosses all tie-lines represents the composition in which each polymer represents 50% of the total volume of the mixture.

All the representative pictures in Figure 2 show spherical droplets, this is probably due to the relative low viscosities of the gelatin and the maltodextrin. The picture at the bottom showed an emulsion where the continuous phase is composed of maltodextrin and the droplets are formed of gelatin, whereas at the top the image represents an emulsion of maltodextrin droplets dispersed in a continuous gelatin phase. The middle picture in Figure 2 represents a system where each phase comprises approximately 50% in volume of the sample, meaning that at the microscopic level none of each will be considered as dispersed in the other, thus both phases are referred as continuous i.e. a bicontinuous system.

The shape of the dispersed phase depends on the viscosities of each phase and the interfacial tension. If one phase is much more viscous than the other, the relaxation time, which is the time necessary for the droplets to return to the spherical shape after shear, τ, would be higher. If the disperse phase becomes a gel, then the droplets would take an infinite time to return to their spherical shape and would appear microscopically as deformed droplets. Interestingly, by applying a shear to the droplets which is perpendicular to the plane

of observation of the microscope and monitoring τ, it is possible to obtain γ for the w/w emulsions, a method called drop relaxation (GUIDO; VILLONE, 1999; RALLISON, 1984).

FIGURE 2. THE PHASE DIAGRAM OF THE BINARY MIXTURE BETWEEN GELATIN AND MALTODEXTRIN. THE SOLID LINE REPRESENTS THE BINODAL WHICH WAS FITTED BY THE EMPTY CIRCLES, WHEREAS THE DOTTED LINE REPRESENTS THE SPINODAL LINE. THE EMPTY SQUARES ARE THE EXPERIMENTALLY DETERMINED PHASE BOUNDARIES. THE FILLED SQUARES FORM THE 50:50 VOLUME FRACTION LINE. A BICONTINUOUS SYSTEM IS OBSERVED BY CLSM ALONG THE 50:50 VOLUME FRACTION LINE (MIDDLE IMAGE), COMPARED TO THE MALTODEXTRIN CONTINUOUS (BOTTOM IMAGE) OR GELATIN CONTINUOUS (TOP IMAGE) SYSTEMS.

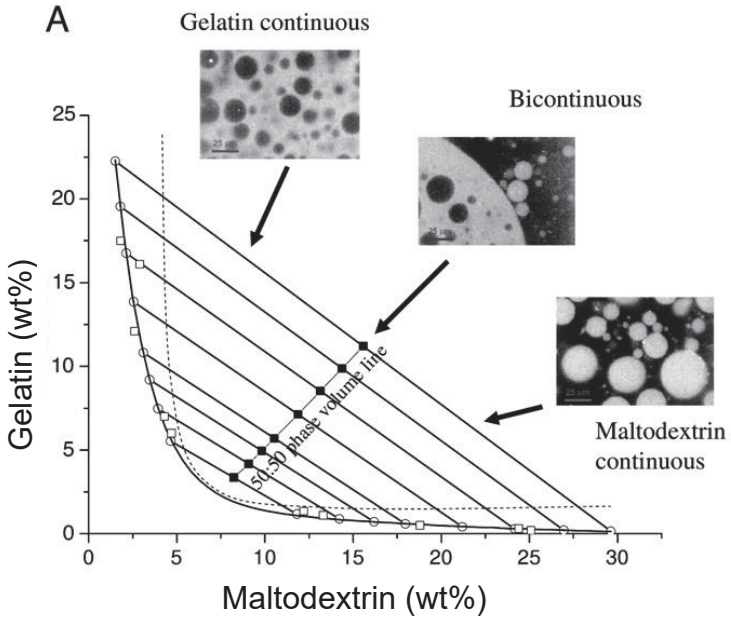

Source: extracted from NORTON; FRITH, 2001.

Due to the formation of aqueous compartments, aqueous two-phase systems (ATPS) or even aqueous multiphase systems (AMPS) have been used to selectively separate metals (ONGHENA; OPSOMER; BINNEMANS, 2015), biomolecules (HATTI-KAUL, 2001), or particles (AKBULUT et al., 2012).

In the case of AMPS formed by three incompatible polymers A and B dispersed in a continuous C phase, there are three different scenarios that can be found depending on the interfacial tensions between the components, see Figure 3. The first one happens when the interfacial tension between A and B (γ_{AB}) is smaller than the sum of interfacial tensions between B and C (γ_{BC}) and A and C (γ_{AC}), so that $\gamma_{AB} < \gamma_{BC} + \gamma_{AC}$. The second a situation

where one phase engulf another phase, in the case presented phase B engulfs phase A and so $\gamma_{AC} > \gamma_{BC} + \gamma_{BC}$ and the third situation is seen when the two dispersed phases do not touch each other, so that $\gamma_{AB} > \gamma_{BC} + \gamma_{AC}$.

FIGURE 3. SCHEMATIC REPRESENTATION OF THE POSSIBLE SCENARIOS FOR THREE INCOMPATIBLE POLYMERS, A AND B DISPERSED IN C.

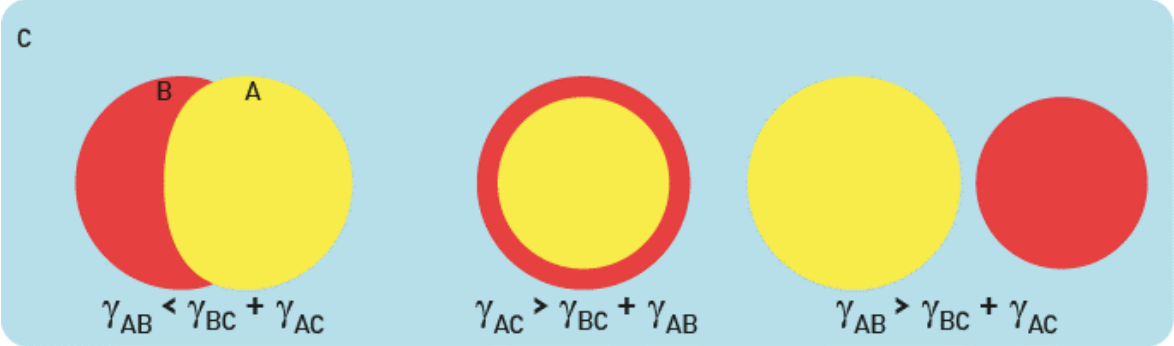

Source: the author (2021).

Figure 4 shows an experimental situation where the droplets of the dispersed liquids associate, forming a three-phase contact angle, if one interfacial tension is known, the other two interfacial tensions can be determined by analyzing the angles, as follows (ROWLINSONS; WIDOM, 1983).

FIGURE 4. CONFOCAL LASER SCANNING MICROSCOPY IMAGE OF TWO ASSOCIATED DROPLETS OF TWO AQUEOUS POLYMER SOLUTIONS A AND B IN A CONTINUOUS C PHASE. THE RESPECTIVE ANGLES FORMED BY THE CONTACT OF THE DROPLETS ARE SHOWN.

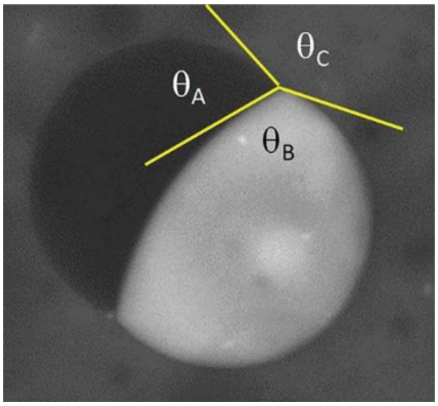

Source: the author (2021).

$$cos(\theta_A) = 0.5\left[\left(\frac{\gamma_{BC}}{\gamma_{AC}}\right)\left(\frac{\gamma_{BC}}{\gamma_{AB}}\right) - \left(\frac{\gamma_{AC}}{\gamma_{AB}}\right) - \left(\frac{\gamma_{AB}}{\gamma_{AC}}\right)\right] \quad 2$$

$$cos(\theta_B) = 0.5\left[\left(\frac{\gamma_{AC}}{\gamma_{AB}}\right)\left(\frac{\gamma_{AC}}{\gamma_{BC}}\right) - \left(\frac{\gamma_{AB}}{\gamma_{BC}}\right) - \left(\frac{\gamma_{BC}}{\gamma_{AB}}\right)\right] \quad 3$$

$$cos(\theta_C) = 0.5\left[\left(\frac{\gamma_{AB}}{\gamma_{BC}}\right)\left(\frac{\gamma_{AB}}{\gamma_{AC}}\right) - \left(\frac{\gamma_{BC}}{\gamma_{AC}}\right) - \left(\frac{\gamma_{AC}}{\gamma_{BC}}\right)\right] \quad 4$$

From Equations 2, 3, and 4 and knowing that:

$$\theta_A+\theta_B+\theta_C = 2\pi \quad 5$$

Then, it is possible to derive three relations of interfacial tension ratios:

$$\frac{\gamma_{AB}}{\gamma_{BC}} = \frac{sin\,(\theta_C)}{sin(\theta_A)} \quad 6$$

$$\frac{\gamma_{AB}}{\gamma_{AC}} = \frac{sin\,(\theta_C)}{sin(\theta_B)} \quad 7$$

$$\frac{\gamma_{AC}}{\gamma_{BC}} = \frac{sin\,(\theta_B)}{sin(\theta_A)} \quad 8$$

For these calculations to be accurate, one must assure that the centers of the droplets are in the same horizontal plane with respect to the *z* axis (perpendicular to the screen). If that is not the case, 3D analysis of the associate droplets is necessary.

Contrary to oil-water interfaces, the interface of w/w emulsions cannot be stabilized by molecular surfactants. The reason why common surfactants cannot adhere at the interface is because the interfacial width of w/w emulsions is not as sharp as that found for conventional interfaces between water and oil. Typically, the length of the interface for w/w is a few dozens of nanometers, whereas that for oil-water interfaces is ~ 1 nm (TROMP; BLOKHUIS, 2013; ZARBAKHSH; BOWERS; WEBSTER, 2005). Therefore, other candidates have been explored to stabilize the w/w interface, such as solid particles or high molar mass polyelectrolytes (ESQUENA, 2016; NICOLAI; MURRAY, 2017; TEA; NICOLAI; RENOU, 2019).

In this context, particles from WPI or β-lg have been largely employed as w/w emulsions stabilizers, due to the demand to produce fat-free products containing a high nutritious content, and w/w emulsions stabilized by WPI particles are an excellent candidate

of a future commercial product (BALAKRISHNAN et al., 2012; DE FREITAS et al., 2016; GONZALEZ-JORDAN; BENYAHIA; NICOLAI, 2017; ZHANG et al., 2021).

By considering a spherical rigid particle attached at the interface of two aqueous solutions A and B, one can calculate the free energy of particle desorption ($\Delta_{des}G$), which is the energy necessary to displace the particle from the interface to the interior of one phase, by (BINKS; HOROZOV, 2006):

$$\Delta_{des}G = \pi R_{part}^2 \gamma_{AB}(1 - |cos\ \theta|)^2 \quad 9$$

where R is the particle radius, and the three-phasic contact angle, θ, is obtained by:

$$cos\ \theta = (\gamma_{AP} - \gamma_{BP})/\gamma_{AB} \quad 10$$

where γ_{AP} and γ_{BP} are the interfacial tension between the particles with phase A and B, respectively, and γ_{AB} is the interfacial tension between the two phases. By looking at Equation 9, it could be expected that the extremely low γ_{AB} found in w/w emulsions may not lead to a significant amount of $\Delta_{des}G$. That is, even thermal fluctuations could be responsible for removing particles from the interface. However, that is not the case, as was observed for a system of poly(ethylene oxide) with dextran in the presence of latex particles. The researchers have proved that once the particles adhere at the interface, they did not spontaneously desorb from it and $\Delta_{des}G \approx 7\ k_BT$, where k_B is Boltzmann's constant. To remove them, shear forces were necessary (BALAKRISHNAN et al., 2012).

Thus, the adsorption energy gain by adhering a particle to the interface can be enough to explain the increase in the stability of the emulsion, provided that the particle size is big enough and the mixture is far from the critical point. Unfortunately, despite the observations showing the interfacial adherence of particles in w/w emulsions, a consistent decrease of droplet coalescence that led to long-term stability is usually not seen (FIROOZMAND; MURRAY; DICKINSON, 2009).

In the same line of thought, analyzing Equation 10, it is possible to observe that particles will spontaneously adsorb at the interface only if $\gamma_{AB} > |\gamma_{PA}\text{-}\gamma_{PB}|$, i.e. when $0° < \theta < 180°$. It is also clear that $\Delta_{des}G$ will be at its maximum value when $\theta = 90°$. That said, it is possible to expect that if one can fine-tune the balance of the interfacial tensions so that the particles would prefer to reside at the interface, an increase in stability against coalescence would be seen.

There are several methods to modulate the partition of solid particles in w/w emulsions, such as modifying the surface (DE FREITAS et al., 2016; GONZALEZ-JORDAN; NICOLAI; BENYAHIA, 2018; KHEMISSI et al., 2018) or the morphology (GONZALEZ-JORDAN; NICOLAI; BENYAHIA, 2016; HAZT et al., 2020) of the particles or by modifying the properties of the media in which the particles are inserted, i.e. the pH, ionic strength, or temperature (DIAMOND; HSU, 1990; IQBAL et al., 2016). One parameter which has not been investigated yet is the effect of adding a third soluble component to the mixture which will be miscible between both phases and does not interact specifically with particles nor the phases but could possibly change the interfacial tensions e.g. a soluble polysaccharide.

Although, as mentioned above, positioning the particles at the interface does not necessary provides stability against coalescence. Therefore, an interesting approach would be to form localized particle-gels at the interface, which can create some resistance against the rupture during coalescence.

In this report, w/w emulsions were studied from a fundamental and from an applicable point of view. Firstly, binary mixtures between several proteins and polysaccharides were investigated followed by a discussion regarding the formation of aqueous multiphase system. Then, a method of fine-tuning the partition of particles in w/w emulsions was explored. The addition of a third soluble polymer to w/w emulsions formed by mixing amylopectin and pullulan at pH 7.0 in the presence of protein microgels was studied for one neutral (xyloglucan) and three anionic (alginate, pectin, and κ-carrageenan) polysaccharides. The findings were generalized by using a different type of w/w emulsion and a different particle. Also, after stablishing the conditions where the particles adhere at the interface, two different methods were employed to achieve interfacial cold-set gels, seeking stabilization against coalescence compared to individual protein microgels. Finally, a brief study on the effect of temperature on the partition of the protein microgels between w/w interfaces was presented.

2 OBJECTIVES

2.1 GENERAL OBJECTIVE

Explore new possibilities and features of w/w emulsions in the presence or absence of protein microgels from both the fundamental and applicable point of view pursuing applications in fat-free food and beverages.

2.2 SPECIFIC OBJECTIVES

- Observe and study the association of incompatible aqueous mixtures of polysaccharides and proteins solutions,
- Investigate the possibility to modulate the partition of particles in w/w emulsions by adding a third soluble component, changing the pH, and by varying the temperature,
- Exploit the findings to other systems to form a generalized concept,
- Explore the influence of two different methods to induce particle attractive interaction by changing the pH on the microstructure of the emulsions.

3 MATERIALS AND METHODS

3.1 PREPARATION OF BIOPOLYMERS STOCK SOLUTIONS

Dextran (DX), alginate (ALG), κ-carrageenan (KC), gelatin from cold-water fish skin (GEL), and poly(ethylene oxide) (PEO) were purchased from Sigma-Aldrich. In order to remove potassium ions from the KC, 0.5 wt% solutions were dialyzed first against 0.1 mol L^{-1} sodium chloride (NaCl) and then extensively against ultrapure water. The KC was subsequently freeze-dried.

Pullulan (PUL) and xyloglucan (XG) were kindly provided from Hayashibara co., DSP Gokyo Food & Chemical co., respectively, whereas low-methylated pectin from lemon peel (PEC), hydroxypropyl methylcellulose (HPMC) were obtained by Cargill. Sodium caseinate (CAS) was purchased from Lactalis Ingredients. PUL, HPMC, PEO, and DX were used as received, whereas PEC (~ 4,1 wt%), ALG (~ 3 wt%), CAS (~ 10%) and XG (~ 2 wt%) stock solutions were centrifuged at 58960 *g* to remove minor insoluble aggregates.

Amylopectin (AMP) from maize was purchased from Sigma-Aldrich and was purified before using following a method previously described (BELLO-PÉREZ et al., 1998; DE FREITAS et al., 2016). Briefly, AMP was dispersed in a dimethyl sulfoxide (DMSO): H_2O 95:5 (v/v) mixture at 5 wt%. After complete dispersion, it was centrifuged at 10000 *g* for 30 min at 20 °C. The supernatant was precipitated in ethanol (99%) and the precipitate was recovered by filtration through a glass filter. The precipitate was washed extensively successively with ethanol, acetone, and diethyl ether. The AMP powder obtained was dried under vacuum and then dispersed in water to obtain an AMP solution.

The pH was adjusted by adding aliquots of either hydrochloric acid (HCl) or sodium hydroxide (NaOH) solutions at 0.1 or 0.01 mol L^{-1}. All the water used in the materials and methods section was ultrapure (Milli-Q system).

The DEX, ALG, KC, PEC, PUL, XG, and AMP were studied more thoroughly, so they were characterized by size-exclusion chromatography combined with on-line light scattering (Dawn EOT, Wyatt technology, Santa Barbara, CA, USA) and refractive index (Shodex RI 71, Showa Denko K.K., Tokyo, Japan) detectors. The column used was a TSK gel G6000PW and 0.1 mol/L $NaNO_3$ at pH 7.0 was used as the eluent. The weight-average molar masses, M_w, determined were the following: DEX = 4.10×10^5, ALG = 7.90×10^4, KC = 8.77×10^4, PEC = 3.72×10^6, PUL = 2.98×10^5, XG = 1.04×10^6, HPMC = 2.91×10^5, and AMP = 1.64×10^8 g mol^{-1}. The refractive index increment used for the mentioned

samples were: DEX = 0.143 (BASEDOW; EBERT; RULAND, 1978), ALG = 0.165 (BUCHNER; COOPER; WASSERMANN, 1961), KC = 0.140 (WITTGREN et al., 1998), PEC = 0.146 (DIMOPOULOU et al., 2019), PUL = 0.152 (DE NOOY et al., 1996), XG = 0.113 (DE FREITAS et al., 2016), HPMC = 0.150 (JUMEL et al., 1996), and AMP = 0.146 (DE FREITAS et al., 2016).

3.2 PRODUCTION OF WHEY PROTEIN MICROGELS

Protein microgels (MG) were prepared from whey protein isolate (WPI - M_w of 2.14×10^4 g mol^{-1} determined by SEC) powder from Bipro Protein following a methodology already described (KHARLAMOVA; CHASSENIEUX; NICOLAI, 2018). Initially, WPI powder was solubilized at 10 wt% for 5 h in water. The solution was then centrifuged at 50000 *g* at 20 °C for 2 h. The supernatant was kept and used to determine the protein concentration in solutions of approximately 0.1 wt% in a spectrophotometer (Jasco V760) at 25°C in quartz cuvettes with a pathlength of 1 cm. The spectra were recorded from 200 to 500 nm at 0.5 nm steps, and the concentration was measured at 278 nm using $\varepsilon = 1.05$ L g^{-1} cm^{-1}.

Then, the solution was diluted to 4 wt% and the pH was set to 5.9 by adding HCl 0.1 mol L^{-1}. Then, the WPI solution was heated at 80 °C for 15 h. At these conditions, the conversion of WPI to MG was 67 %. Light scattering measurements gave values for the radius of gyration R_g and M_w of 125 nm and 3.30×10^8 g mol^{-1}, respectively. The remaining proteins were strand-shape fractal aggregates with hydrodynamic radius (R_h) = 38 nm. After preparation, sodium azide was added to as a bacteriostatic agent at 0.02 wt% to all protein and polysaccharide solutions.

3.3 PREPARATION OF COMPLEXES OF MICROGELS AND ANIONIC POLYSACCHARIDES

MG were complexed electrostatically by adding the anionic polysaccharides PEC, KC or ALG individually into the dispersion. Different concentration ratios of MG:anionic polysaccharides were tested (1:1, 1:0.75,1:0.5, 1:0.2, 1:0.1, and 1:0.075). The polysaccharide solution was added to the MG dispersion at rest, then during stirring the pH was adjusted with HCl solution until pH 5.0. The mixtures were left at different amount of time (24, 15, 10, 5, 4, 3, 2 or 1 h) at this same pH where complexation should take place.

Then, NaOH solution was added to return the pH to 7.0, which was the condition used to dilute the samples and to analyze by laser light scattering (0,01 wt%) and confocal laser scanning microscopy (1 wt%).

3.4 DETERMINATION OF R_h, R_g AND M_w BY LIGHT SCATTERING

Static (SLS) and dynamic (DLS) light scattering measurements were performed in a correlator ALV-CGS3 equipped with a laser emitting vertically polarized light at a wavelength of 632 nm (ALG-Langen). The samples were diluted to a total protein concentration of 0.01 wt% in a 0.1 mol L^{-1} NaCl aqueous solution and then were analyzed at a controlled temperature set to 20.0 ± 0.2 °C through a range of angles from 13° to 150°. The relative scattering intensity (R), so-called the Rayleigh ratio, was calculated as follows (MCCLEMENTS, 2007):

$$R = \frac{(I - I_S)R_{tol}}{I_{tol}} \quad 11$$

Where I, I_s, and I_{tol} are respectively the intensities from the solution, from the solvent, and from the toluene. R_{tol} is the Rayleigh constant of toluene ($R_{tol} = 1.35x10^{-5}$ cm^{-1} for $\lambda = 632$ nm). In dilute solutions, R is related to the M_w and the structure factor (S(q)), as follows:

$$\frac{R}{KC} = M_W S(q) \quad 12$$

Where C is the concentration of the solute and q is the scattering vector defined as:

$$q = \frac{4\pi n}{\lambda} sen\left(\frac{\theta}{2}\right) \quad 13$$

where n is the refractive index of the solvent (for water, n = 1.333) and K is an optical constant given by:

$$K = \frac{4\pi^2 n_s^2}{\lambda^4 N_A}\left(\frac{\partial n}{\partial C}\right)^2 \left(\frac{n_{tol}}{n_s}\right)^2 \frac{1}{R_{tol}} \quad 14$$

With $\partial n/\partial C$ being the refractive index increment (0.19 mL/g for WPI), N_A Avogadro's number, n_{tol} and n are the refractive index of the toluene and the solvent, respectively.

For small values of q the structure factor can be described as:

$$S(q) = \left(1 + \frac{q^2 R_g^2}{3}\right)^{-1} \quad 15$$

Which gives the z-average radius of gyration, R_g. DLS experiment provides information regarding the diffusion of the particles in the solution. The z-average diffusion coefficient (D), which was given by the average relaxation, provides us the R_h extrapolating the value of D to $q = 0$ using Stokes-Einstein equation:

$$D = \frac{k_B T}{6\pi\eta R_h} \quad 16$$

Where T and η are the absolute temperature and the viscosity of the solvent, respectively.

3.5 PREPARATION OF THE EMULSIONS AND MACROSCOPIC EVALUATION

The binary mixtures were investigated macroscopically by determining firstly the phase-behavior. The methodology used is described schematically in Figure 5. Basically, the binary mixture was prepared at pH 7.0 in the absence of added salt and homogenized to assure the mixing of the components. Then, this mixture was centrifuged mildly to accelerate the phase separation if it happened. If a homogeneous mixture was observed, the concentration of the polymers was increased. If the system continuously behaved as a homogeneous mixture, it was assumed that it was a compatible binary mixture. If the system behaved as a heterogeneous mixture after centrifugation, the relative heights of each phase were calculated allowing the estimation of the tie-lines. Then, by adding water and repeating the procedure continuously until the phase separation stops, it was possible to determine the binodal line.

FIGURE 5. FLOWCHART USED TO DETERMINE THE PHASE-BEHAVIOR OF BINARY MIXTURES AND TO SKETCH THE PHASE DIAGRAM.

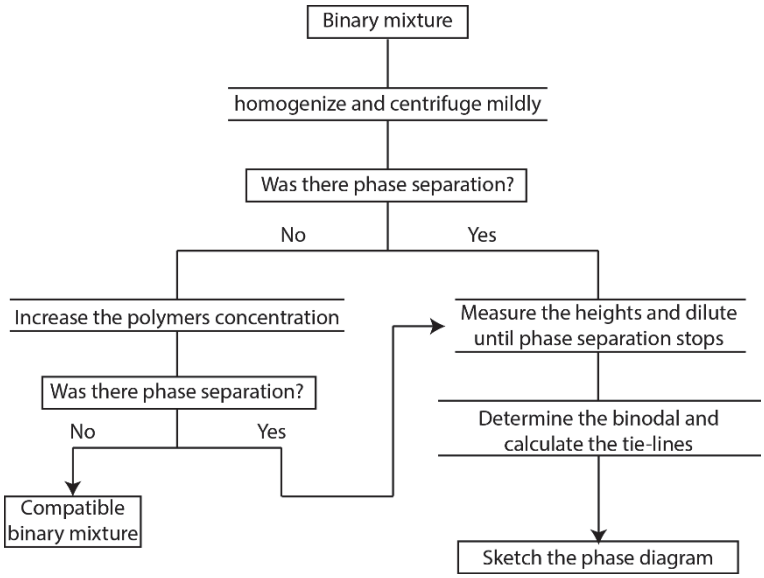

3.6 MICROSCOPIC INVESTIGATION OF THE EMULSIONS

Confocal laser scanning microscopy (CLSM) images were obtained with a Zeiss LSM800 (Carl Zeiss Microscopy GmbH, Germany) using water immersion objectives: HC×PL APO 63× (NA = 1.2) and HC×PL APO 25× (NA = 0.7). The samples were either labeled by adding 5 ppm of Rhodamine B (RodB) or Nile blue (NB). The samples were analyzed in a concave slides hermetically sealed by a cover glass slip. The excitation wavelength used for RodB and NB were 551 and 640 nm, respectively, whereas the emission was detected at 627 nm (RodB) and 674 nm (NB). PEC was covalently labeled with fluorescein isothiocyanate (FITC) by adapting a method described (BUI et al., 2019). Briefly, 1 g of PEC was dispersed in 20 mL of DMSO followed by the addition of 0.5 mL of HCl 1 mol L^{-1}. Then, 0.04 g of FITC and 40 µL of dibutyltin dilaurate were added to the mixture, which was left stirring at 80 °C for 2 days. The was then precipitated and washed with ethanol 99 % until the solvent became colorless and it was denominated PEC-FITC. The precipitate was subsequently dissolved in water and dialyzed against to remove any free FITC. A few insoluble aggregates of PEC-FITC formed during the labeling process were observed in the experiments, but they did not interfere in the system. Glucono-δ-lactone (GDL) was used to decrease the pH of the system *in-situ*. GDL is an acidifier that releases H^+ during aqueous dissociation (LIU; ZHOU; NICOLAI, 2020a, 2020b). The pH of the samples was measured in parallel to the microscopic observations.

The temperature dependent experiments were performed in a RheOptiCAD ®, in which the samples were introduced between two planar glass slides separated by 500 µm distance gap. The equipment allows controlled temperature experiments as well as rheological analysis. For a detailed description, please see BOITTE et al., 2013. All CLSM images obtained were treated with the ImageJ software.

3.7 MEASUREMENT OF THE MG PARTITION

The partitioning of the MG between the phases was quantified by measuring the absorbance at a wavelength of 280 nm using a UV-visible spectrometer (Jasco PAC-743). After macroscopic phase separation, both the AMP and PUL-rich phase was analyzed at different PUL volume fractions Φ_{PUL} = 0.13, 0.50, and 0.87 at different PEC concentrations and a fixed MG concentration of 0.4 wt%. For the PEC-FITC quantification, emulsions at Φ_{PUL} = 0.13, 0.26, 0.32, 0.50, 0.55, 0.65, 0.87 in the presence of 0.1 wt% FITC-PEC were prepared, and the top PUL-rich phases were analyzed after centrifugation to quantify the FITC-PEC while the concentration in the AMP-rich phase was deduced from them. The centrifugation was at a sufficient low speed, so that it did not perturb the partition but only accelerated the phase separation.

4 RESULTS AND DISCUSSION

Results and discussion section will be divided as follows. The first subsection (4.1) regards the general aspects of mixtures of both binary and multi-phase systems formed of polymers solutions, an overview of phase-separated mixtures between several polysaccharides and proteins will be presented. The second subsection (4.2) will show the results on the complexation between MG with themselves and MG with anionic polysaccharides, which will help us to understand the formation and the stability of protein-polysaccharide complexes. It will be shown the influence of adding the protein:polysaccharide complexes to an emulsion of amylopectin and pullulan. The effect caused by adding a third polysaccharide on the partition of MG particles in w/w emulsions of amylopectin and pullulan will be exposed and a plausible explanation to the effect will be given in subsection 4.3. Then, in subsection 4.4 the influence of the pH on the stability and the microstructure of the emulsions with protein microgels will be shown, followed by a briefly observation on how the temperature changes the preference of MG between phases in w/w emulsions.

4.1 OVERVIEW OF PHASE SEPARATION IN AQUEOUS MIXTURES OF POLYMERS

The phase behaviors of binary mixtures of proteins and polysaccharides solutions at pH 7.0 are summarized in Tables 1 and 2, where it is shown in the first row a fixed polymer and in the respective column the polymer(s) with which it phase separated.

It was observed that among the polysaccharides investigated, AMP was the one that had more incompatibilities, whereas among the proteins GEL is incompatible with 6 different components. For some of the binary mixtures shown in Tables 1 and 2, preliminary phase diagrams were created based in the procedure described in section 3.4. These phase diagrams will not be discussed in detail and are shown in the Appendix III.

TABLE 1. SUMMARY OF THE MACROSCOPICALLY EVALUATION OF BINARY MIXTURES THAT RENDERED AQUEOUS TWO-PHASE SYSTEMS AT pH 7.0. HERE THE FIXED COMPONENT IS A POLYSACCHARIDE AND IT IS PRESENTED IN THE FIRST ROW.

XG	**DX**	**AMP**	**ALG**	**HPMC**	**PEC**	**KC**	**PUL**	**PEO**
DX	XG	XG	CAS	DX	CAS	AMP	DX	XG
GEL	GEL	DX		GEL		CAS	GEL	DX
AMP	AMP	GEL		AMP			AMP	GEL
WPI	HPMC	HPMC		PUL			HPMC	AMP
PEO	PUL	KC					PEO	PUL
	PEO	PUL						WPI
		WPI						
		PEO						

The concentrations of the polysaccharides aqueous solutions were: XG (2 wt%), DX (20 wt%), AMP (15 wt%), ALG (3 wt%), PEC (4.1 wt%), KC (3 wt%), PUL (10 wt%), HPMC (1%) and PEO (15 wt%).

TABLE 2. SUMMARY OF THE MACROSCOPICALLY EVALUATION OF BINARY MIXTURES THAT RENDERED AQUEOUS TWO-PHASE SYSTEMS AT pH 7.0. HERE THE FIXED COMPONENT IS A PROTEIN AND IT IS PRESENTED IN THE FIRST ROW.

GEL	**CAS**	**WPI**
XG	ALG	XG
DX	PEC	AMP
AMP	KC	HPMC
HPMC		PEO
PUL		
PEO		

The concentrations of the proteins aqueous solutions were: GEL (20 wt%), CAS (10 wt%), and WPI (30 wt%).

From the analysis of Tables 1 and 2, it can be proposed that by mixing for instance XG, DX and GEL an AMPS could be formed, provided that all three components are incompatible between themselves. This hypothesis was investigated more thoroughly by mixing three or more stock solutions of different polymers.

Strictly speaking, when three incompatible macromolecules A, B, and C are mixed in solution, so that A and B are dispersed in C, the droplets of A and B will associate if $\gamma_{AB} < \gamma_{BC} + \gamma_{AC}$.

The measurement of the angles formed by the contact of the dispersed phases led to inaccuracy, thus an alternative method was developed. It consisted in tracing circles around the dispersed droplets (A and B) and then a third circle, C, that goes along with the interface of the two droplets. In Figure 6, this method is applied in an AMPS formed by DX (phase A) and AMP (phase B) dispersed phases in PEO (phase C).

FIGURE 6. SCHEME REPRESENTING THE ASSOCIATED DROPLETS OF FIGURE 4 WITH CIRCLES DREW TRACING THE INTERFACES. THE DISTANCE BETWEEN THE CENTERS OF CIRCLE B AND C IS PRESENTED, d_{BC}.

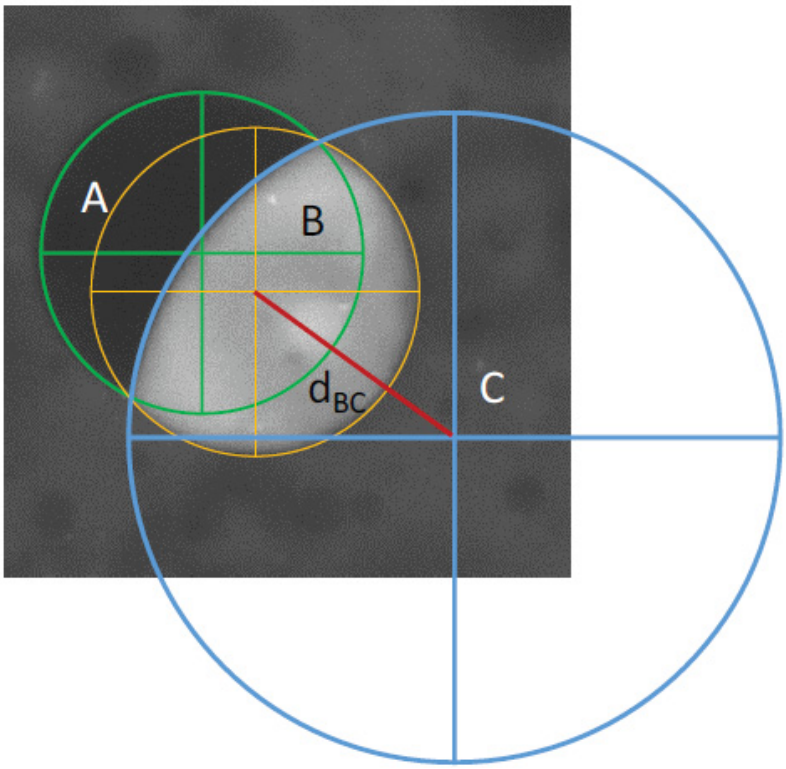

In this case, equations related to the circles' radii and the distance between the centers of the circles arise:

$$cos(\theta_A) = \left(\frac{r_A^2 + r_B^2 - d_{AC}^2}{2r_A r_C}\right) \quad 17$$

$$cos(\theta_B) = \left(\frac{r_B^2 + r_C^2 - d_{BC}^2}{2r_B r_C}\right) \quad 18$$

$$cos(\theta_C) = \left(\frac{r_A^2 + r_B^2 - d_{AB}^2}{2r_A r_B}\right) \quad 19$$

Where r_A, r_B and r_C are the circles' radii and d_{AB}, d_{AC} and d_{BC} are the distances between the center of the circles A-B, A-C, and B-C, respectively. Equations 17, 18 and 19, give $\theta_{DX} = 70°$, $\theta_{AMP} = 140°$, and $\theta_{PEO} = 160°$. Substituting these values into Equations 6, 7 and 8 one can obtain the following:

$$\gamma_{AMP-DX} = 1.46\gamma_{PEO-DX} \quad 20$$

$$\gamma_{PEO-AMP} = 0.54\gamma_{PEO-DX} \quad 21$$

After mixing the three components their respective compartments were formed, which after phase separation, allowed the determination of the concentration of each component in their separated phases. The approximate concentration ratio between AMP (C_{AMP}), DX (C_{DX}), and PEO (C_{PEO}) in the separated phases of was found to be C_{AMP}:C_{DX}:C_{PEO} = 4:2:1. The unequal partition of the RodB among each phase allowed the visualization of each component individually by a brightness contrast in CLSM, see Figure 7 where the continuous phase (the phase with the highest volume fraction) sequentially among AMP, DX and PEO.

FIGURE 7. CLSM IMAGES OF MIXTURES OF AMP, DX, AND PEO WITH EITHER AMP (A), DX (B), OR PEO (C) AS CONTINUOUS PHASE. THE SCALES ARE SHOWN IN THE IMAGES. THE BRIGTHNESS DECREASES AS AMP > PEO > DX.

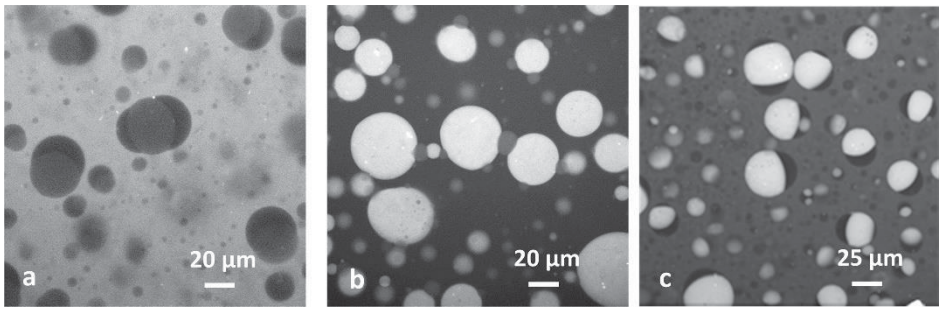

The effect of diluting with water the three-phase emulsion of AMP and DX droplets in a continuous PEO phase is shown in Figure 8. Provided that the compositions were very far from the binodal of the binary mixtures (AMP-DX, PEO-DX and PEO-AMP), the dilution of 1.5× had small effect on the ratio of the interfacial tensions, since the angles

changed slightly. Less than 20% difference was seen at a dilution factor of 2.5. This is a remarkable observation, since the binary mixture of PEO-DX is strongly dependent on the dilution, namely the tie-line length (TLL): $\gamma_{PEO-DX} \propto TLL^{3.9}$ (BALAKRISHNAN et al., 2012).

FIGURE 8. CLSM IMAGES OF AMP AND DX DROPLETS DISPERSED IN A CONTINUOUS PEO PHASE AT DIFFERENT DILUTIONS FACTORS INDICATED BELOW EACH PICTURE. THE BRIGHT REGION CORRESPONDS TO AMP PHASE WHEREAS THE DARKER REGION CORRESPONDS TO THE DX PHASE.

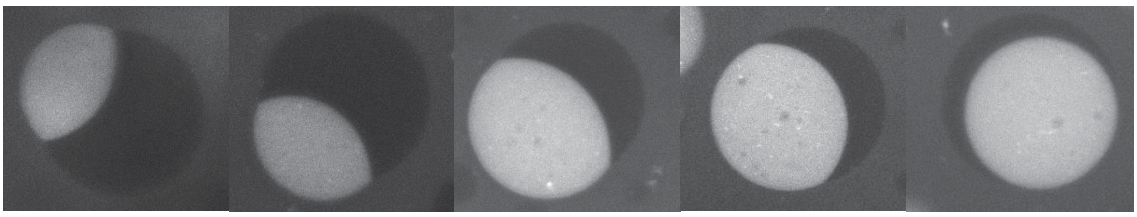

When the dilution factor was higher than 2.5, the DX phase started to surround the AMP phase, giving an $\theta_{DX} = 7°$ whereas θ_{AMP} and θ_{PEO} approached 180°. This can be understood by the increase in miscibility by DX and PEO at this dilution, which caused an abrupt decrease in γ_{PEO-DX} compared to the other two interfacial tensions.

When DX and PUL were mixed with PEO, a completely different scenario was observed. The PUL phase was entirely covered by DX when they were dispersed in PEO. Similarly, when PEO and DX were dispersed in PUL, the DX stayed in between PEO and PUL. In this situation, since there are no angles to measure, the interfacial tension between DX/PUL could not be determined, but what can be stated is: $\gamma_{PUL-DX} < (\gamma_{PEO-PUL} - \gamma_{PEO-DX})$. Likewise, DX formed a layer around PUL phase when GEL was the continuous phase and PUL formed a layer around the XG when dispersed in PEO.

Other sets of AMPS were investigated (APPENDIX IV) and the resulting interfacial tensions of binary mixtures were expressed in relation to the γ_{PEO-DX} which is a well-studied w/w emulsion, see Figure 9. It was noticed that the deviation of interfacial tension ratios associated with tracing circles of different associated droplets within the same sample was approximately 10 %.

It is worth mentioning that this should not be taken as strict interfacial tension values and are only valid far from the critical point, where the interfacial tension is less

influenced by the composition, therefore the error associated with the measurement should not have a major influence.

FIGURE 9. SCHEMATIC COMPARISON BETWEEN THE INTERFACIAL TENSIONS OF SEVERAL BINARY MIXTURES WITH RESPECT TO THE INTERFACIAL TENSION BETWEEN PEO-DX.

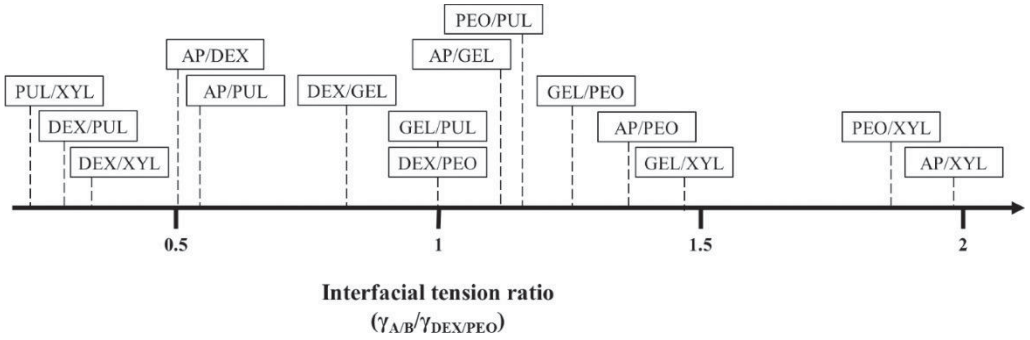

By mixing more than three incompatible polymeric aqueous solutions, more elaborated structures were formed. For instance, when AMP, DX, PUL were dispersed in a continuous PEO phase. The AMP and PUL droplets connected whereas the DX formed a halo around the PUL phase, protecting it from meeting the PEO phase, see Figure 10A. If a small amount of GEL is added to this system, it laid between the interface of DX and PEO, see Figure 10B.

FIGURE 10. AMPS FORMED BY MIXING AMP, DX, AND PUL IN A CONTINUOUS PEO PHASE (A). THE SAME SYSTEM BUT AFTER ADDING A GEL (B).

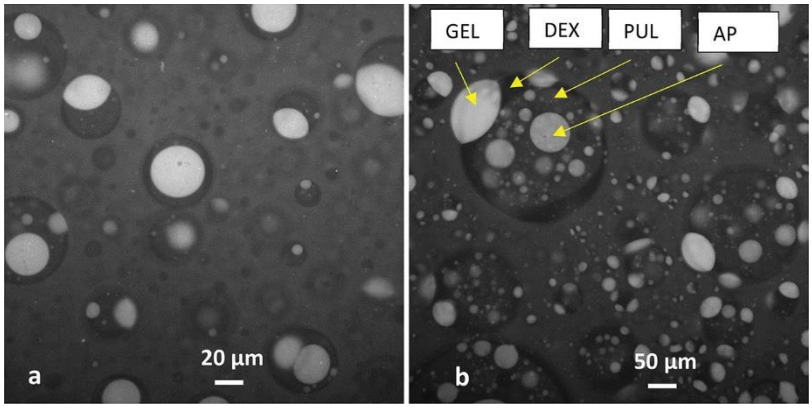

The AMPS formed by dispersing GEL, PEO, and AMP in a continuous PUL phase is presented in Figure 11. This situation led to the association of the PEO and AMP droplets in a string-like form (FIGURE 11A). Upon adding DX to this system, the droplets of PEO were covered with DX. This kind of association can be rationalized by considering the

relative interfacial tensions between the phases, which tells us that $\gamma_{PEO\text{-}PUL} > \gamma_{DX\text{-}PUL} + \gamma_{DX\text{-}PEO}$.

FIGURE 11. AMPS FORMED BY MIXING AMP, GEL, AND PEO IN A CONTINUOUS PUL PHASE (A). THE SAME SYSTEM BUT AFTER ADDING A DX (B).

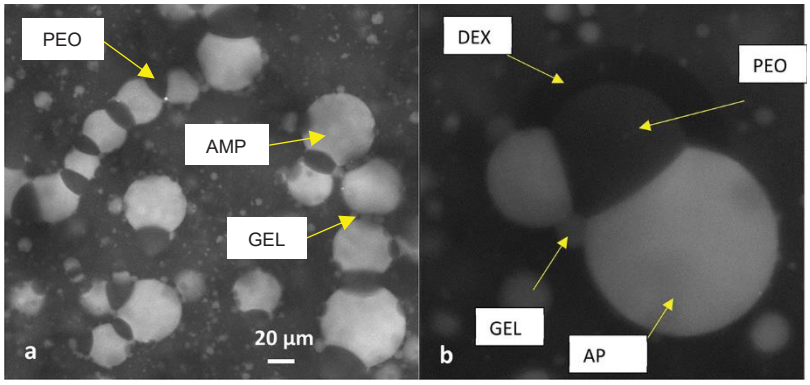

The influence of adding MG particles in AMPS was investigated in different systems. Based on previous studies, it is known that MG adsorb at the interface between PEO and DX and can provide stabilization against coalescence in certain situations (GONZALEZ-JORDAN; NICOLAI; BENYAHIA, 2016). Here, it was found that these protein particles also reside at the interface between PEO-AMP, PEO-PUL and PEO-XG. For any other system investigated, the MG preferred to stay within one phase, so that it was possible to stablish the preference of this particle for the polymer solutions studied. The preference increased in the following order: XG < AMP < PUL < PEO < DX < GEL, which can be used as an indicative to distinguish between unknown phases when RodB is used, because this fluorophore binds strongly to the MG.

Interesting observations were found by permutation of DX, AMP and PUL in a continuous PEO phase in the presence of MG. In Figure 12, it is shown one more time that when DX is present with PUL in a continuous PEO phase, the DX forms a layer around the PUL droplets. In the presence of MG, the outer layer of the DX phase is covered with MG and no excess of particles is seen elsewhere. When PUL is substituted by AMP, association of DX and AMP droplets is found, and the MG adsorb only at the DEX-PEO interface. In the AMPS formed by dispersing AMP and PUL in PEO, the MG migrated towards the interfaces between PEO-AMP and PEO-PUL only.

FIGURE 12. AMPS FORMED BY PERMUTATION OF THE DISPERSED PHASES OF AMP, DX, AND PUL IN A CONTINUOUS PEO PHASE IN THE PRESENCE OF 0.1 wt% MG PARTICLES: DX+PUL IN PEO (LEFT), DX+AMP IN PEO (MIDDLE), AND PUL+AMP IN PEO (RIGHT).

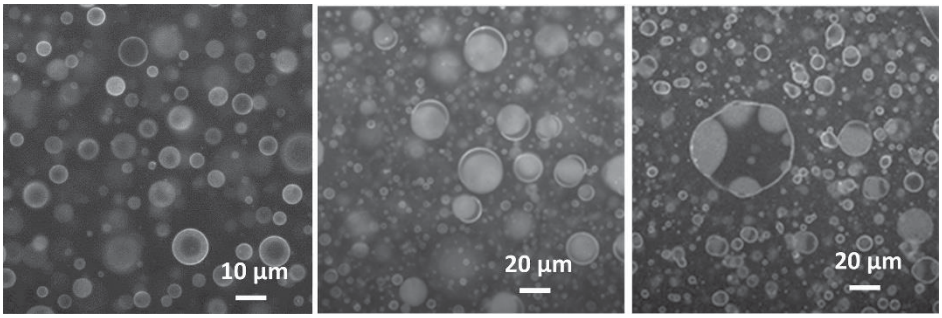

Curiously, the presence of a MG layer around the droplets did not cause significant change in the angles between the components, see Figure 13. One can assume that the MG particles are a different phase that either stay within one phase or adsorb at the interface, depending on the interfacial tension of the particles with each phase. However, the MG cannot deform, so that the angles created with the other phases are fixed.

FIGURE 13. EMULSIONS OF AMP AND PEO DISPERSED IN PUL WITH (LEFT) AND WITHOUT (RIGHT) 0.1 wt% MG. AS STATED BEFORE, THE RodB BINDS STRONGLY TO THE MG, SO THAT IN THE PRESENCE OF THE PARTICLES, THE PEO PHASE BECOMES BRIGHTER DUE TO THE MIGRATION OF THE MG TOWARDS THIS PHASE, AND A BRIGHT RING OF PARTICLES IS SEEN AT THE PEO-PUL INTERFACE.

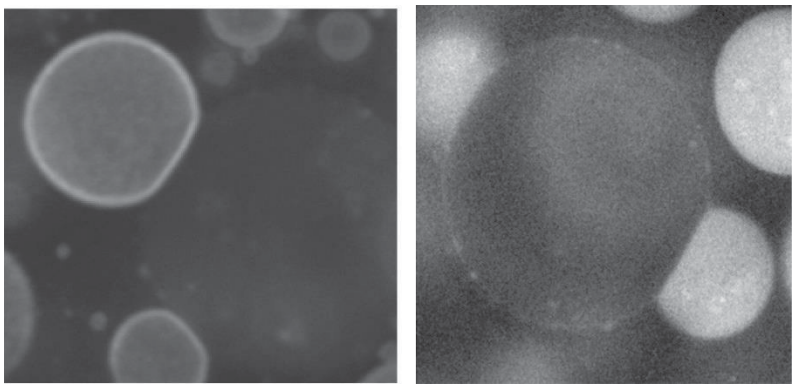

In the presence of MG, both PUL and AMP droplets dispersed in PEO could be stabilized against coalescence. The PEO, however, could only be stabilized by MG when dispersed in PUL.

The evaluation of the stability against coalescence for the AMPS formed by mixing AMP and PUL in PEO in the presence of MG showed to be stable for at least one week despite the sedimentation of the associated droplets, see Figure 14.

FIGURE 14. AMPS FORMED BY DISPERSING AMP AND PUL IN PEO IN THE PRESENCE OF APPROXIMATELY 0.1 wt% MG. THE IMAGE WAS TAKEN 1 WEEK AFTER PREPARATION AND REPRESENT THE A MACROSCOPIC SEDIMENTED LAYER OF STABLE DROPLETS.

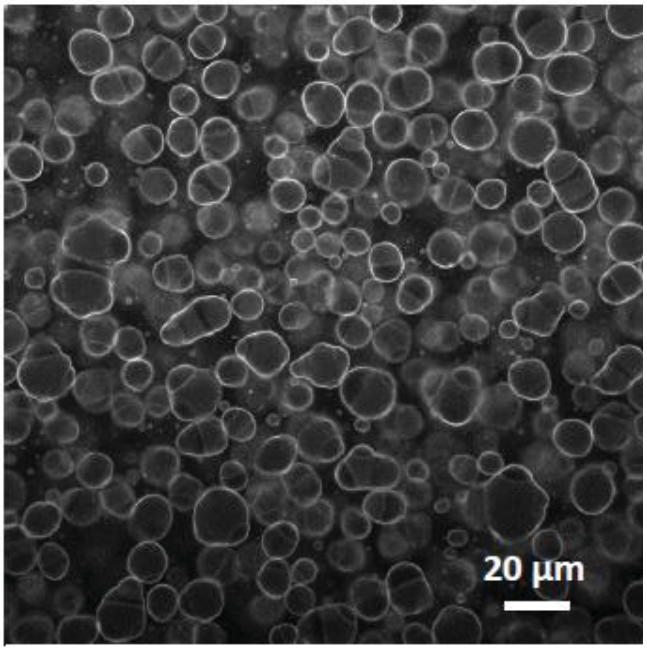

Even more impressive was the network formed by dispersing AMP and PEO in PUL in the presence of MG after 1 week of evaluation, see Figure 15. In this case, the MG formed a layer only around the PEO phase protecting it against coalescence whereas the AMP phase had very few particles protecting it. Even though the AMP was partially covered with particles, the system as a whole did not destabilize due to the alternating association of stable PEO droplets and AMP droplets. Macroscopically, this system behaved as a viscous liquid but not a gel.

FIGURE 15. AMPS FORMED BY DISPERSING AMP AND PEO IN PUL IN THE PRESENCE OF APPROXIMATELY 0.1 wt% MG. THE IMAGE WAS TAKEN 1 WEEK AFTER PREPARATION AND REPRESENT A NETWORK FORMED BY ALTERNATING AMP AND PEO DROPLETS.

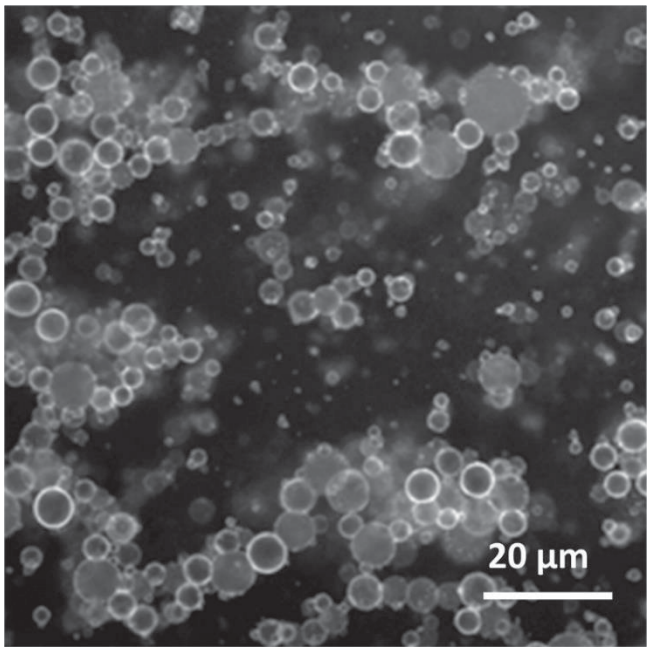

As a short summarization for this section, it was stablished an overview of the phase behavior for several binary mixtures which allowed one to elaborate AMPS. By mixing three or more incompatible polymer solutions together, it was possible to determine a scale of relative interfacial tensions of binary mixtures. The presence of MG led to the stabilization against coalescence in certain AMPS.

4.2 FORMATION AND USE OF PROTEIN:POLYSACCHARIDE COMPLEXES IN WATER-IN-WATER EMULSIONS

4.2.1 Complexation of microgels with anionic polysaccharides

At pH ≈ IEP, MG tend to aggregate irreversibly. However, this transition from individual MG particles to clusters of MG takes time, as is shown in Figures 16 and 17, where MG suspensions were left at pH 5.0 for different periods of time, then set back to pH 7.0, and analyzed by light scattering and CLSM. One can see that the aggregation was still largely reversible until 5 h showing only small increases in M_w and R_h.

FIGURE 16. R/KC DEPENDENCE ON THE SCATTERING WAVE VECTOR *q* FOR MG SUSPENSIONS AFTER DIFFERENT TIMES AT pH 5.0. NOTE THAT THE EXPERIMENT WAS CONDUCTED AT pH 7.0 AND THE SAMPLES WERE AT A TOTAL PROTEIN CONCENTRATION OF 0.01 wt%.

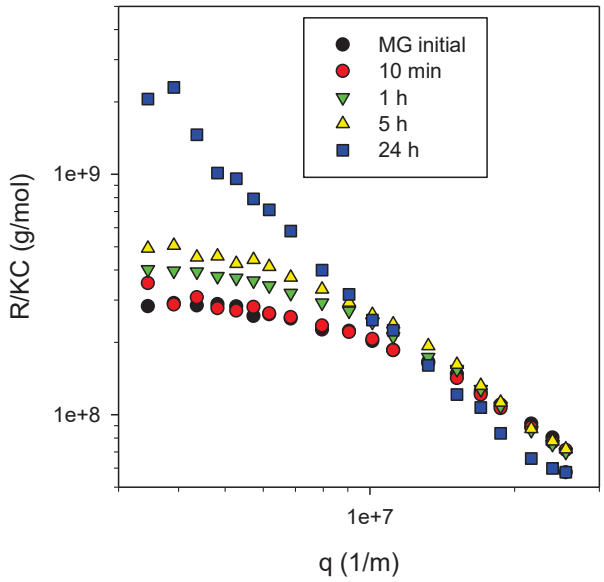

By CLSM, the increase in size and mass of the MG within 1 h was not clearly seen, however at 5 and 24 h it was possible to see the clusters formed by several individual MG. Notice that in order to observe the structures by CLSM, higher MG concentrations were used, thus that is probably the reason why aggregated structures are seen at 5 h in Figure 17.

FIGURE 17. CLSM IMAGES OF MG SUSPENSIONS AT A TOTAL PROTEIN CONCENTRATION OF 0.1 wt% SHOWING THE EFFECT OF TIME ON THE AGGREGATION OF INDIVIDUAL PARTICLES INTO CLUSTERS AT pH 5.0. NOTE THAT THE IMAGES WERE OBSERVED AT pH 7.0. THE SCALE BAR REPRESENTS 20 µm.

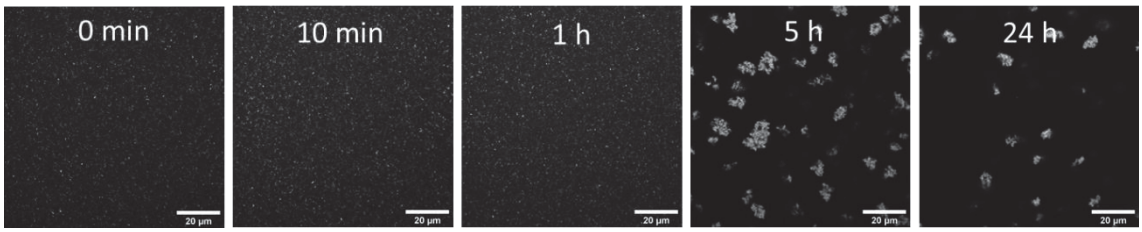

The aggregation of heat-denatured protein particles, so-called cold-gelation or cold-set gel, is a known behavior and is caused by the decrease of electrostatic repulsion in aqueous media by either increase of the ionic strength or by pH reduction (ALTING et al., 2003, 2004; GONZALEZ-JORDAN; BENYAHIA; NICOLAI, 2017; KHARLAMOVA;

CHASSENIEUX; NICOLAI, 2018; MCCLEMENTS; KEOGH, 1995; SCHMITT et al., 2010b).

After noticing that the irreversible formation of MG clusters took more than 5 h to happen at pH 5.0, the effect of adding an anionic polysaccharide at the same pH for 24 h was investigated in order to form individual protein-polysaccharide complexes that could be used as stabilizers in emulsions. Figures 18, 20, and 22 show the scattering vector dependence on R/KC (A) and on R_h (B), whereas Figures 19, 21, and 23 present CLSM images for the protein-polysaccharide mixtures with PEC, ALG, and KC at pH 7.0 after being kept at pH 5.0 for 24 h.

For the complexes made by mixing MG and PEC it is possible to see from the R/KC *vs* q dependence that the complexes had a higher M_w compared to the initial MG, although it was not possible to determine the exact value for the mixtures at 1:1, 1:0.75, and 1:0.1 probably due to the presence of a few aggregates, since SLS is very sensitive for the presence of aggregates. Specifically, the 1:0.075 ratio for both SLS and DLS experiments showed the presence of aggregates, indicating that this amount of polysaccharide was not sufficient to protect the MG, see Figures 18 A and B. When there is limited amount of polysaccharides, complex coacervation is usually seen, thus leading to bridging, i.e. one polysaccharide adsorbing to more than one protein particle (KRUIF; TUINIER, 2001). As mentioned before, the aggregates observed by CLSM in Figure 19 for the 1:1, 1:0.75 and 1:0.5 are probably an artifact due to the concentration.

FIGURE 18. DEPENDENCE OF THE SCATTERING VECTOR ON R/KC (A) AND ON R_h (B) FOR THE MIXTURE OF MG (1 wt%) AND PEC AT DIFFERENT CONCENTRATION RATIOS EXPRESSED ON THE FIGURES AFTER 24 AT pH 5.0.

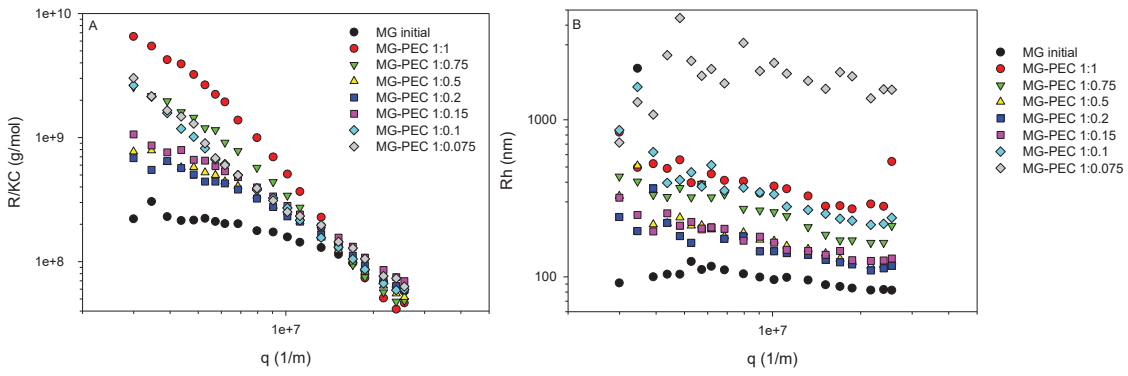

FIGURE 19. CLSM IMAGES OF AQUEOUS DISPERSIONS OF MG-PEC STRUCTURES AT 1 wt% FORMED AT DIFFERENT CONCENTRATION RATIOS AT pH 5.0 AFTER 24 H. NOTE THAT THE pH OF THE EXPERIMENT WAS 7.0. THE SCALE BARS ARE THE SAME AND REPRESENT 20 µm.

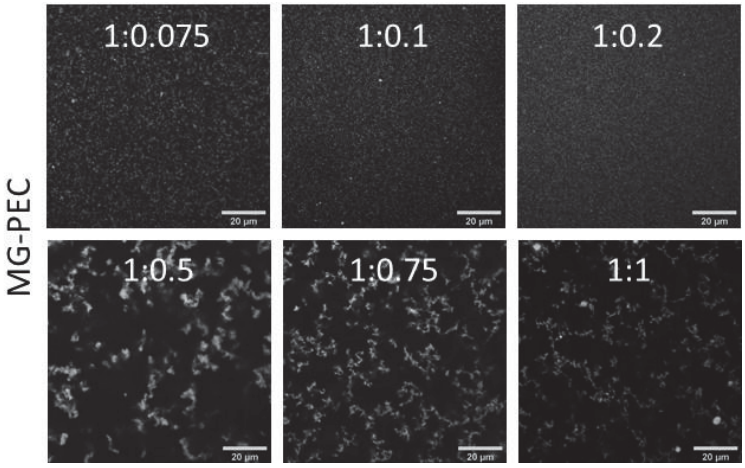

Similar results were found when ALG was used. Observing Figure 20 A and B it is possible to affirm that at higher MG:ALG ratios (1:1 and 1:0.75) the aggregates formed dominated the scattering, giving no trustworthy results for M_w, contrary to what was obtained for lower ratios. In contrast to the highest ratio investigated for PEC (1:0.075), the presence of ALG at the same ratio rendered controlled-sized particles (FIGURE 21). Curiously, when a lower protein:polysaccharide ratio of 1:1 and 1:0.75 was used, the curves did not superimpose over the initial particle profile at high q range, indicating a difference in the structure of the formed complexes. This observation was no further investigated.

FIGURE 20. DEPENDENCE OF THE SCATTERING VECTOR ON R/KC (A) AND ON R_h (B) FOR THE MIXTURE OF MG (1 wt%) AND ALG AT DIFFERENT CONCENTRATION RATIOS EXPRESSED ON THE FIGURES AFTER 24 AT pH 5.0.

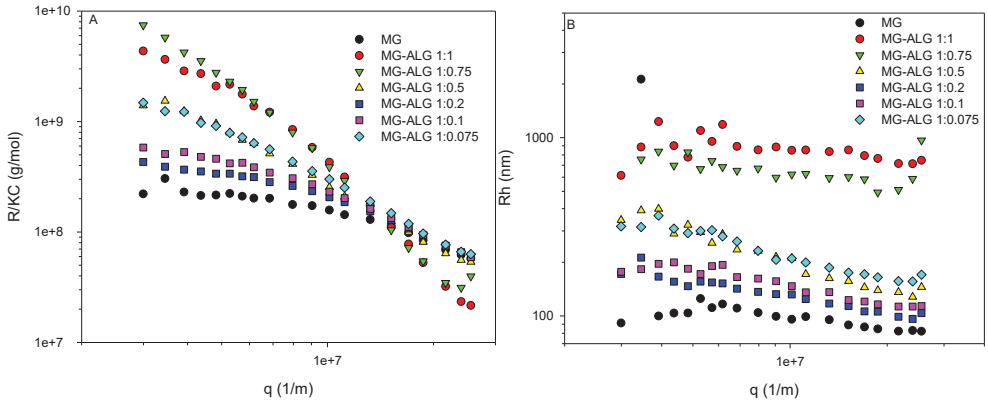

FIGURE 21. CLSM IMAGES OF AQUEOUS DISPERSIONS OF MG-ALG STRUCTURES AT 1 wt% FORMED AT DIFFERENT CONCENTRATION RATIOS AT PH 5.0 AFTER 24 H. NOTE THAT THE PH OF THE EXPERIMENT WAS 7.0. THE SCALE BARS ARE THE SAME AND REPRESENT 20μm.

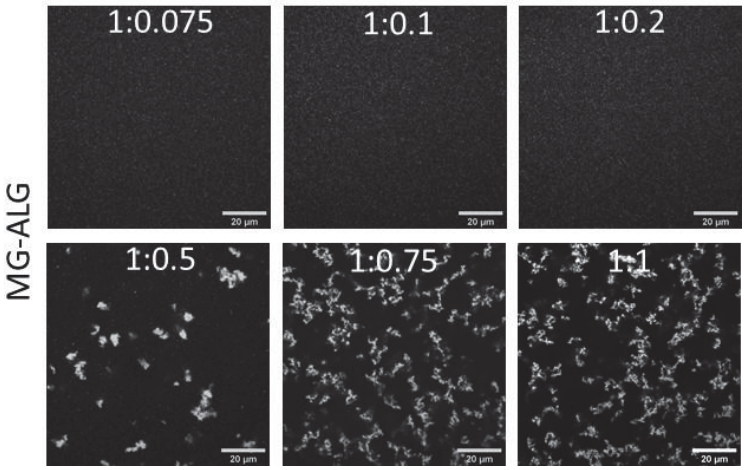

When KC was used, large-sized aggregates were formed at all protein:polysaccharide concentration ratios, as can be seen in Figure 22 and 23. These particles apparently remained aggregated even lowering the concentration to perform the light scattering experiment.

FIGURE 22. DEPENDENCE OF THE SCATTERING VECTOR ON R/KC (A) AND ON R_h (B) FOR THE MIXTURE OF MG (1 wt%) AND KC AT DIFFERENT CONCENTRATION RATIOS EXPRESSED ON THE FIGURES AFTER 24 AT pH 5.0.

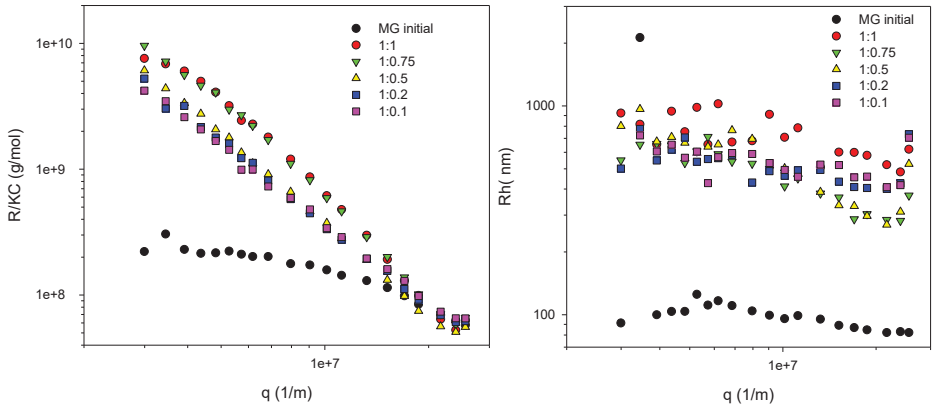

FIGURE 23. CLSM IMAGES OF AQUEOUS DISPERSIONS OF MG-KC STRUCTURES AT 1 wt% FORMED AT DIFFERENT CONCENTRATION RATIOS AT pH 5.0 AFTER 24 H. NOTE THAT THE pH OF THE EXPERIMENT WAS 7.0. THE SCALE BARS ARE THE SAME AND REPRESENT 20 μm.

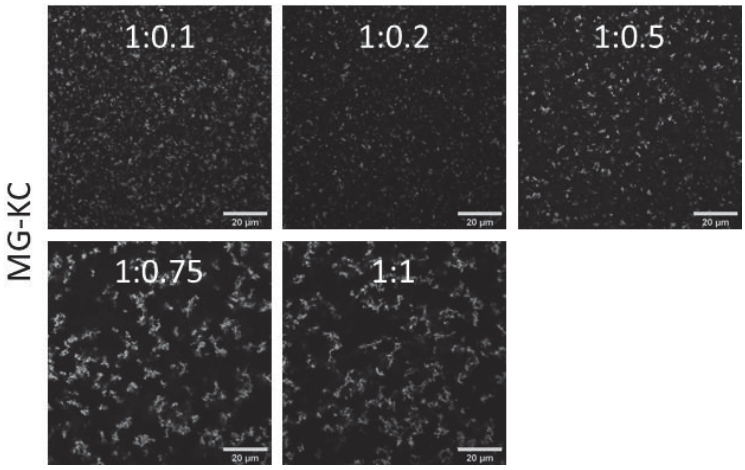

Then, the effect of time on the complexation was investigated for mixtures of MG with PEC, ALG, and KC at a fixed concentration ratio of 1:0.5. Figures 24, 26 and 28 show the light scattering results for the mixtures with PEC, ALG, and KC, respectively.

It can be seen by both the escalating increase in molar mass and R_h of the particles formed that the complexation is a progressive process that has its rate of reaction decreased substantially after approximately 10h. This is conceivable since the adsorbed layers should decrease the net charge density of the formed complex, hindering the electrostatic attraction with the polyelectrolyte in solution, until a surface saturation is observed.

FIGURE 24. DEPENDENCE OF THE SCATTERING VECTOR ON R/KC (A) AND R_h (B) FOR THE MIXTURE OF MG (1 wt%) AND PEC AT FIXED 1:0.5 CONCENTRATION RATIO AND AT DIFFERENT TIMES AT pH 5.0 EXPRESSED ON THE FIGURES.

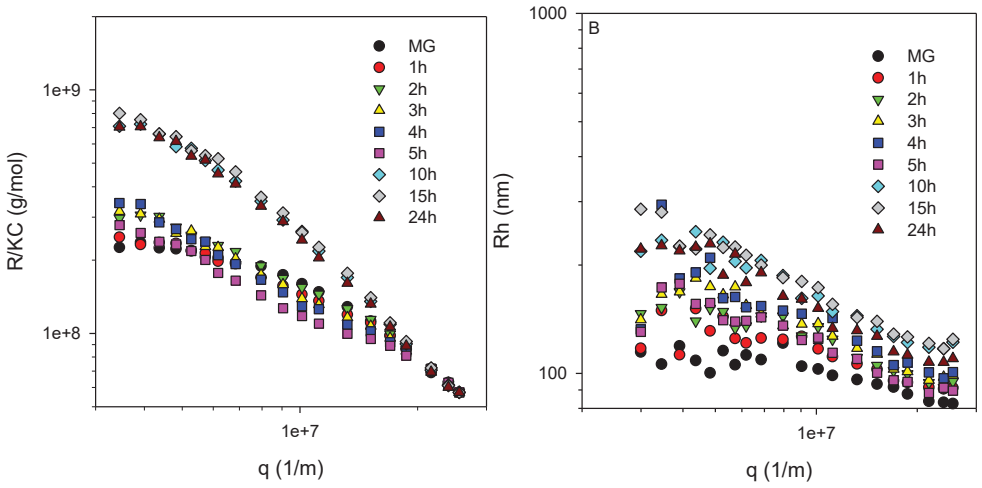

CLSM images for the mixtures with PEC (FIGURE 25) agreed with the light scattering results: a considerable increase in size was observed after 10 h of reaction. Whereas for the mixtures with ALG and KC (FIGURE 27 and 29, respectively), aggregates appeared independent on the time of reaction.

FIGURE 25. CLSM IMAGES OF AQUEOUS DISPERSIONS OF MG-PEC STRUCTURES AT 1 wt% FORMED AT A FIXED 1:0.5 CONCENTRATION RATIO AND AT DIFFERENT TIMES AT pH 5.0 EXPRESSED IN THE FIGURES. NOTE THAT THE pH OF THE EXPERIMENT WAS 7.0. THE SCALE BARS ARE THE SAME AND REPRESENT 20 µm.

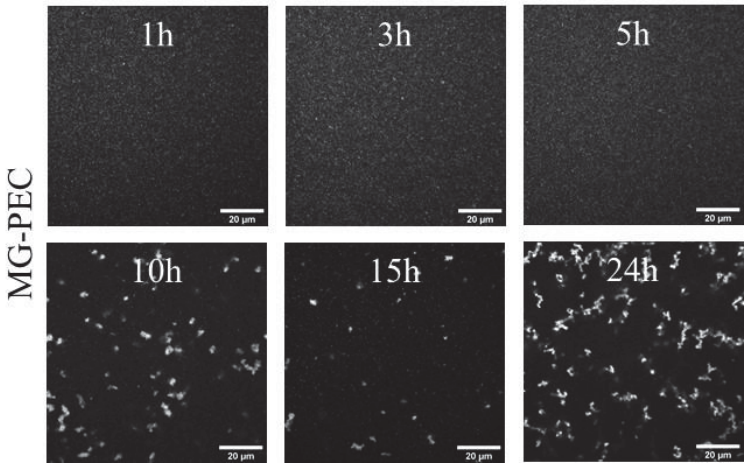

FIGURE 26. DEPENDENCE OF THE SCATTERING VECTOR ON R/KC (A) AND R_h (B) FOR THE MIXTURE OF MG (1 wt%) AND ALG AT FIXED 1:0.5 CONCENTRATION RATIO AND AT DIFFERENT TIMES AT pH 5.0 EXPRESSED ON THE FIGURES.

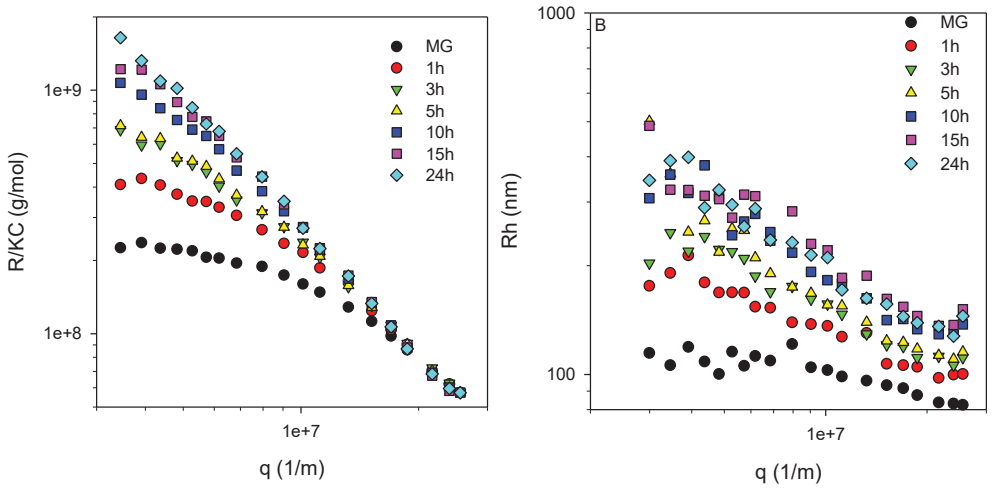

FIGURE 27. CLSM IMAGES OF AQUEOUS DISPERSIONS OF MG-ALG STRUCTURES AT 1 wt% FORMED AT A FIXED 1:0.5 CONCENTRATION RATIO AND AT DIFFERENT TIMES AT pH 5.0 EXPRESSED IN THE FIGURES. NOTE THAT THE pH OF THE EXPERIMENT WAS 7.0. THE SCALE BARS ARE THE SAME AND REPRESENT 20 µm.

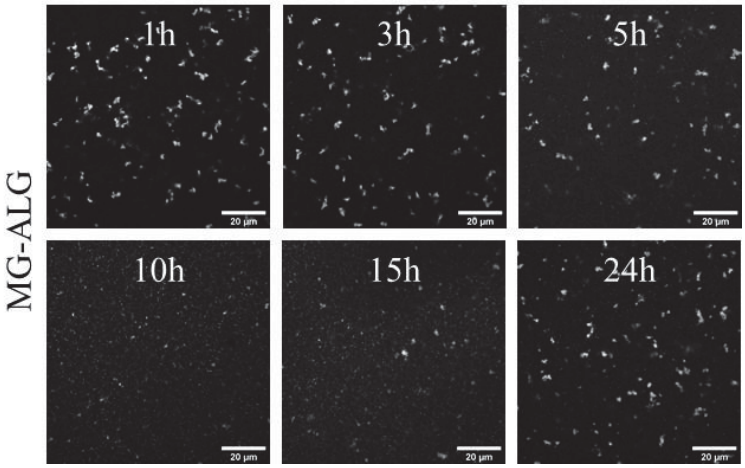

FIGURE 28. DEPENDENCE OF THE SCATTERING VECTOR ON R/KC (A) AND R_h (B) FOR THE MIXTURE OF MG (1 wt%) AND KC AT FIXED 1:0.5 CONCENTRATION RATIO AND AT DIFFERENT TIMES AT pH 5.0 EXPRESSED ON THE FIGURES.

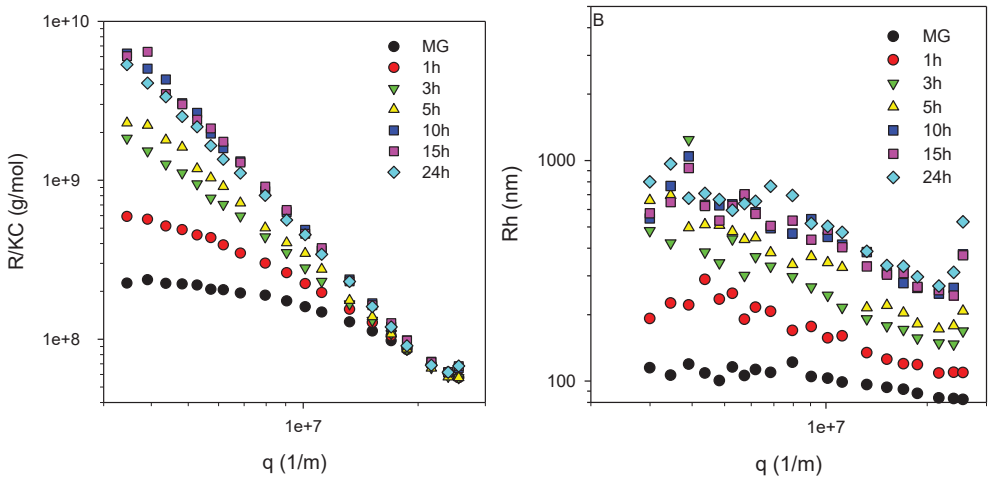

FIGURE 29. CLSM IMAGES OF AQUEOUS DISPERSIONS OF MG-KC STRUCTURES AT 1 wt% FORMED AT A FIXED 1:0.5 CONCENTRATION RATIO AND AT DIFFERENT TIMES AT pH 5.0 EXPRESSED IN THE FIGURES. NOTE THAT THE pH OF THE EXPERIMENT WAS 7.0. THE SCALE BARS ARE THE SAME AND REPRESENT 20 μm.

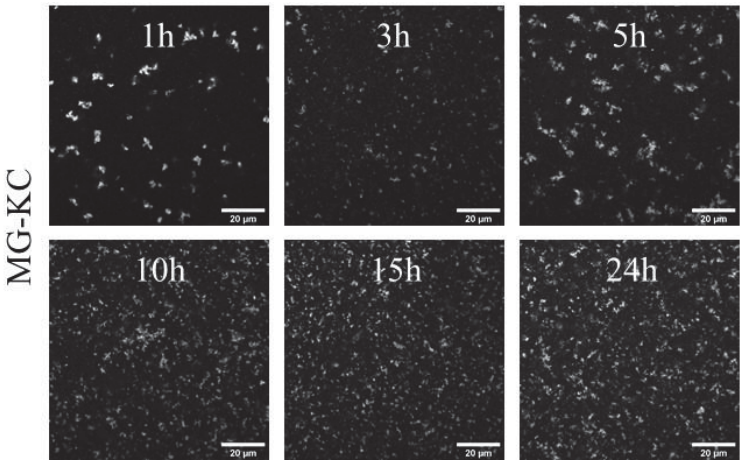

All the above-mentioned results suggest that one of the two following statements is occurring: The protein-polysaccharide complexes formed at pH 5.0 resist the further increase in pH, indicating that the electrostatic interactions become permanent if the system is kept for enough time at pH 5.0; or the irreversible aggregates of MG formed at pH 5.0 by the decrease of electrostatic repulsion the distinction between MG aggregates and complex is unavoidable by either LS or CLSM results. These hypotheses were investigated afterwards.

4.2.2 Application of the complexes in water-in-water emulsions

The complexes formed were used aiming stabilization in a not-yet investigated w/w emulsion composed of AMP and PUL. The phase diagram of PUL-AMP is shown in Figure 30. For this system, the critical point was situated at 2.8 wt % AMP and 2.1 wt % PUL. Two compositions were used to determine the tie-line, as indicated in Figure 17: 7.8 wt % AMP, 1.4 wt % PUL and 1.2 wt % AMP, 5.1 wt % PUL. Emulsions of PUL in AMP (P/A) and AMP in PUL (A/P) were studied along the same tie-line but at different Φ_{PUL}. At the tie-line studied, it was found about 0.8 wt% PUL in the AMP-rich phase, whereas the fraction of AMP in the PUL-rich phase was negligible.

FIGURE 30. PHASE DIAGRAM OF AQUEOUS MIXTURES OF AMP AND PUL. THE BINODAL (SOLID) AND THE 50:50 VOLUME FRACTION (DOTTED) LINE ARE SHOWN. THE SQUARES AND CIRCLES REPRESENT THE PHASE-SEPARATED AND HOMOGENEOUS SYSTEMS, RESPECTIVELY. THE LINE IN BETWEEN THEM REPRESENTS THE BINODAL. THE TRIANGLES REPRESENT THE SYSTEMS USED TO CALCULATE THE TIE-LINE STUDIED (DASHED).

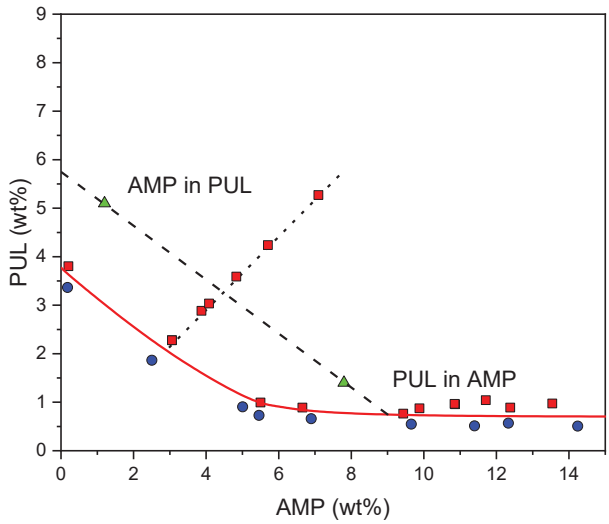

CLSM images of A/P emulsions at Φ_{PUL} = 0.75 and at pH 7.0 containing pure MG or complexes formed at different concentration ratios (1:0.2 and 1:0.5) are shown in Figure 31. The MG and the complexes formed at 1:0.2 concentration ratio preferred to reside in the PUL phase, and no interfacial adsorption was observed. Interestingly, at the concentration ratio of 1:0.5 a few particles were seen at the interface, except for MG-KC 1:0.5.

FIGURE 31. CLSM IMAGES OF A/P EMULSIONS AT Φ_{PUL} = 0.75 AT pH 7.0 WITH 0.1 wt% OF EITHER MG, MG-PEC, MG-ALG, OR MG-KC IN DIFFERENT CONCENTRATIONS RATIOS EXPRESSED IN THE IMAGES. THE SCALE REPRESENTS 20 µm.

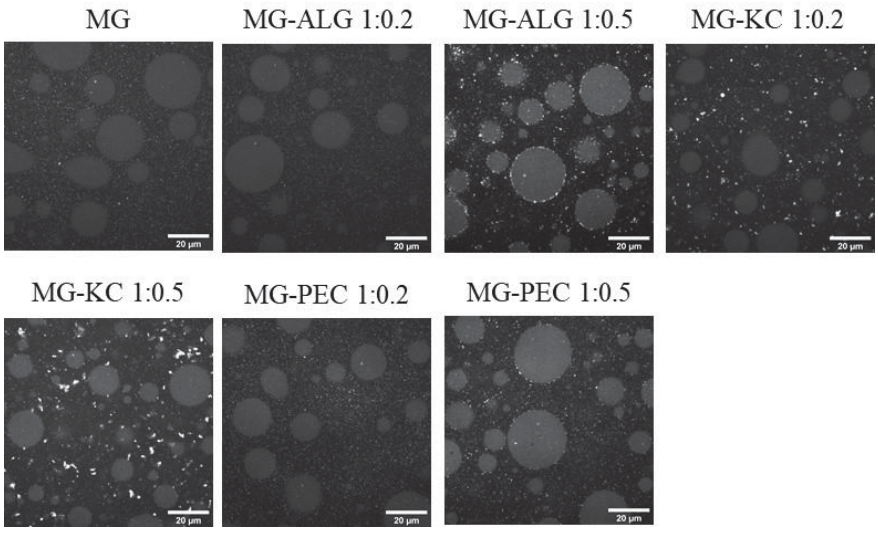

It can be seen in Figure 32 that at pH 5.0 and 4.0 the MG associate into large flocs which adhered to the interface, in agreement with the literature (GONZALEZ-JORDAN; BENYAHIA; NICOLAI, 2017). When the pH was further decreased to 4.0, they changed their wettability, and the flocs migrated towards the AMP phase. That is an interesting observation because it indicates that flocculation of the MG led to a surface change along with aggregation. Regarding the mixtures with polysaccharides, the particles seen at the interface at pH 7.0 have released it at pH < 5.5 and remained in the PUL phase down to pH 4.0. At 1:0.2 ratio, large aggregates were seen for all polysaccharides tested when the pH was set to 4.0, suggesting that there is a minimum amount of polysaccharide needed to hinder the MG flocculation.

So far, it was not clear whether the complexation between the MG and the polysaccharides that happened at pH 5.0 persisted after adjusting the pH to 7.0, as investigated during Section 4.1. Usually, complexes formed solely by electrostatic interactions have lower dissociation stability against changes in pH, salt concentration, or temperature when compared to heated-induced complexes formed through covalent binding between the two species, through the so-called Maillard reaction (GABER et al., 2018).

FIGURE 32. CLSM IMAGES OF A/P EMULSIONS AT Φ_{PUL} = 0.75 AT DIFFERENT pH 6.0, 5.5, 5.0, AND 4.0 WITH 0.1 wt% OF EITHER MG, MG-PEC, MG-ALG, OR MG-KC IN DIFFERENT CONCENTRATIONS RATIOS EXPRESSED IN THE IMAGES. THE SCALE REPRESENTS 20 μm.

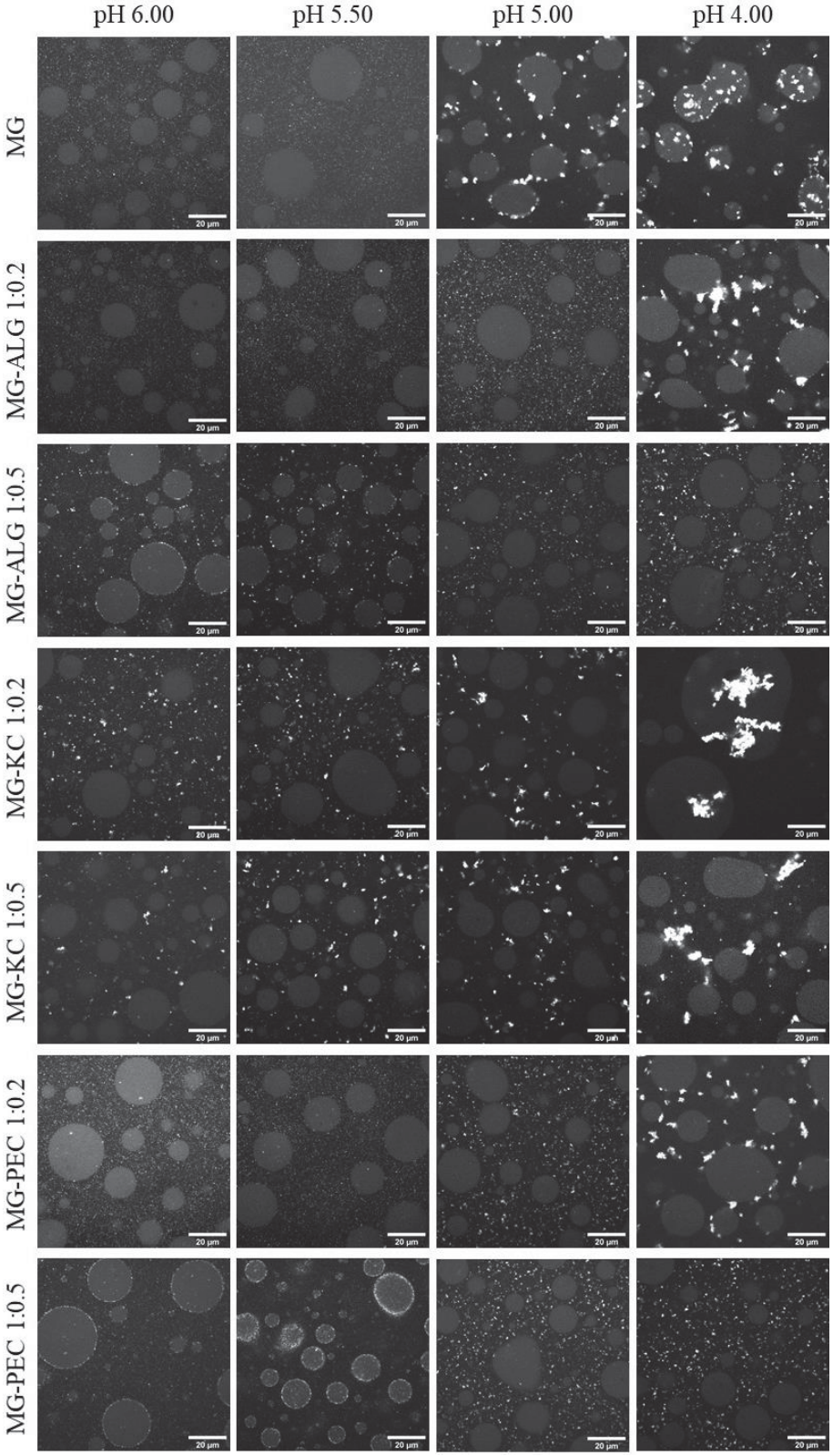

To visualize if the resulting particles after pH treatment were indeed complexes or only MG aggregates, observations were done in A/P emulsions with MG and by substituting the PEC with the FITC-labeled version, PEC-FITC.

Subsequent steps of the experiment are depicted as a scheme showing the complexation between 0.1 wt% MG and 0.05 wt% PEC-FITC (added as separated ingredients) in A/P emulsion (Φ_{PUL} =0.75) in Figure 33. Initially, only the MG are adsorbed at the interface and the excess is in the PUL phase (step 1). At pH 7.0, no attractive interaction is expected since the MG have a negative net charge as well as the PEC. At pH 5.0 (step 2), complexes are formed, as there is superposition of PEC-FITC and the MG signals, and these complexes are both in the continuous phase and at the interface. Remarkably, after 24 (step 3), the interfacial accumulation increases, and the droplets became stable against coalescence. When the system was diluted by a factor of 1.18 at pH 5.0 (step 4) the droplets as well as the complexes remained stable. However, when the pH was increased to 7.0 (step 5), the complexes dissociated and only the MG adhered to the interface, as seen initially.

Three striking observations should be highlighted here. First, the MG migrated towards the interface in the presence of 0.05 wt% PEC-FITC at pH 7.0, indicating that, although there is no specific interaction between the two negatively charged species, the presence of the latter altered the partition of the MG. Care should be taken that some unexpected interactions between proteins and anionic polymers carrying the same net charge can happening. It was seen that when the protein and the anionic branched polymer have the same negative charge, complexation may take place as the so-called positive “patches” that remained positive above the IEP of the protein start to interact with the negative groups of the polymer (DE VRIES, 2004; WITTEMANN; BALLAUFF, 2006). In this work, however, we did not intent to investigate this possibility.

Second, at pH 5.0, the adsorption of complexes at the interface increased with time, which eventually led to droplets’ stabilization. Third, the acid-induced complexation between MG and anionic polysaccharides is reversible even after 24 at pH 5.0, suggesting that the results obtained at Section 4.1 were artifacts due to a few flocs of MG that aggregated irreversibly. These findings motivated us to study the influence of adding a third non-interacting polysaccharide to the emulsions.

FIGURE 33. SCHEME OF THE COMPLEXATION BETWEEN 1 wt% MG AND 0.05 wt% PEC-FITC IN A/P EMULSIONS. SEVERAL STEPS ARE PRESENTED SHOWING THE PROCESSES THAT THE SYSTEM WENT THROUGH. ALL IMAGES AND INSERTS HAVE THE SAME DIMENSION 101 AND 25 μm, RESPECTIVELY. THE CONTRAST WAS ADJUSTED TO HELP THE VISUALIZATION. CARE WAS TAKEN TO ENSURE THAT THERE WAS NO INFLUENCE OF ONE FLUOROPHORE ON THE OTHER'S SIGNAL. SMALL AGGREGATES OF PEC-FITC WERE FOUND INSIDE THE AMP PHASE, BUT THEY DID NOT DISTURB THE EXPERIMENT.

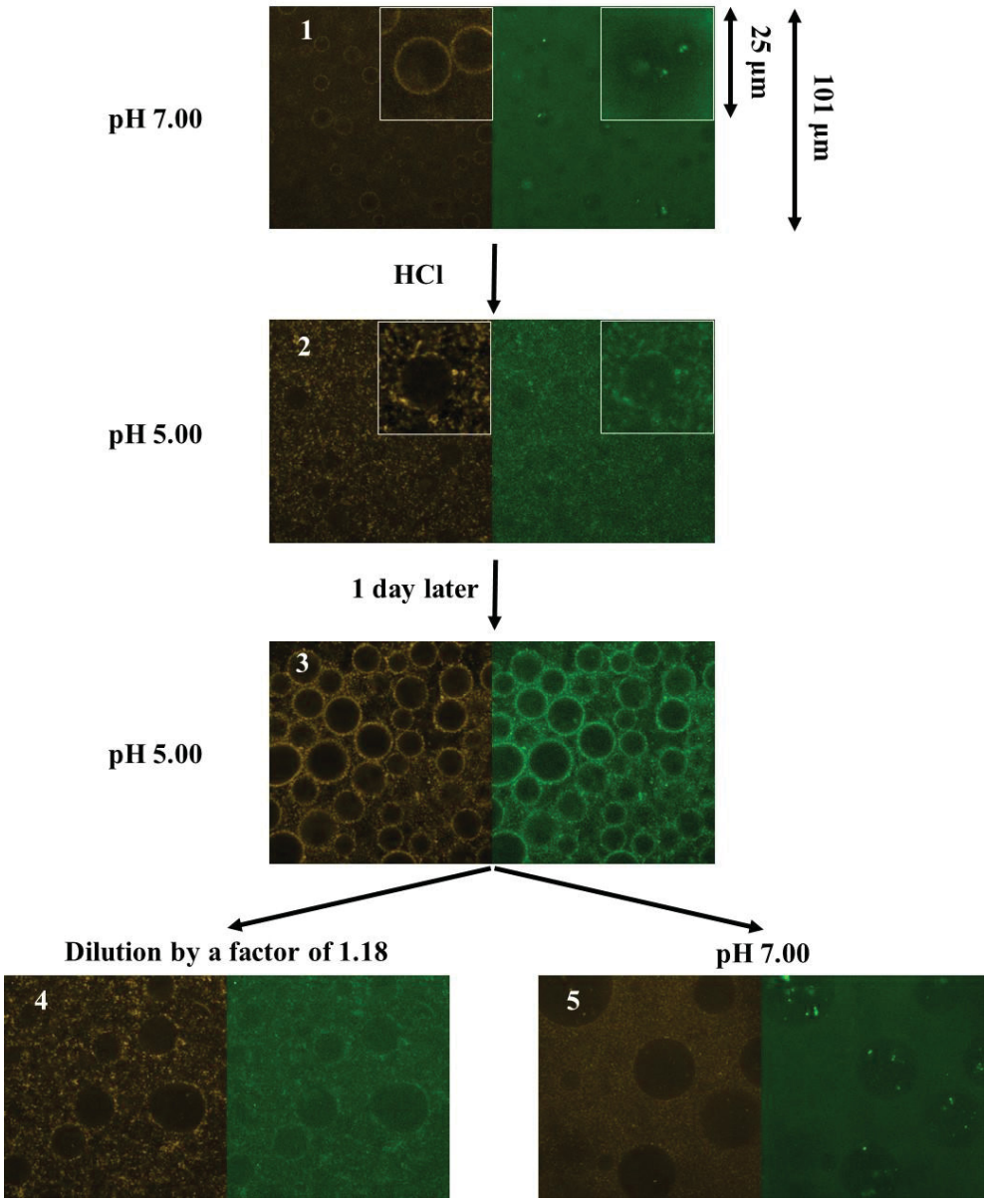

In summary, the complexation of the protein MG with anionic polysaccharides at pH 5.0 has happened by means of electrostatic interaction but the complexes dissociated when the pH was increased independently on how much time they stayed at pH 5.0. For

some reason which will be thoroughly studied in the next section, the presence of the anionic polysaccharide caused the MG to change their partition.

4.3 EFFECT OF ADDING A THIRD POLYSACCHARIDE TO WATER-IN-WATER EMULSIONS CONTAINING PROTEIN MICROGELS

This section will focus on the effect caused on the MG partition by adding different amounts of polysaccharides to the AMP-PUL emulsions. First, the effect of adding PEC was investigated in more detail. Then, the findings were extended to other situations to pursue generalization.

When MG were added to A/P or P/A emulsions, they did not adsorb at the interface but were situated mostly in the PUL phase. By adding PEC to the systems, the MG started to move to the interface, see Figure 34. At higher PEC concentrations (C_{PEC}) the excess MG were found in the AMP phase. The transition of the MG from PUL to the AMP were observed at both A/P and P/A emulsions but at different C_{PEC}. The MG were seen at the interface of A/P emulsions at 0.03 wt% $\leq C_{PEC} \leq$ 0.1 wt%, whereas for P/A emulsions at 0.005 wt% $\leq C_{PEC} \leq$ 0.02 wt%. At higher C_{PEC}, the MG preferred the AMP phase.

FIGURE 34. CLSM IMAGES OF FRESHLY PREPARED P/A AND A/P EMULSIONS AT Φ_{PUL} = 0.13 AND 0.87, RESPECTIVELY, CONTAINING 0.4 wt% MG AND DIFFERENT PEC CONCENTRATIONS AS INDICATED. ALL IMAGES ARE AT THE SAME SCALE, AND THE INSERTS ADDED TO SOME IMAGES REPRESENT ZOOMS (20 μm × 20 μm) OF A PART OF THE MAIN IMAGE.

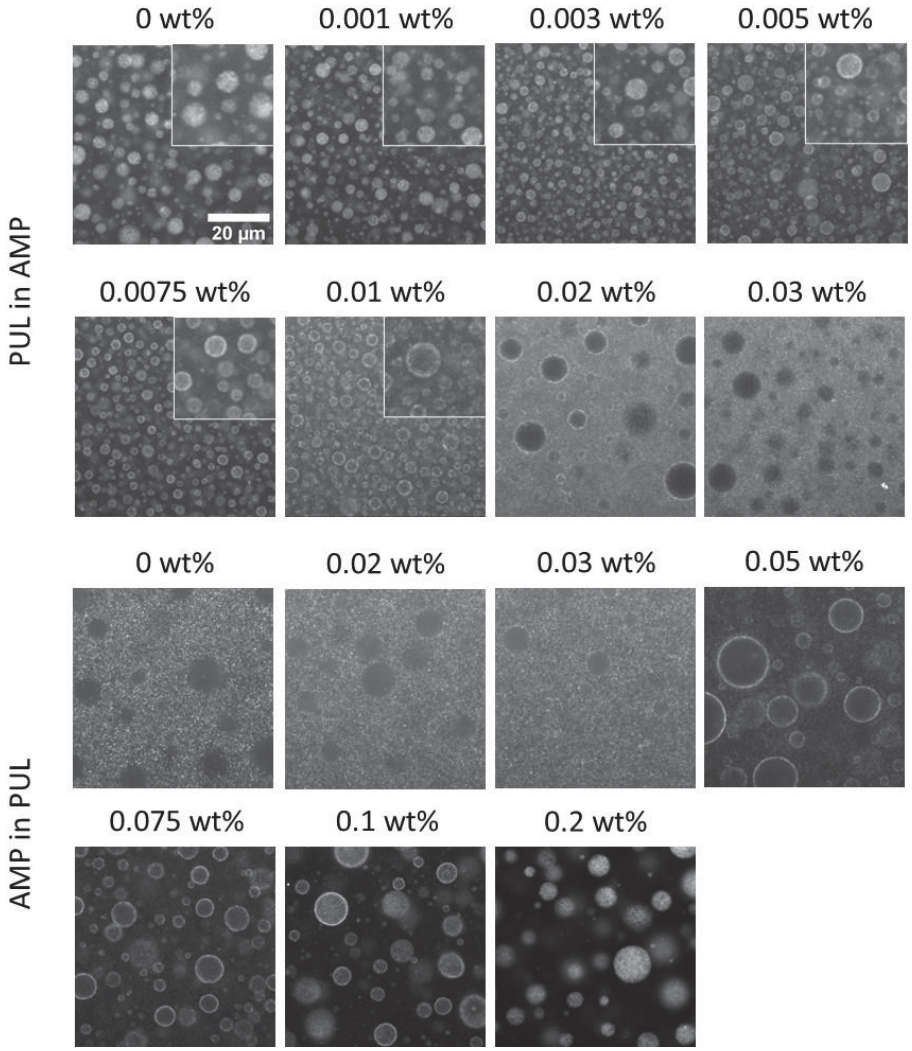

As the MG gave a turbid aspect to the phase in which they were dispersed, their transition from the PUL to the AMP phase could be observed after macroscopic phase separation (FIGURE 34). Notice that PUL solutions were transparent, whereas AMP solutions were opalescent due to the presence of a small amounts of large aggregates. A slight shift in the C_{PEC} necessary to cause the transition of the MG was noticed when RodB was used, see Figures 34 and 35. In P/A emulsions, the transition happened between 0.005 – 0.0075 wt% in the absence of RodB, whereas it happened between 0.01 – 0.02 wt% when it was added.

FIGURE 35. MACROSCOPIC PHASE SEPARATION SAMPLES OF P/A (Φ_{PUL} = 0.13) AND A/P (Φ_{PUL} = 0.87) EMULSIONS CONTAINING 0.4 wt% MG AND DIFFERENT PEC CONCENTRATIONS AS INDICATED IN THE FIGURE.

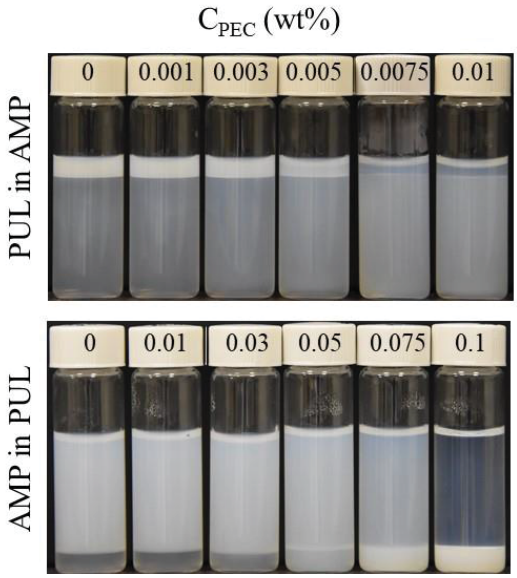

The ratio of the MG concentration in the AMP phase over that in the PUL phase ($R_{[MG]}$) as a function of both C_{PEC} and Φ_{PUL} was determined from the absorbance at a wavelength of 278 nm of both phases in the absence of RodB. Figure 36 shows that the change of the partition of the MG between the PUL to the AMP phases happened progressively with increasing C_{PEC} and the concentration where $R_{[MG]} = 1$ depended on Φ_{PUL}.

FIGURE 36. $R_{[MG]}$ AS A FUNCTION OF C_{PEC} FOR EMULSIONS AT 3 DIFFERENT Φ_{PUL} AS INDICATED IN THE FIGURE. THE SOLID LINES ARE GUIDES TO THE EYE.

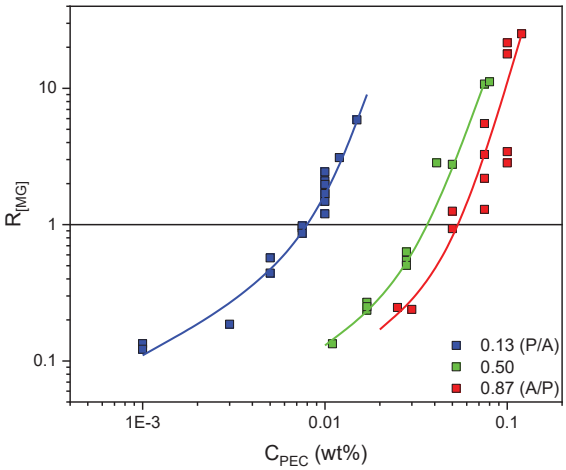

As discussed in the introduction, it was expected that MG should spontaneously adsorb at the interface when $\gamma_{PUL\text{-}AMP} > |\gamma_{MG\text{-}PUL} - \gamma_{MG\text{-}AMP}|$. The observation that MG adsorbed

at the interface when PEC was added implies that the term $\gamma_{PUL-AMP}$ increased and/or $|\gamma_{MG-PUL}-\gamma_{MG-AMP}|$ decreased. Initially, the term γ_{MG-PUL} starts to increase with the addition of PEC, causing a decrease in the term $|\gamma_{MG-PUL}-\gamma_{MG-AMP}|$ until $R_{[MG]} = 1$, when $\gamma_{MG-AMP} = \gamma_{MG-PUL}$. Further increase of C_{PEC} increased once more $|\gamma_{MG-PUL}-\gamma_{MG-AMP}|$, but now the left-hand term becomes higher than the right-hand one. At high C_{PEC}, the term $|\gamma_{MG-PUL}-\gamma_{MG-AMP}|$ became again larger than $\gamma_{PUL-AMP}$ so that MG no longer adsorbed at the interface. Whatever is the effect of PEC on $\gamma_{PUL-AMP}$, the fact that MG do not adsorb at high PEC concentrations shows that it does not increase as much as γ_{MG-AMP}.

Following this discussion, another consequence of tuning the system such that $R_{[MG]} = 1$ is the following: when there is no preference for the particles to reside in either phase, they should remain at the interface as long as there is appreciable phase separation between both phases, i.e. as long as $\gamma_{AB} > 0$. This hypothesis was tested by diluting an A/P emulsion in the presence of 0.06 wt% PEC where $R_{[MG]} \approx 1$ and $|\gamma_{PA}-\gamma_{PB}|$ is close to zero and it was found that indeed MG remained at the interface even very close to the binodal (FIGURES 37 and 38).

FIGURE 37. CLOSE-UP ON THE PHASE DIAGRAM BETWEEN AMP-PUL MIXTURE AT DIFFERENT DILUTION FACTORS. THE INITIAL COMPOSITION OF A/P EMULSION WAS 1.2 wt % AMP AND 5.1 wt % PUL. THE EXPERIMENT WAS PERFORMED AT $R \approx 1$ (C_{PEC} = 0.5 wt%).

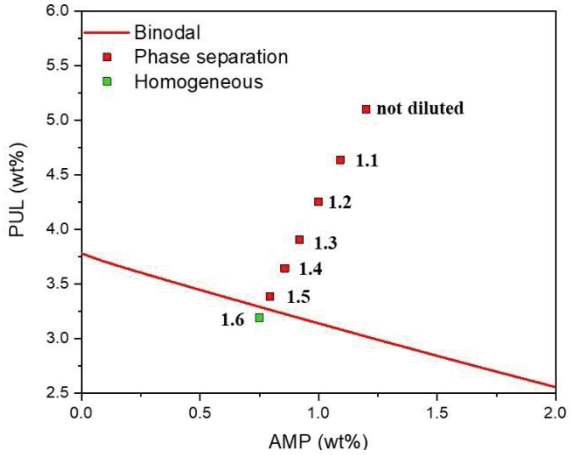

FIGURE 38. CLSM IMAGES OF A/P EMULSIONS WITH 0.4 wt% MG AS A FUNCTION OF THE DILUTION FACTOR PRESENTED IN FIGURE 24. ALL IMAGES ARE ON THE SAME SCALE. THE COMPOSITION OF THE UNDILUTED EMULSION WAS 1.2 wt % AMP AND 5.1 wt % PUL.

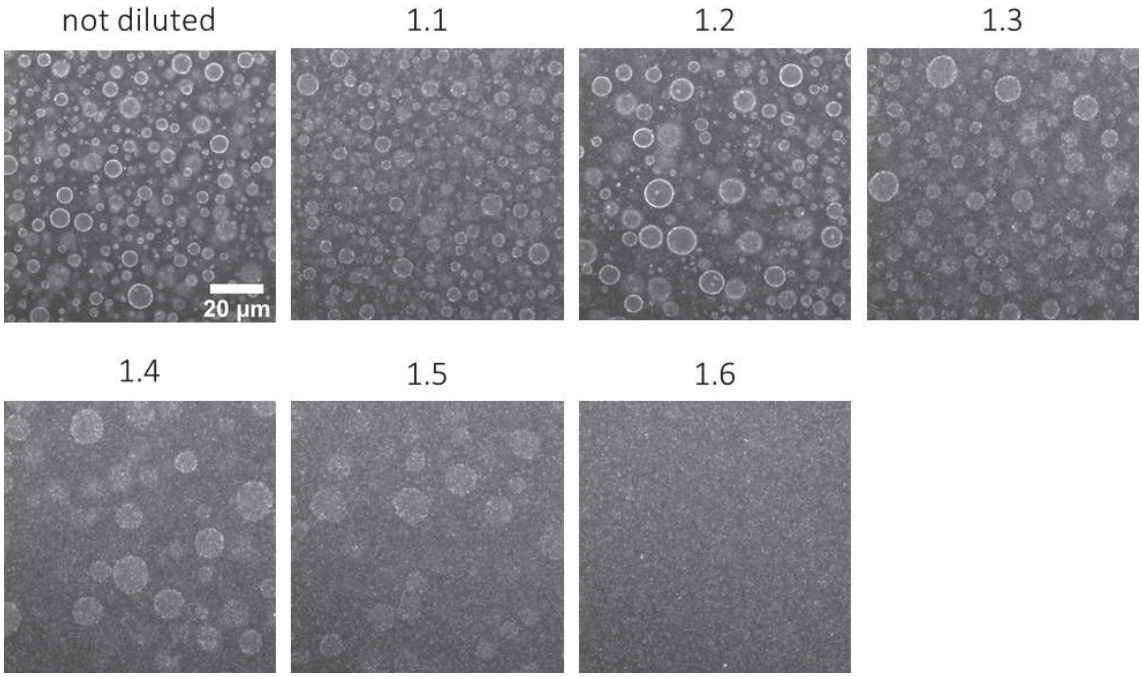

When PEC was substituted by ALG or KC, similar effects on the partition of the MG were observed, see Figure 39.

The transition of the MG from the PUL phase to the AMP phase occurred approximately at the same concentration for the three anionic polysaccharides. Also, it is expected that the factor controlling the transition of the MG depends on the concentration of PEC in PUL and not the total PEC concentration, since it prefers PUL over AMP (see Figure 33). Thus, it can be shown in Figure 40 that by multiplying the PEC concentration by the volume fraction of PUL it is possible to superimpose the data from Figure 36.

FIGURE 39. CLSM IMAGES OF FRESHLY PREPARED P/A (Φ_{PUL} = 0.13) AND A/P (Φ_{PUL} = 0.87) EMULSIONS IN THE PRESENCE OF 0.4 wt% MG AND DIFFERENT ALG AND KC CONCENTRATIONS AS INDICATED IN THE FIGURE. ALL IMAGES ARE AT THE SAME SCALE.

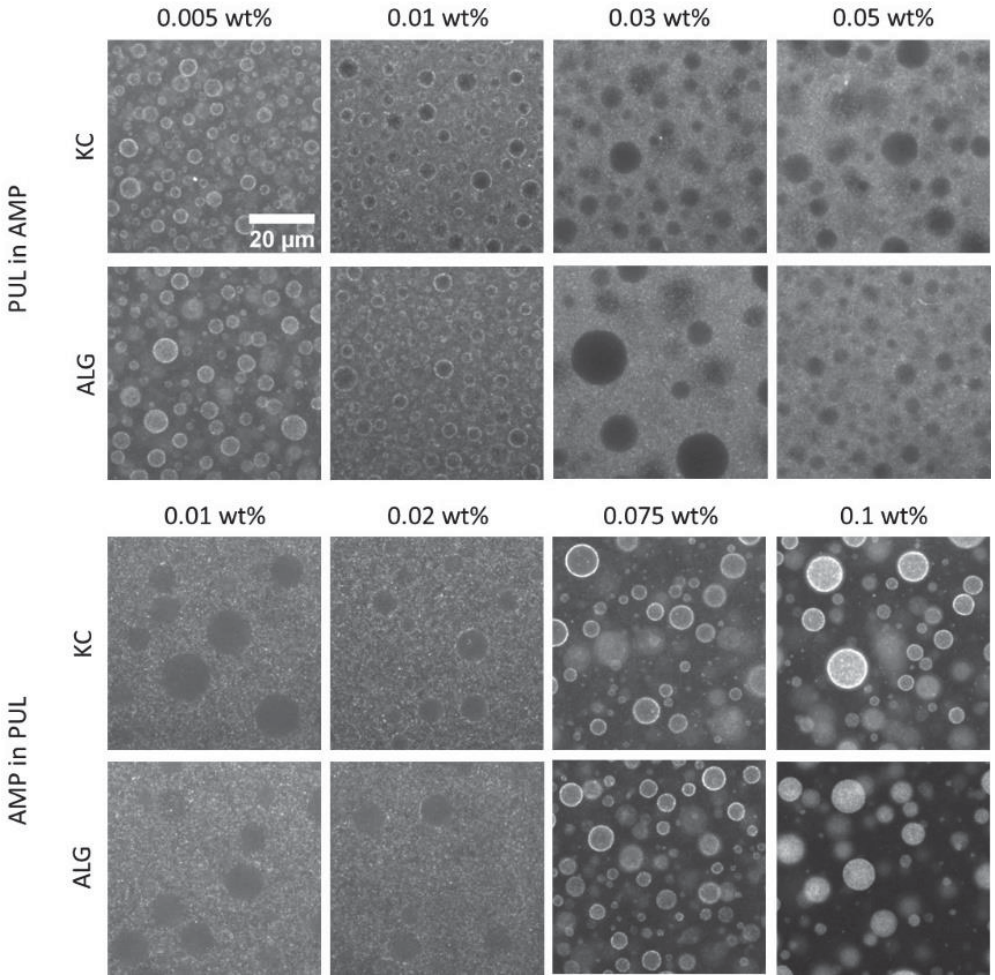

FIGURE 40. THE RATIO OF THE MG CONCENTRATIONS (R) IN THE AMP AND PUL PHASES AS A FUNCTION OF C_{PEC} FOR EMULSIONS AT 3 DIFFERENT Φ_{PUL} AS INDICATED IN THE FIGURE. THE SOLID LINES ARE GUIDES TO THE EYE.

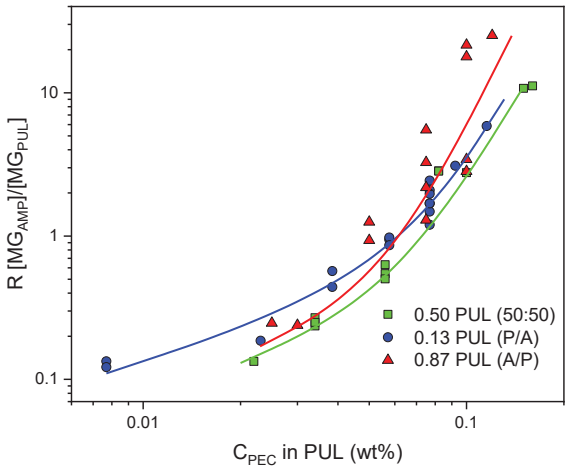

At this point, one may ask whether the transition was occurring due to the negative charges on the polysaccharides, which were causing an electrostatic repulsion with the net negative charges on the surface of the MG. To address this question, the anionic polysaccharides (KC, ALG and PEC) were substituted by xyloglucan which is expected to be nonionic. Again, very comparable results were seen, except that the concentration needed to induce the transition was higher than that for the anionic polysaccharides (FIGURE 41). For XG, the transition happened between 0.2 and 0.5 wt% and between 0.1 and 0.2 wt% for the A/P and P/A emulsions, respectively. Notice that mixtures of XG and AMP phase separate only at higher polymer concentrations than those used here. In phase separated mixtures of XG and AMP, MG prefers to reside in the AMP phase from pH 7.0 until pH 5.0. At lower pH, the MG changed the preference towards the XG (DE FREITAS et al., 2016; HAZT et al., 2020). Therefore, it is likely that XG entered the PUL phase in AMP-PUL emulsions rendering it less compatible for the MG and, thereby, driving the MG towards the AMP phase.

FIGURE 41. CLSM IMAGES OF A/P (Φ_{PUL} = 0.13) AND P/A (Φ_{PUL} = 0.87) EMULSIONS WITH 0.4 wt% MG AND DIFFERENT XG CONCENTRATIONS. ALL IMAGES ARE ON THE SAME SCALE.

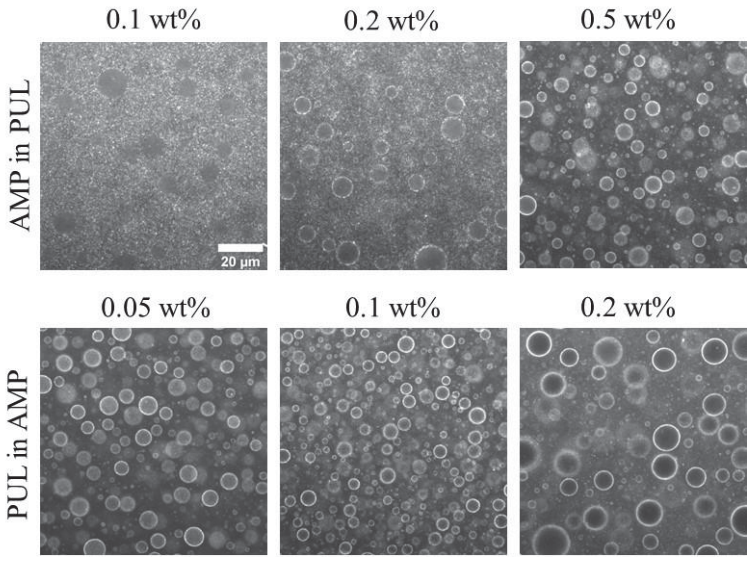

The phenomenon observed in PUL-AMP emulsions was extended to another emulsion of DX-AMP, where the MG partitioned preferentially to the DX in the absence of the third polysaccharide. Adding PEC led to adsorption of the MG at the interface, and at larger PEC concentrations drove the MG to the AMP phase (FIGURES 42 and 43).

FIGURE 42. MACROSCOPIC PHASE-SEPARATED MIXTURES OF AMP IN DX AND DX IN AMP EMULSIONS (DISPERSED PHASE VOLUME FRACTION EQUALS TO 0.25) WITH 0.4 wt% MG AT DIFFERENT PEC CONCENTRATIONS AS INDICATED IN THE FIGURE.

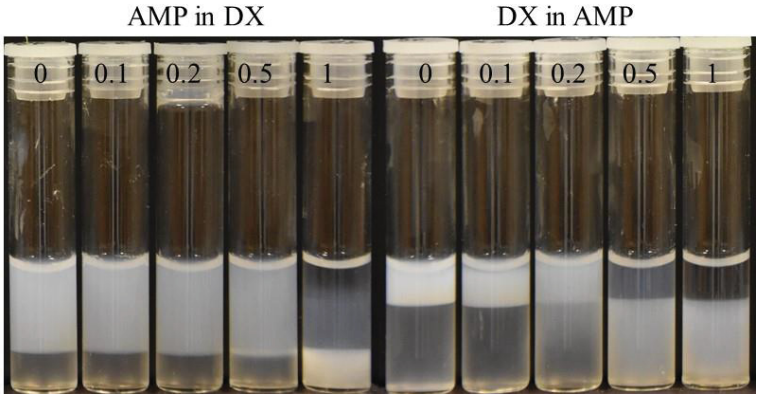

FIGURE 43. CLSM IMAGES OF FRESH EMULSIONS OF AMP AND DEX IN THE PRESENCE OF 0.4 wt% MG, AND AT DIFFERENT PEC CONCENTRATIONS AS INDICATED IN THE FIGURE. ALL IMAGES ARE AT THE SAME SCALE.

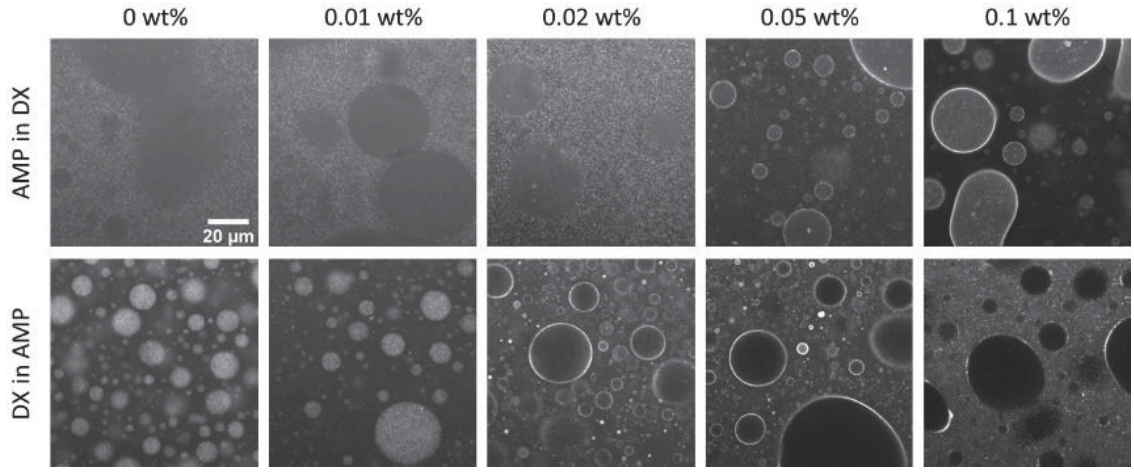

Finally, to investigate the possibility to fine-tune the positioning of other particles in w/w emulsions, cellulose nanocrystals (CNC) were added instead of MG in AMP-PUL emulsions. The partition was monitored as a function of C_{PEC} (FIGURE 44). Although the contrast was faint, it is possible to see the migration of the cellulose nanocrystals from the PUL phase to the interface and the AMP phase.

FIGURE 44. CLSM IMAGES OF A/P EMULSIONS WITH 0.2 wt% CNC WITHOUT PEC (LEFT), 0.11 wt% PEC (MIDDLE) AND 0.8 wt% PEC (RIGHT). THE CONTRAST WAS ENHANCED TO FACILITATE VISUALIZATION. THE BRIGHTNESS ARE DUE TO THE 5 ppm NB USED TO LABEL THE CNC. ALL IMAGES ARE AT THE SAME SCALE.

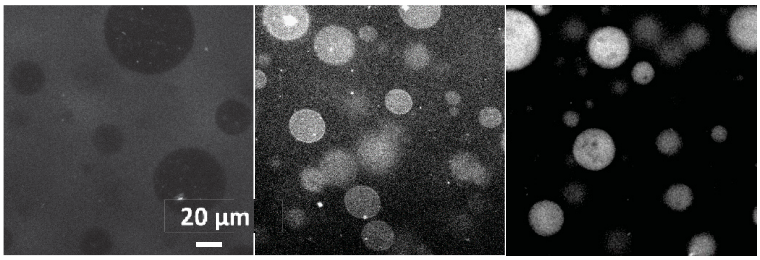

It appears that the modulation of the partition of particles due to the addition of a third non-interacting component that is miscible with one or both phases is quite general. It is suggested that the effect is caused by subtle changes in the interfacial tension between the particles and the phases. This change can be induced in two ways: either by adding a component that has a higher affinity for the particle and that partitions to the phase that had lower particle concentration, therefore pulling them or by adding a component that has a lower affinity for the particles and that partitions to the phase that had a higher affinity for them, pushing them. The latter was the case here as all the added polysaccharides preferred the PUL phase. By fine-tuning the addition of the component so that the particles partition equally to both phases, it is possible to maintain the particles at the interface even very close to the binodal. It should be noticed that specific interactions can change completely the partition of the solid particle, as one would expect when using for instance XG to change the partition of CNC in w/w emulsions. Although it is an interaction between a charged and a non-charged component, precise sites of the XG backbone appears to interact through van der Waals interactions and hydrogen bonds forming a combined network with CNC, which would change completely the concept generalized in this part of the work (DAMMAK et al., 2015; VILLARES et al., 2015).

Briefly, this section has shown that the presence of a polymer that has no apparent specific interaction with solid particles can nevertheless modulate their partition in w/w emulsions. Apparently, the net interaction of this third soluble component depends partially on its own charge, but is not limited to it, as it was shown that a neutral polysaccharide could modulate and control the positioning of MG in the emulsion of AMP-PUL. Perhaps, since PEC preferred to reside mostly in the PUL phase as well as the particles in the absence of PEC, there may be some depletion effect caused by the presence of another polymeric

component within the same environment as the MG particles (FLEER et al., 1998; JENKINS; SNOWDEN, 1996). This could cause the particles to be expelled from the PUL phase towards a more thermodynamically favorable environment.

Sadly, all the w/w emulsions studied thus far were unstable and phase separated even when the particles were preferentially at the interface. In the next section, methods to induce the gelation of the MG will be explored seeking the stabilization of emulsions of AMP and PUL.

4.4 EFFECT OF pH ON THE MICROSTRUCTURE OF AMYLOPECTIN-PULLULAN EMULSIONS IN THE PRESENCE OF MICROGELS

4.4.1 Acidification while vortexing

Since no stabilization against coalescence was observed in the previous sections even though it was possible to tune the adsorption of most of the particles at the interface, a different approach aiming the stabilization was investigated. To start the discussion of the effect of the pH on the stability, MG were applied in A/P emulsions in the absence of any other polysaccharide added (FIGURE 45).

FIGURE 45. CLSM IMAGES OF A/P EMULSIONS IN THE PRESENCE OF 0.4 wt% MG AT DIFFERENT pH SHOWN IN THE FIGURE. THE FLUORESCENCE FROM THE LABELLED MG IS SHOWN IN WHITE. THE TOP AND THE BOTTOM ROWS CORRESPOND, RESPECTIVELY, TO IMAGES TAKEN JUST AFTER PREPARATION AND 1 WEEK LATER. ALL IMAGES ARE ON THE SAME SCALE (101 μm × 101 μm). NOTE THAT THE IMAGES AT pH 7.0, 5.6, AND 3.5 WERE TAKEN AT THE INTERFACE BETWEEN THE TWO MACROSCOPIC PHASES.

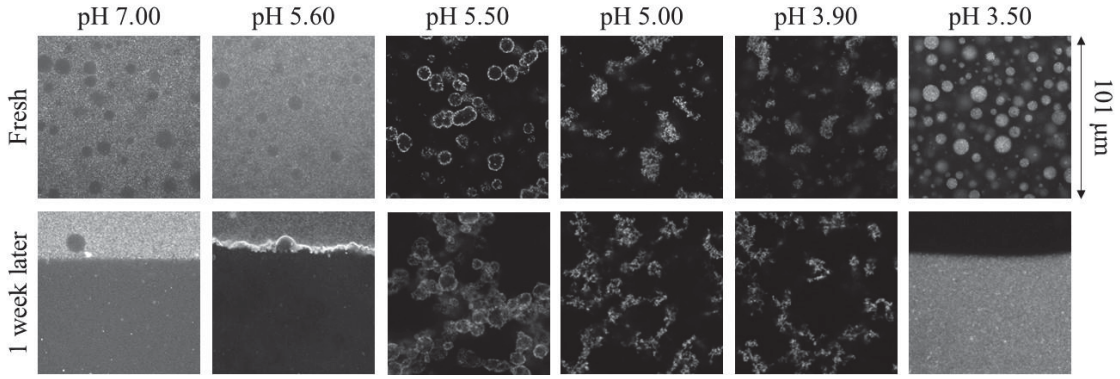

It was found that the pH influenced the partition of the MG in the absence of added polysaccharides, see Figure 46. At pH 7.0, the MG resided at the PUL phase completely, whereas, with decreasing pH from pH 5.5, they started to aggregate and migrate towards the interface and the AMP phase. Eventually, at pH 3.5, they partitioned completely to the AMP phase. This effect occurred possibly due to an increased hydrophobicity of the MG with decreasing pH. It is not clear whether the change in the net charge density of the MG (IEP = 5.0) had an effect considering that PUL and AMP are neutral. It is worth mentioning that at pH 3.5, the MG were no longer aggregated and were presented as individual particles.

FIGURE 46. CLSM IMAGES OF P/A EMULSIONS IN THE PRESENCE OF 0.4 wt% MG AT DIFFERENT pH INDICATED IN THE FIGURE. THE TOP AND THE BOTTOM ROWS CORRESPOND, RESPECTIVELY, TO IMAGES TAKEN JUST AFTER PREPARATION AND 1 WEEK LATER. NOTE THAT THE IMAGES AT pH 7.0, 5.9, AND 3.5 AFTER ONE WEEK WERE TAKEN AT THE INTERFACE BETWEEN THE TWO MACROSCOPIC PHASES. ALL IMAGES ARE ON THE SAME SCALE (101 μm × 101 μm).

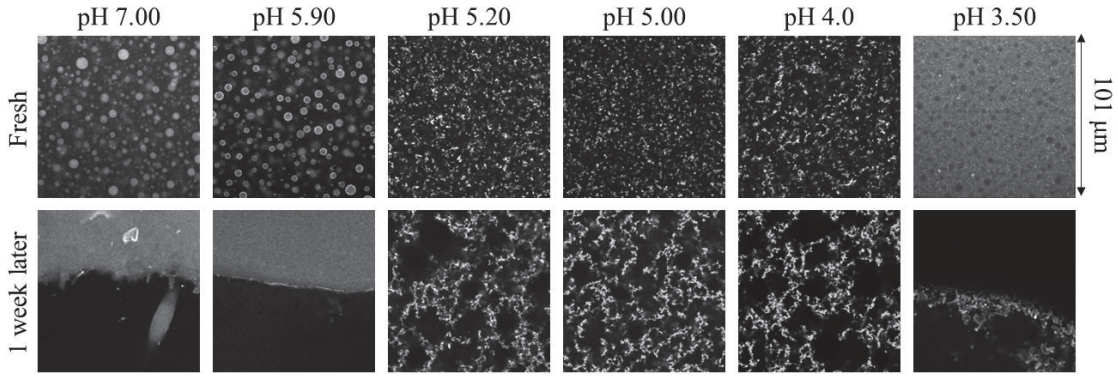

4.4.2 Acidification under quiescent conditions

The use of GDL allows one to follow the influence of pH decrease *in-situ* on the microstructure of the emulsion, as seen in Figure 47. The MG initially dispersed as individual particles in the continuous PUL phase started to form aggregates close to pH 5.5 and subsequently adhered irreversibly at the interface of the droplets as small clusters. Curiously, the interfacial adsorption did not prevent droplets from coalescing, resulting in macroscopic phase separation when pH 5.0 was reached (FIGURE 48). If more GDL was added initially, seeking a rapid formation of a gelled MG layer at the interface (final pH ~3.7), the clusters of MG flocculated into large regions.

The resulting microstructure for P/A emulsions when GDL was used to reduce the pH was considerably different from those using HCl, see Figure 48. The MG, initially at the

dispersed PUL phase, adhered at the interface protecting relatively small droplets (around 10 μm) and formed a strong gelled layer that prevent coalescence for at least 1 week. After this one week no sedimentation was observed.

FIGURE 47. CLSM IMAGES OF A/P EMULSIONS WITH 0.4 WT% MG AT DIFFERENT pH VALUES DUE TO THE USE OF GDL AS EXPRESSED IN THE IMAGES. ALL IMAGES ARE AT THE SAME SCALE (50 μm × 50 μm).

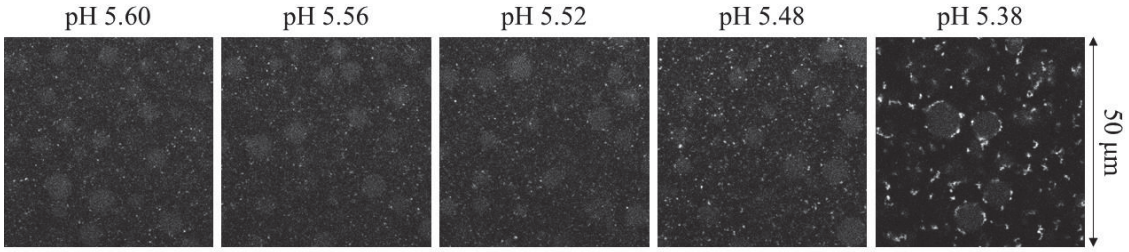

The remarkable difference in behavior between A/P and P/A emulsions relies on the fact that in the latter system the MG are confined inside the droplets, rendering it more easily the migration towards the interface. Another argument can be made regarding the viscosity of the AMP phase which is approximately 10 times higher than that of the PUL phase (APPENDIX V).

FIGURE 48. CLSM IMAGE OF A/P AND P/A EMULSIONS WITH 0.4 wt% MG ONE WEEK AFTER ADDING GDL.

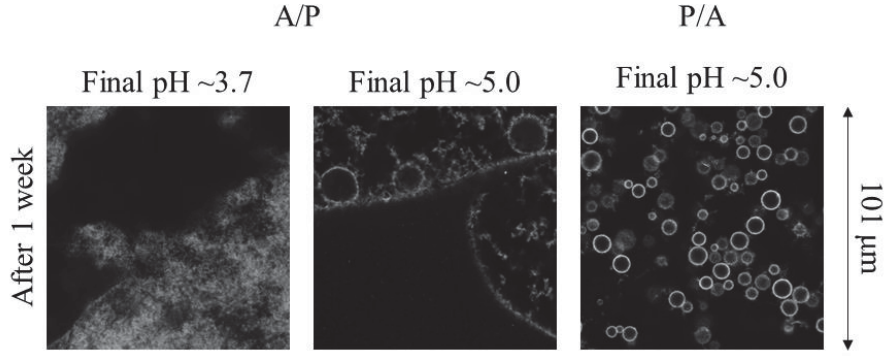

4.4.3 Impact of polysaccharides on the acidification under vortexing

When ALG was added to the emulsions, the partition as a function of the pH was also changed, see Figure 49. As previously explained in section 4.2, MG were at the interface and the excess was in the PUL phase in between pH 7.0 and 5.6. When the pH was further

decreased to pH 5.0, the amount of MG adsorbed at the interface decrease as they migrated towards the PUL phase, contrary to what was seen when no ALG was added. The change between pH 5.6 and 5.5 can be explained by the fact that complexation between MG and ALG started close to pH 5.6 and, since the ALG preferred the PUL phase, the complexes are expected to reside in that phase preferentially. This argument endorses the observation that no clusters of MG were seen at this pH range.

At pH 5.6 and higher, macroscopic phase separation was observed after 1 week, whereas sedimented droplets were seen when the pH was set between 5.5 and 5.0 (FIGURE 49). These droplets appeared to be bigger than the ones seen in the fresh emulsion, indicating that coalescence was slowed, which was investigated in greater detail, see Figure 50.

FIGURE 49. CLSM IMAGES OF A/P EMULSIONS WITH 0.05 wt% ALG AND 0.4 wt% MG AT DIFFERENT pH AS INDICATED IN THE FIGURE. THE TOP AND THE BOTTOM ROWS CORRESPOND, RESPECTIVELY, TO IMAGES TAKEN JUST AFTER PREPARATION AND 1 WEEK LATER. NOTE THAT THE IMAGES AT pH 7.0 AND 5.6 AFTER ONE WEEK WERE TAKEN AT THE INTERFACE BETWEEN THE TWO MACROSCOPIC PHASES AND THAT THE SCALE IS NOT THE SAME FOR THE IMAGES IN THE TOP AND BOTTOM ROWS.

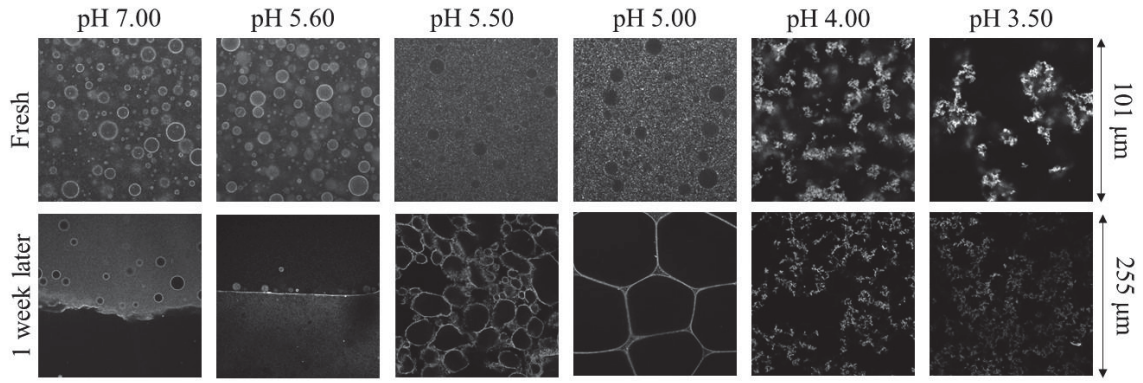

After setting the pH to 5.0, CLSM images were taken as a function of time to follow the formation of the microstructure seen in Figure 50. 2 h after preparation, the accumulation of MG is more clearly seen at the interface. After 4 h, the coalescence was slowed considerably and the droplets sedimented, and after 1 week the droplets grown due to late stages of coalescence.

This shows that the complexes formed at the PUL rich phase slowly decrease the rate of coalescence as they interact at the interface with each other. It can be argued thus that if the complexes were formed in the PUL phase previously to the addition of AMP to form the emulsion, the rate of coalescence would be reduced such that the droplets would be

smaller after 1 week. This statement was tested by letting the MG and the ALG complex in the PUL phase for 24 h at pH 5.0. Then, the AMP was added, and the system was emulsified. However, the emulsion destabilized within the first 24 h after preparation.

FIGURE 50. CLSM IMAGES SHOWING THE EVOLUTION WITH TIME OF A/P EMULSIONS WITH 0.4 wt% MG AND 0.05 wt% ALG AT pH 5.0. ALL IMAGES ARE ON THE SAME SCALE (255 μm × 255 μm).

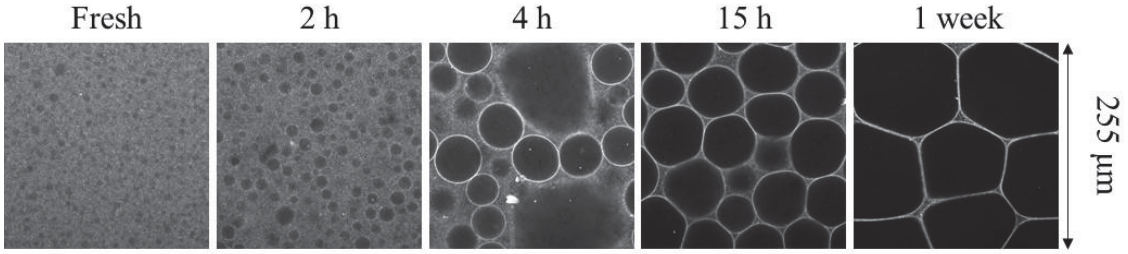

Figure 51 shows the effect of varying the ALG concentration at pH 5.0. In the presence of 0.03 wt% ALG amount investigated, the complexes aggregated rapidly and adhered to the interface in the form of clusters, similarly to the results found in the absence of ALG. At lower concentrations, the clusters did not migrate to the interface. When 0.05 wt% ALG was added, the excess complexes remained in the PUL phase, whereas pure MG clusters partitioned to the AMP phase below pH 5.6. It shows that complexation even with little ALG was sufficient to render the MG compatible with PUL. As the ALG concentration increased from 0.05 wt% towards 0.2 wt%, smaller droplets were observed after one week of standing, and the MG layer appeared more strongly gelled. These droplets sedimented, contrary to the structures obtained at lower concentrations, where a gelled network was able to sustain its own weight. Apparently, the attraction between the MG increased again with high ALG concentrations, perhaps caused by bridging of ALG between the MG. Similar behaviors were observed when ALG was substituted by PEC or KC, see Figure 52.

FIGURE 51. CLSM IMAGES OF A/P EMULSIONS AT pH 5.0 WITH 0.4 wt% MG AND DIFFERENT CONCENTRATIONS OF ALG AS INDICATED IN THE FIGURE. THE TOP AND THE BOTTOM ROWS CORRESPOND, RESPECTIVELY, TO IMAGES TAKEN JUST AFTER PREPARATION AND 1 WEEK LATER. ALL IMAGES ARE AT THE SAME SCALE (101 μm × 101 μm).

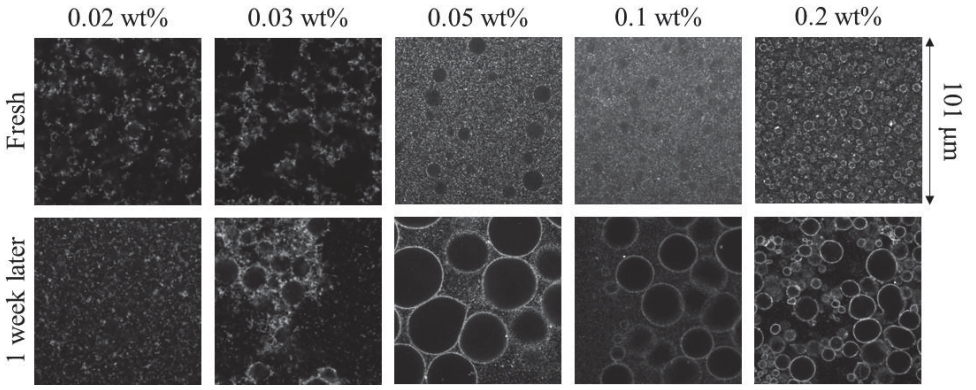

FIGURE 52. CLSM IMAGES OF A/P EMULSIONS AT pH 5.0 WITH 0.4 wt% MG AND DIFFERENT CONCENTRATIONS OF PEC (TWO TOP ROWS) AND KC (TWO BOTTOM ROWS) AS INDICATED IN THE FIGURE. FOR EACH POLYSACCHARIDE, THE UPPER AND THE LOWER ROWS CORRESPOND, RESPECTIVELY, TO IMAGES TAKEN JUST AFTER PREPARATION AND 1 WEEK LATER. ALL IMAGES ARE AT THE SAME SCALE (101 μm × 101 μm).

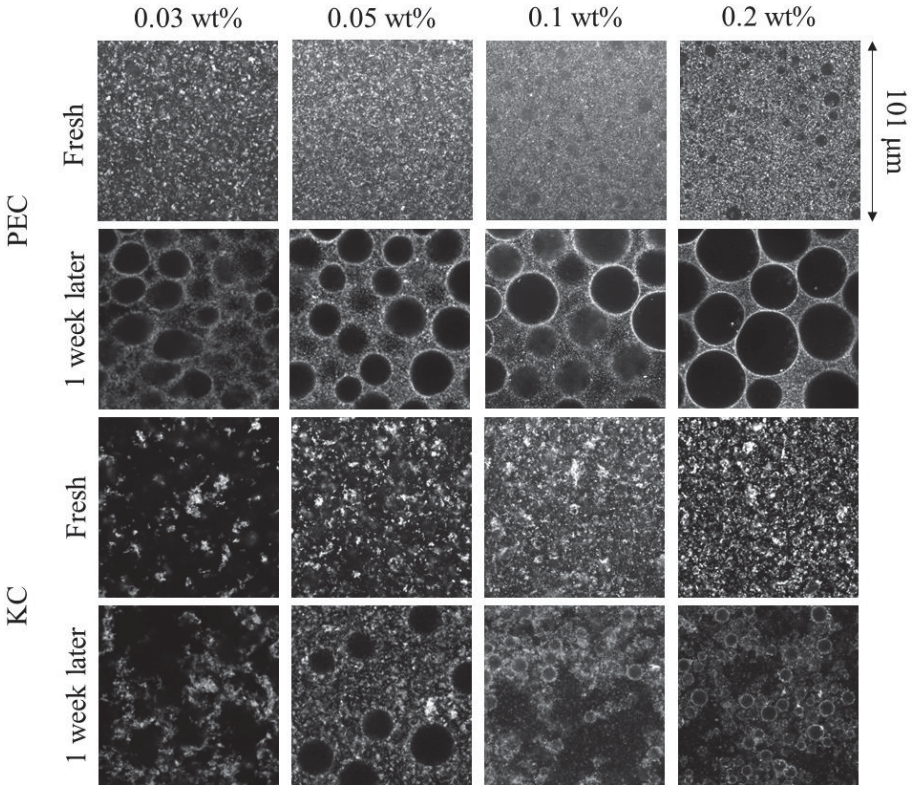

The microstructure of P/A emulsions with 0.05 wt% ALG at different pH is shown in Figure 53. As shown previously, the MG at pH 7.0 partitioned to the AMP phase at this concentration of ALG, and no interfacial layer was observed. It was hypothesized that this was due to the higher concentration of the ALG in the PUL phase when the volume fraction of the latter was smaller. When complexes are formed below pH < 5.6, a layer of MG is clearly visible around the PUL droplets, which decreased in size with decreasing pH, until pH 4.5 was reached. These droplets were present even after 1 week. If the pH was decreased even further, the clusters aggregated too strongly and sedimented, which is the bottom layer seen at pH 4.0 in Figure 53. At pH 5.0 and lower, excess MG partitioned to the PUL phase.

FIGURE 53. CLSM IMAGES OF P/A EMULSIONS WITH 0.05 wt% ALG AND 0.4 wt% MG AT DIFFERENT pH AS INDICATED IN THE IMAGE. THE TOP AND THE BOTTOM ROWS CORRESPOND, RESPECTIVELY, TO IMAGES TAKEN JUST AFTER PREPARATION AND 1 WEEK LATER. NOTE THAT THE IMAGES AT pH 7.0, 5.6, AND 4.0 AFTER 1 WEEK WERE TAKEN AT THE INTERFACE BETWEEN THE TWO MACROSCOPIC PHASES. ALL IMAGES ARE ON THE SAME SCALE (101 μm × 101 μm).

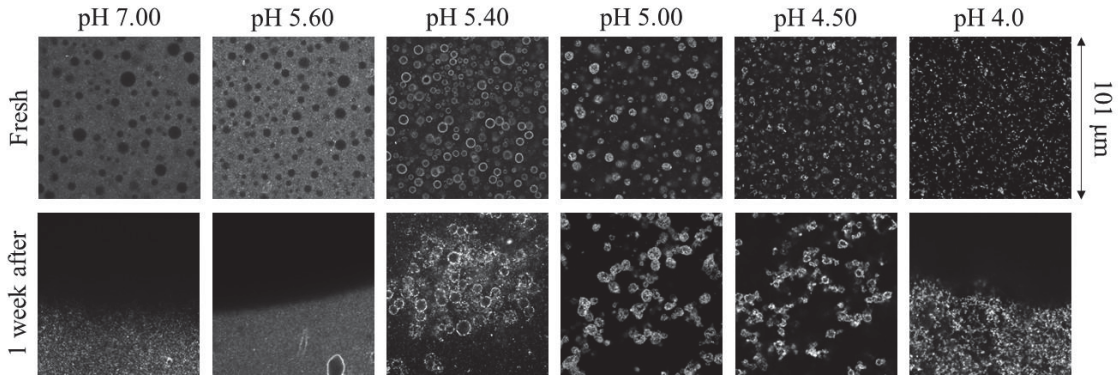

The influence of the ALG concentration on P/A emulsions at pH 5.0 is presented in Figure 54. At ALG concentrations lower than 0.05 wt%, the resulting microstructure was alike those found in the absence of the latter (FIGURE 46), suggesting that the amount of polysaccharide was insufficient to inhibit aggregation of the MG. At ALG concentration of 0.05 wt%, the formation of stable PUL droplets that associated into clusters or a weak gel was observed. This structure remained stable without signs of sedimentation for 1 week and no significant difference was seen with increasing ALG concentration.

FIGURE 54. CLSM IMAGES OF P/A EMULSIONS AT pH 5.0 WITH 0.4 wt% MG AND DIFFERENT CONCENTRATIONS OF ALG AS INDICATED IN THE FIGURE THE TOP AND THE BOTTOM ROWS CORRESPOND, RESPECTIVELY, TO IMAGES TAKEN JUST AFTER PREPARATION AND 1 WEEK LATER. ALL IMAGES ARE AT THE SAME SCALE (101 μm× 101 μm).

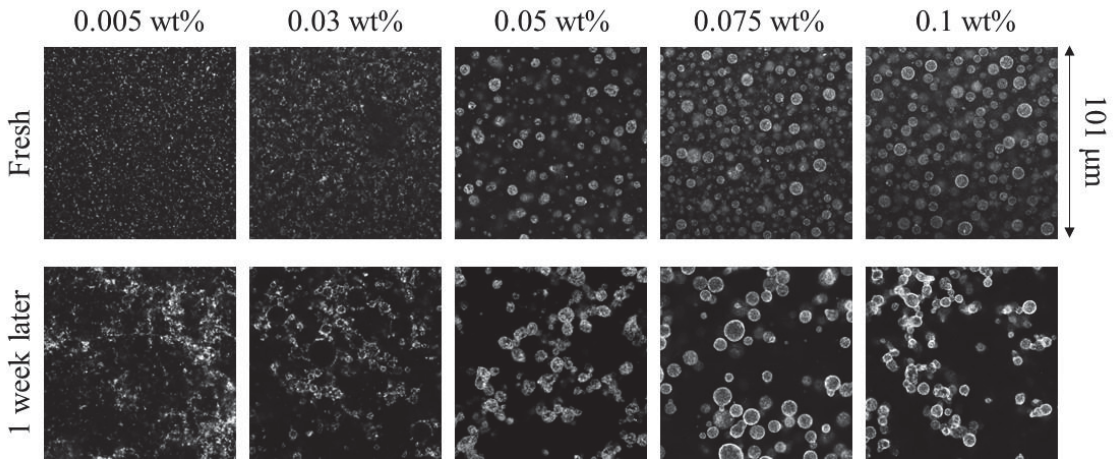

The substitution of ALG by PEC or KC in P/A emulsions as a function of the concentration of these polysaccharides is presented in Figure 55. The minimum amount to prevent the flocculation of MG when using KC seemed to be slightly higher than that for PEC and ALG.

FIGURE 55. CLSM IMAGES OF P/A EMULSIONS AT pH 5.0 WITH 0.4 wt% MG AND DIFFERENT CONCENTRATIONS OF PEC (TWO TOP ROWS) AND KC (TWO BOTTOM ROWS) AS INDICATED IN THE FIGURE. FOR EACH POLYSACCHARIDE, THE UPPER AND THE LOWER ROWS CORRESPOND, RESPECTIVELY, TO IMAGES TAKEN JUST AFTER PREPARATION AND 1 WEEK LATER. ALL IMAGES ARE AT THE SAME SCALE (101 μm × 101 μm).

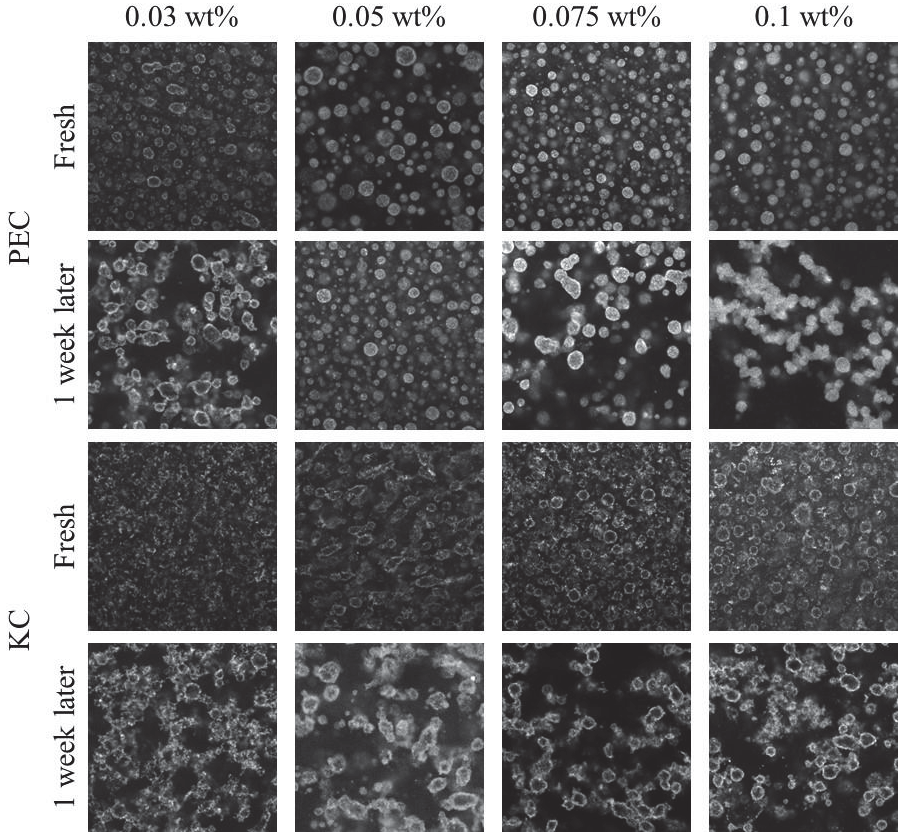

4.4.4 Impact of polysaccharides on the acidification under quiescent conditions

In the presence of 0.05 wt% ALG, KC or PEC, the MG were situated at the interface of A/P emulsions already at pH 7.0, and when the pH was acidified to pH 5.0 *in-situ* under quiescent conditions they remained there. CLSM images obtained during the acidification under quiescent conditions for A/P emulsions in the presence of both MG and ALG are presented in Figure 56.

FIGURE 56. CLSM IMAGES OF A/P EMULSIONS WITH 0.4 WT% MG AND 0.05 wt% ALG AT DIFFERENT pH VALUES DUE TO THE USE OF GDL AS EXPRESSED IN THE IMAGES. ALL IMAGES ARE AT THE SAME SCALE (50 μm × 50 μm).

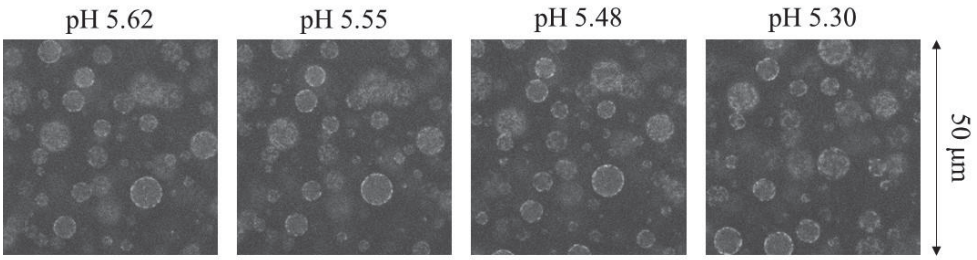

To reduce the time needed to reach pH values were complexation occurred, GDL was added to solution prepared at pH 5.7 for the A/P emulsions. However, this did not inhibit coalescence during the decrease of the pH, so that large droplets sedimented after 1 week (FIGURE 57). Curiously, the final size of the droplets appeared to depend on the polysaccharide added. The reason for this behavior, however, remains unknown. For the A/P emulsions, the method chosen to reduce the pH to 5.0, either HCl or GDL, appears to have little significance, compare Figures 49 and 52 with 57.

FIGURE 57. CLSM IMAGES OF A/P EMULSIONS AT pH 5.0 WITH 0.4 wt% MG AND 0.05 wt% ALG (A), KC (B) OR PEC (C). THE IMAGES WERE TAKEN ONE WEEK AFTER PREPARATION. THE SCALE OF IMAGE (A) IS 255 μm × 255 μm, WHEREAS THAT OF (B) AND (C) IS 101 μm × 101 μm.

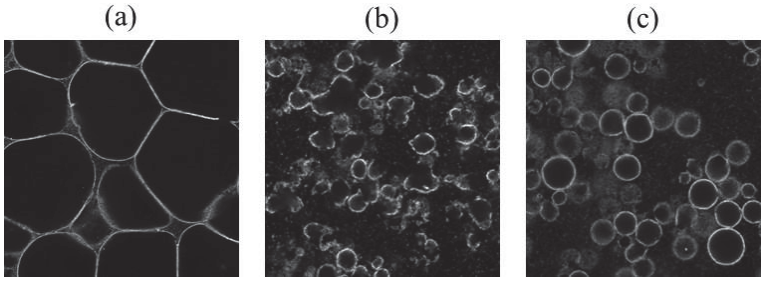

P/A emulsions were investigated at a lower polysaccharide concentration, because at 0.05 wt% the MG are no longer at the interface at pH 7.0, but partition to the AMP phase. Thus, in the presence of 0.005 wt% ALG, KC, or PEC the MG are at the interface at pH 7.0, and quiescent *in-situ* decrease of the pH led to the formation of a gelled layer of MG around spherical AMP droplets close to what was observed in the absence of anionic polysaccharide, (FIGURE 58). The droplets were relatively small and remained stable in suspension for at least a week.

FIGURE 58. CLSM IMAGES OF P/A EMULSIONS AT pH 5.0 WITH 0.4 wt% MG AND 0.005 wt% ALG (A), KC (B), OR PEC (C). THE IMAGES WERE TAKEN ONE WEEK AFTER PREPARATION. ALL IMAGES ARE AT THE SAME SCALE (101 μm × 101 μm).

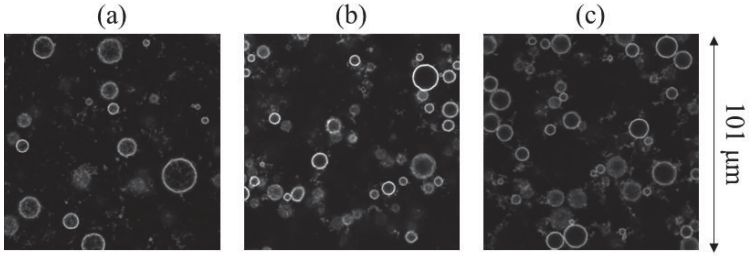

A few measurements at different MG and ALG concentrations were done, see Figure 59. At 2 wt% MG, similar stable PUL droplets were formed, but at 1 wt% MG, macroscopic phase separation occurred, suggesting that the MG concentration at the interface was insufficient to inhibit coalescence. There was significant influence of ALG on the size and stability of the PUL droplets when its concentration was 0.005 wt% or lower. However, at 0.05 wt% ALG the emulsion was not stable, and macroscopic phase separation was observed even though the MG did absorb at the interface as the pH was decreased *in-situ.* Probably, the complexes at the interface were somewhat less connected when there was more ALG so that coalescence happened.

FIGURE 59. CLSM IMAGES OF P/A EMULSIONS RIGHT AFTER PREPARATION (TOP ROW) AND 1 WEEK LATER (BOTTOM ROW) WITH DIFFERENT MG:ALG RATIOS INDICATED ABOVE EACH COLUMN. GDL WAS USED TO REDUCE THE pH FROM 7.0 TO ~5.0. ALL IMAGES ARE AT THE SAME SCALE (101 μm × 101 μm). NOTICE THAT THE IMAGES FROM THE FRESH SAMPLES WERE TAKEN AFTER COMPLETE GDL DEGRADATION (24 h LATER).

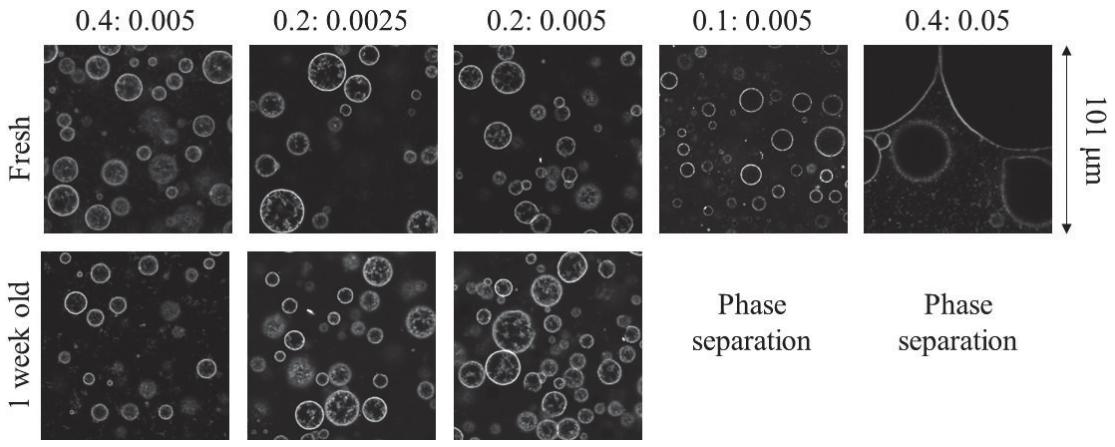

To estimate the strength of the interfacial gel layer formed with 0.4 wt% MG and 0.005 wt% of polysaccharide, the droplets went through several procedures and were observed 5 days after each procedure, see Figure 60. The first observable influence of the type of the polysaccharides was that the excess MG formed gelled strands within the droplets, whereas this was not seen with PEC or KC. When the emulsions were diluted by a factor of 0.5 – concentrations where phase separation is no longer expected – the gelled layer in the presence of PEC did not resist, contrary to what was observed for the KC and ALG. By adding NaOH proportionally to the amount of H^+ released by GDL degradation, the pH is expected to return to 7.0, and then by gently homogenizing the sample apparently did not have significant effect on the particle layer when ALG and PEC but was responsible to disrupt the gelled particles in the presence of PEC. Apparently, new droplets are formed by returning the pH to 7.0, indicating that that AMP-PUL mixture has a secondary phase separation induced by the pH. Remarkably, by submitting the samples to vortex all the droplets resisted, independent on the polysaccharide used.

FIGURE 60. CLSM IMAGES OF P/A EMULSIONS WITH 0.4 wt% MG AND 0.005 wt% PEC (LEFT), KC (MIDDLE) OR ALG (RIGHT) SUBMITTED TO GLD ACIDIFICATION. THE FIRST ROW REPRESENTS IMAGES NOT PROCESSED, WHEREAS THE OTHER ROWS WERE THE SAMPLES THAT WENT THROUGH DIFFERENT PROCESSES. THE IMAGES WERE TAKEN RIGHT AFTER THE PROCESSING AND 5 DAYS LATER. ALL IMAGES ARE AT THE SAME SCALE (101 μm × 101 μm).

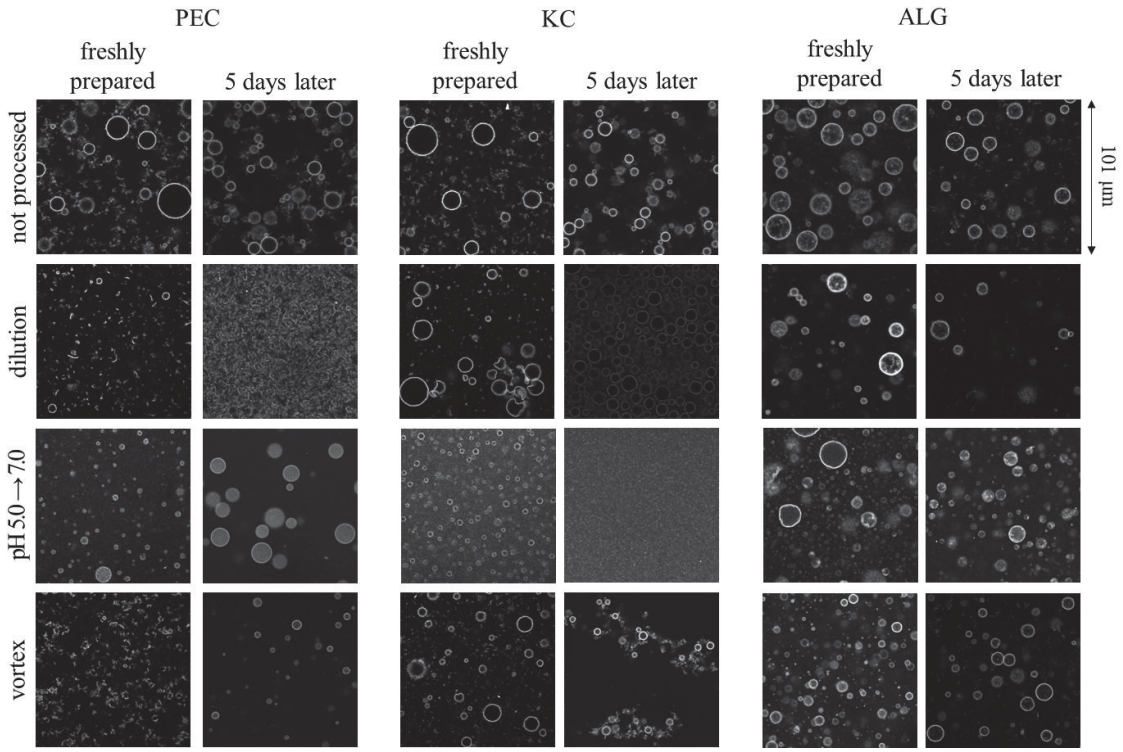

Based on the results above mentioned, the droplets formed by 0.2 wt% MG and 0.0025 wt% ALG were submitted to a scanning electron microscopy analysis. Unfortunately, the vacuum was enough to damage the particle gelled layer so that only the profile of the destroyed droplets was seen (FIGURE 61).

FIGURE 61. SCANNNING ELECTRON MICROSCOPY IMAGES OF THE P/A EMULSION WITH 0.2 wt% MG AND 0.0025 wt% ALG SUBMITTED TO GDL ACIDIFICATION.

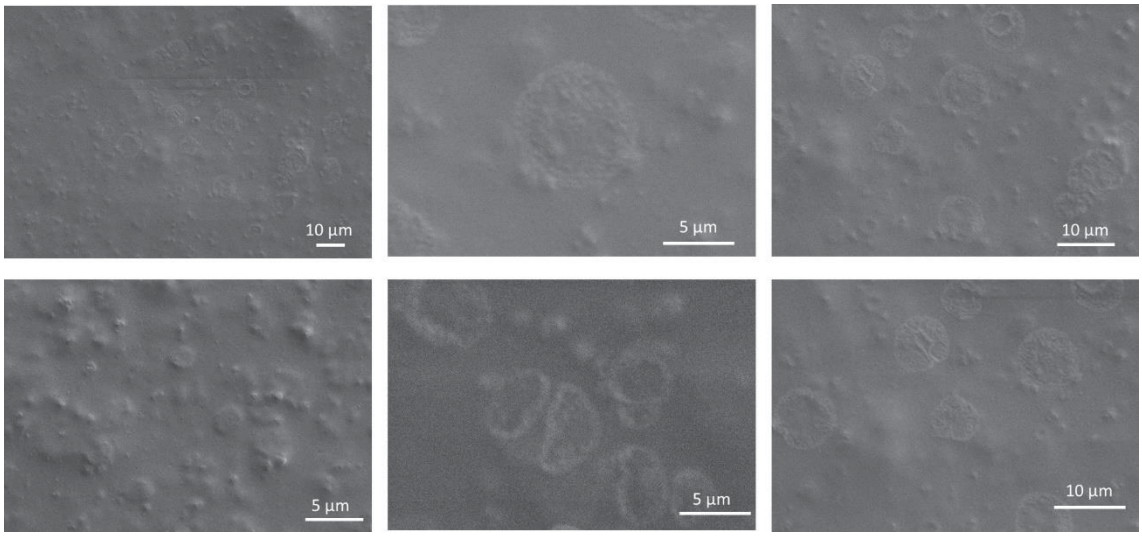

4.4.5 Influence of temperature on the partition of microgels in amylopectin-pullulan emulsions

The influence of temperature on the partition of the MG in A/P emulsions in the presence of 0.05 wt% ALG is shown in Figure 62. At 20 °C the MG are located at the interface. The excess can be seen both in AMP and PUL phase, due to the presence of RodB, as discussed above. As the temperature is increased, more MG seemed to populate the AMP phase, so that there is no clear distinction between the ring of particles at the interface and the interior of the droplets at 50 °C. The migration is reversible since similar contrast between the interface and both phases is seen as the temperature decreases. Care was taken in order to use the same laser intensity and sensibility of the detector.

FIGURE 62. CLSM IMAGES OF THE A/P EMULSIONS WITH 0.4 wt% MG AND 0.05 wt% ALG AT DIFFERENT TEMPERATURES. ALL IMAGES HAVE THE SAME DIMENSION (64 µm × 64 µm). NOTICE THAT COALESCENCE CAUSED THE DECREASE IN THE AMOUNT OF DROPLETS SHOWN.

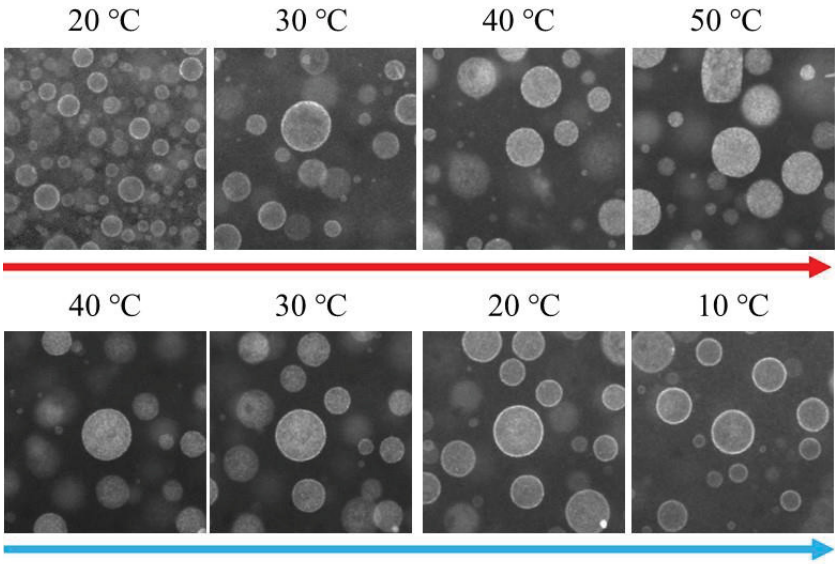

With changing the temperature in P/A emulsions, a very close behavior was observed, except this time the MG migrated towards the continuous phase, rendering the interior of the droplets darker, see Figure 63. A slight hysteresis on the partition was seen as the temperature decreased for P/A emulsion.

FIGURE 63. CLSM IMAGES OF THE P/A EMULSIONS WITH 0.4 wt% MG AND 0.005 wt% ALG AT DIFFERENT TEMPERATURES. ALL IMAGES HAVE THE SAME DIMENSION (64 µm × 64 µm).

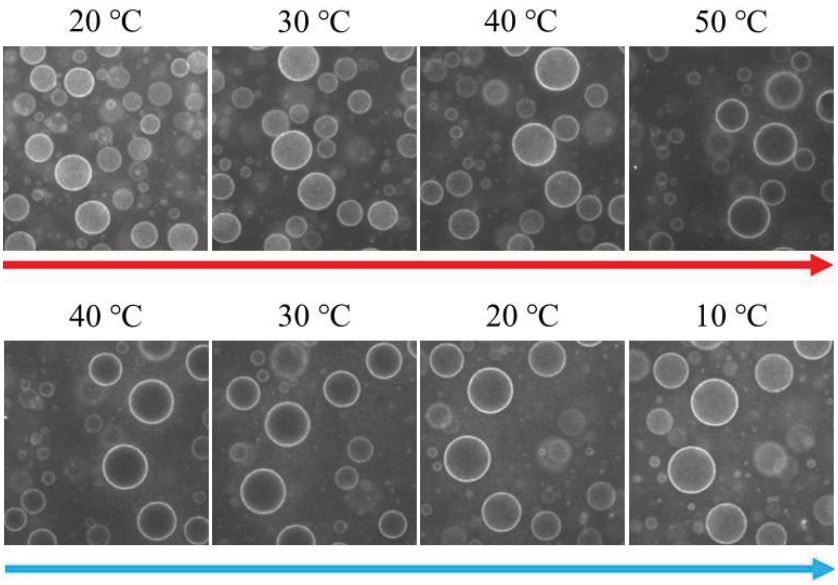

When no ALG was added, the MG remained dispersed in the PUL phase, without indications of interfacial adsorption, see Figure 64. This suggests that the temperature influences the partition of the ALG, so that the ALG concentration in the PUL phase increases with increasing the temperature, rendering this phase worse to accommodate the MG.

FIGURE 64. CLSM IMAGES OF THE A/P EMULSIONS WITH 0.4 wt% MG AT DIFFERENT TEMPERATURES. ALL IMAGES HAVE THE SAME DIMENSION (64 μm × 64 μm).

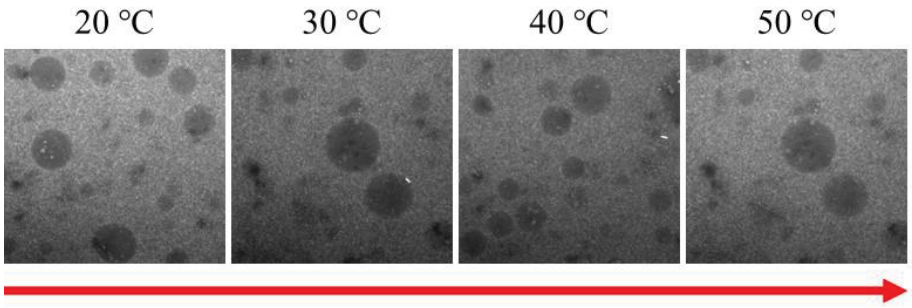

In this final section, the impact of the acidification method to induce the cold-gelation of the MG on the stabilization of AMP-PUL emulsions was explored. Initially, it was seen that pH is a factor that can control the partition of the MG as well as the temperature. Then, it seemed clear that using HCl to acidify the media was interesting in situations where there was an anionic polysaccharide to complex with the MG, which led to stable individual droplets. The acidification with GDL under quiescent conditions appeared to be more indicated since, upon flocculation the MG could arrange at the interface in a more favorable and controllable way, avoiding undesired aggregation of the droplets so that at the end of the acidification process, very resistant droplets were produced.

5 FINAL REMARKS AND CONCLUSION

The results reported here showed the possibility to form stable AMPS by forming different networks of associated droplets. The morphology of the AMPS is dictated by the interfacial tension ratios, assuming that none of the interfacial tension is higher than the sum of the two others and the measurement of the angles formed by the association of the droplets allows the determination of relative interfacial tensions. Curiously, the addition of MG had small influence on the relative interfacial tensions.

The adsorption of particles at the interface of w/w emulsions could be fine-tuned by adding a third polymer that mixes homogeneously with one or both phases and has no

specific interactions with the particles. For the case of MG particles in AMP-PUL emulsions, it was shown that adding either of three anionic (ALG, PEC, and KC) or a neutral (XG) polysaccharide led to a change in the partitioning of the MG between the phases even in small amounts, passing through their adsorption at the interface. It is hypothesized that the origin of this phenomenon is that the added polymer modifies the interfacial tension between the particles and each of the two phases differently. When the interfacial tension between the particles and each phase is equal, adsorption of particles at the interface occurs even if the interfacial tension between the phases is extremely small, i.e. close to the binodal. The effect was also found in emulsions formed by mixing AMP with DX and using a different type of particle, namely CNC. Thus, this behavior is apparently universal.

Even though it was possible to adhere most of the particles at the interface, the stabilization of AMP-PUL emulsions was only found when the pH was decreased down to the point where the MG-polysaccharide complexes started to be formed. The pH by itself was also responsible to change the partition of the MG from the PUL phase at pH 7.0 to AMP phase at pH 3.5 in the absence of added polysaccharide. When the MG are located at the interface at pH 7.0, GDL can cause the acid-induced gelation locally. The behavior using GDL as acidifier was not very different from the use of HCl for the A/P emulsions. However, in the case of P/A emulsions, the weak gel formed at the interface was able to procure stability to small droplets for at least 1 week.

The influence of temperature on the partition of MG in PUL-AMP emulsions was briefly investigated. Without the addition of a third polysaccharide, the partition of the MG was independent on the temperature. However, when ALG was added, the MG seemed to migrate towards the AMP phase. The reason for this effect probably lies on the change in the partition of the ALG, which consequently caused the preference for the MG to change.

REFERENCES

AKBULUT, O. et al. Separation of Nanoparticles in Aqueous Multiphase Systems through Centrifugation. **Nano Letters**, v. 12, n. 8, p. 4060–4064, 8 ago. 2012.

ALTING, A. C. et al. Cold-set globular protein gels: Interactions, structure and rheology as a function of protein concentration. **Journal of Agricultural and Food Chemistry**, v. 51, n. 10, p. 3150–3156, 2003.

ALTING, A. C. et al. Acid-Induced Cold Gelation of Globular Proteins: Effects of Protein Aggregate Characteristics and Disulfide Bonding on Rheological Properties. **Journal of Agricultural and Food Chemistry**, v. 52, n. 3, p. 623–631, 2004.

ASENJO, J. A.; ANDREWS, B. A. Aqueous two-phase systems for protein separation: Phase separation and applications. **Journal of Chromatography A**, v. 1238, n. September 2011, p. 1–10, 2012.

BALAKRISHNAN, G. et al. Particles trapped at the droplet interface in water-in-water emulsions. **Langmuir**, v. 28, n. 14, p. 5921–5926, 2012.

BASEDOW, A. M.; EBERT, K. H.; RULAND, U. Specific refractive index increments of dextran fractions of different molecular weights. **Makromolekulare Chemie**, v. 179, n. 5, p. 1351–1353, 1978.

BELLO-PÉREZ, L. A. et al. Macromolecular Features of Starches Determined by Aqueous High-performance Size Exclusion Chromatography. **Journal of Cereal Science**, v. 27, n. 3, p. 267–278, 1998.

BINKS, B. P.; HOROZOV, T. S. (EDS.). **Colloidal Particles at Liquid Interfaces**. Cambridge: Cambridge University Press, 2006.

BOITTE, J. et al. A novel rheo-optical device for studying complex systems under controlled double plate shear A novel rheo-optical device for studying complex fluids in a double shear plate geometry. n. January, 2013.

BUCHNER, P.; COOPER, R. E.; WASSERMANN, A. 774. Influence of counter-ion fixation on molecular weight and shape of a polyelectrolyte. **Journal of the Chemical Society (Resumed)**, n. 0, p. 3974–3983, 1961.

BUI, V. T. N. T. et al. Mobility of carrageenan chains in iota- and kappa carrageenan gels. **Colloids and Surfaces A: Physicochemical and Engineering Aspects**, v. 562, p. 113–118, 2019.

DAMMAK, A. et al. Exploring architecture of xyloglucan cellulose nanocrystal complexes through enzyme susceptibility at different adsorption regimes. **Biomacromolecules**, v. 16, n. 2, p. 589–596, 2015.

DE FREITAS, R. A. et al. Stabilization of Water-in-Water Emulsions by Polysaccharide-Coated Protein Particles. **Langmuir**, v. 32, n. 5, p. 1227–1232, 2016.

DE NOOY, A. E. J. et al. TEMPO-Mediated Oxidation of Pullulan and Influence of Ionic Strength and Linear Charge Density on the Dimensions of the Obtained Polyelectrolyte Chains. **Macromolecules**, v. 29, n. 20, p. 6541–6547, 1 jan. 1996.

DE VRIES, R. Monte Carlo simulations of flexible polyanions complexing with whey proteins at their isoelectric point. **Journal of Chemical Physics**, v. 120, n. 7, p. 3475–3481, 2004.

DIAMOND, A. D.; HSU, J. T. Protein Partitioning in PEG / Dextran Aqueous Two-Phase Systems. v. 36, n. 7, p. 1017–1024, 1990.

DIMOPOULOU, M. et al. Pectin recovery and characterization from lemon juice waste streams. **Journal of the Science of Food and Agriculture**, v. 99, n. 14, p. 6191–6198, 1 nov. 2019.

ESQUENA, J. Water-in-water (W/W) emulsions. **Current Opinion in Colloid and Interface Science**, v. 25, p. 109–119, 2016.

FIROOZMAND, H.; MURRAY, B. S.; DICKINSON, E. Interfacial structuring in a phase-separating mixed biopolymer solution containing colloidal particles. **Langmuir**, v. 25, n. 3, p. 1300–1305, 2009.

FLEER, G. J. et al. **Polymers at interfaces**. [s.l.] Springer, 1998. v. 1999

FLORY, J. P. **Principles of Polymer Chemistry**. [s.l.] Cornell University Press, 1954.

GABER, M. et al. Protein-polysaccharide nanohybrids: Hybridization techniques and drug delivery applications. **European Journal of Pharmaceutics and Biopharmaceutics**, v. 133, n. September, p. 42–62, 2018.

GONZALEZ-JORDAN, A.; BENYAHIA, L.; NICOLAI, T. Cold gelation of water in water emulsions stabilized by protein particles. **Colloids and Surfaces A: Physicochemical and Engineering Aspects**, v. 532, n. January, p. 332–341, 2017.

GONZALEZ-JORDAN, A.; NICOLAI, T.; BENYAHIA, L. Influence of the Protein Particle Morphology and Partitioning on the Behavior of Particle-Stabilized Water-in-Water Emulsions. **Langmuir**, v. 32, n. 28, p. 7189–7197, 2016.

GONZALEZ-JORDAN, A.; NICOLAI, T.; BENYAHIA, L. Enhancement of the particle stabilization of water-in-water emulsions by modulating the phase preference of the particles. **Journal of Colloid and Interface Science**, v. 530, p. 505–510, 2018.

GONZALEZ ORTIZ, D. et al. Current Trends in Pickering Emulsions: Particle Morphology and Applications. **Engineering**, v. 6, n. 4, p. 468–482, 2020.

GUIDO, S.; VILLONE, M. Measurement of Interfacial Tension by Drop Retraction Analysis. **Journal of Colloid and Interface Science**, v. 209, n. 1, p. 247–250, 1999.

HATTI-KAUL, R. Aqueous two-phase systems: A general overview. **Applied Biochemistry and Biotechnology - Part B Molecular Biotechnology**, v. 19, n. 3, p. 269–277, 2001.

HAZT, B. et al. Effect of pH and protein particle shape on the stability of amylopectin–xyloglucan water-in-water emulsions. **Food Hydrocolloids**, p. 105769, 2020.

IQBAL, M. et al. Aqueous two-phase system (ATPS): an overview and advances in its applications. **Biological Procedures Online**, v. 18, n. 1, p. 1–18, 2016.

JENKINS, P.; SNOWDEN, M. Depletion flocculation in colloidal dispersions. **Advances in Colloid and Interface Science**, v. 68, n. 1–3, p. 57–96, 1996.

JUMEL, K. et al. Molar mass and viscometric characterisation of hydroxypropylmethyl cellulose. **Carbohydrate Polymers**, v. 29, n. 2, p. 105–109, 1996.

JUNG, J. M. et al. Structure of heat-induced β-lactoglobulin aggregates and their complexes with sodium-dodecyl sulfate. **Biomacromolecules**, v. 9, n. 9, p. 2477–2486, 2008.

KHARLAMOVA, A.; CHASSENIEUX, C.; NICOLAI, T. Acid-induced gelation of whey protein aggregates: Kinetics, gel structure and rheological properties. **Food Hydrocolloids**, v. 81, p. 263–272, 2018.

KHEMISSI, H. et al. Exploiting Complex Formation between Polysaccharides and Protein Microgels to Influence Particle Stabilization of W/W Emulsions. **Langmuir**, v. 34, n. 39, p. 11806–11813, 2018.

KINSELLA, J. E. Texturized proteins: Fabrication, flavoring, and nutrition. **C R C Critical Reviews in Food Science and Nutrition**, v. 10, n. 2, p. 147–207, 1978.

KINSELLA, J. E. Functional properties of proteins: Possible relationships between structure and function in foams. **Food Chemistry**, v. 7, n. 4, p. 273–288, 1981.

KRUIF, C. G. DE; TUINIER, R. Polyssacharides- protein interactions. **Food Hydrocolloids**, v. 15, p. 555–563, 2001.

LIU, D.; ZHOU, P.; NICOLAI, T. Effect of Kappa carrageenan on acid-induced gelation of whey protein aggregates. Part I: Potentiometric titration, rheology and turbidity. **Food Hydrocolloids**, v. 102, n. November 2019, p. 105589, 2020a.

LIU, D.; ZHOU, P.; NICOLAI, T. Effect of kappa carrageenan on acid-induced gelation of whey protein aggregates. Part II: Microstructure. **Food Hydrocolloids**, v. 102, n. November 2019, p. 105590, 2020b.

MCCLEMENTS, D. J. **Understanding and controlling the microstructure of complex foods**. first ed. [s.l.] CRC Press, 2007.

MCCLEMENTS, D. J.; KEOGH, M. K. Physical properties of cold-setting gels formed from heat-denatured whey protein isolate. **Journal of the Science of Food and Agriculture**, v. 69, n. 1, p. 7–14, 1995.

MEHALEBI, S.; NICOLAI, T.; DURAND, D. Light scattering study of heat-denatured globular protein aggregates. **International Journal of Biological Macromolecules**, v. 43, n. 2, p. 129–135, 2008.

NICOLAI, T.; BRITTEN, M.; SCHMITT, C. β-Lactoglobulin and WPI aggregates: Formation, structure and applications. **Food Hydrocolloids**, v. 25, n. 8, p. 1945–1962, 2011.

NICOLAI, T.; MURRAY, B. Particle stabilized water in water emulsions. **Food Hydrocolloids**, v. 68, p. 157–163, 2017.

NORTON, I. T.; FRITH, W. J. Microstructure design in mixed biopolymer composites. **Food Hydrocolloids**, v. 15, n. 4–6, p. 543–553, 2001.

ONGHENA, B.; OPSOMER, T.; BINNEMANS, K. Separation of cobalt and nickel using a thermomorphic ionic-liquid-based aqueous biphasic system. **Chemical Communications**, v. 51, n. 88, p. 15932–15935, 2015.

PICKERING, S. U. CXCVI.—Emulsions. **Journal of the Chemical Society, Transactions**, v. 91, n. 0, p. 2001–2021, 1907.

PICULELL, L.; BERGFELDT, K.; NILSSON, S. Factors determing phase behavior of multi component polymer systems. In: HARDING, S. E.; HILL, S. E.; MITCHELL, J. E. (Eds.). . **Biopolymer mixtures**. first ed. [s.l: s.n.].

RALLISON, J. M. The deformation of small viscous dropls and bubbles in shear flow. **Ann. Rev. Fluid Mech.**, v. 16, p. 45–66, 1984.

RAMSDEN, W. Separation of solids in the surface-layers of solutions and suspensions. **Proc. R. Soc. Lond.**, v. 72, p. 156–164, 1903.

ROWLINSONS, J. S.; WIDOM, B. **Molecular Theory of Capillarity**. Mineola: Dover, 1983. v. 34

SARKAR, A.; DICKINSON, E. Sustainable food-grade Pickering emulsions stabilized by plant-based particles. **Current Opinion in Colloid and Interface Science**, v. 49, p. 69–81, 2020.

SCHMITT, C. et al. Whey protein soluble aggregates from heating with NaCl: Physicochemical, interfacial, and foaming properties. **Langmuir**, v. 23, n. 8, p. 4155–4166, 2007.

SCHMITT, C. et al. **Multiscale Characterization of Individualized β-Lactoglobulin MicrogelsLangmuir**, 2009.

SCHMITT, C. et al. Internal structure and colloidal behaviour of covalent whey protein microgels obtained by heat treatment. **Soft Matter**, v. 6, n. 19, p. 4876–4884, 2010a.

SCHMITT, C. et al. Internal structure and colloidal behaviour of covalent whey protein microgels obtained by heat treatment. p. 4876–4884, 2010b.

STEPHEN, A. M.; PHILIPS, G. O.; WILLIAMS, P. A. (EDS.). **Food Polysaccharides and Their Applications**. second edi ed. [s.l.] Taylor and Francis, 2006.

TAMBE, D. E.; SHARMA, M. M. The effect of colloidal particles on fluid-fluid interfacial properties and emulsion stability. **Advances in Colloid and Interface Science**, v. 52, n. C, p. 1–63, 1994.

TEA, L.; NICOLAI, T.; RENOU, F. Stabilization of Water-In-Water Emulsions by Linear Homo-Polyelectrolytes. **Langmuir**, v. 35, n. 27, p. 9029–9036, 2019.

TROMP, R. H.; BLOKHUIS, E. M. Tension , Rigidity , and Preferential Curvature of Interfaces between Coexisting Polymer Solutions. 2013.

VILLARES, A. et al. Kinetic aspects of the adsorption of xyloglucan onto cellulose nanocrystals. **Soft Matter**, v. 11, n. 32, p. 6472–6481, 2015.

VIS, M.; ERNÉ, B. H.; TROMP, R. H. Chemical physics of water–water interfaces. **Biointerphases**, v. 11, n. 1, p. 018904, 2016.

WITTEMANN, A.; BALLAUFF, M. Interaction of proteins with linear polyelectrolytes and spherical polyelectrolyte brushes in aqueous solution. **Physical Chemistry Chemical Physics**, v. 8, n. 45, p. 5269–5275, 2006.

WITTGREN, B. et al. Conformational change and aggregation of κ-carrageenan studied by flow field-flow fractionation and multiangle light scattering. **Biopolymers**, v. 45, n. 1, p. 85–96, 1 jan. 1998.

YANG, Y. et al. An overview of pickering emulsions: Solid-particle materials, classification, morphology, and applications. **Frontiers in Pharmacology**, v. 8, n. MAY, p. 1–20, 2017.

ZARBAKHSH, A.; BOWERS, J.; WEBSTER, J. R. P. Width of the Hexadecane - Water Interface : A Discrepancy Resolved. n. 4, p. 11596–11598, 2005.

ZHANG, J. et al. Microgel-Stabilized Hydroxypropyl Methylcellulose and Dextran Water-in-Water Emulsion : In fl uence of pH , Ionic Strength , and Temperature. 2021.

APPENDIX I

Academic information

TABLE A1 – Lectures attended or to be attended by the student.

Lecture	Period	Situation (Score)
Rheology – flow and linear viscoelasticity	*20-22/01/2019*	*Approved*
Documentary research	*28/11/2019*	*Approved*
Scattering techniques applied to soft matter	*10-11/03/2021*	*Approved*
Understanding polymers' physical properties	*22-23/04/2021*	*Approved*
Introduction to light scattering and zeta potential	*19/04/2021*	*Approved*
Use of Illustrator	*20-29/04/2021*	*Approved*
Scientific integrity and research data	*01/07/2021*	*Approved*
Métodos estatísticos em pesquisa científica	*17/03-23/06/21*	*Approved (B)*
Prática de docência	*30/04-16/07/21*	*Approved (A)*
Seminários D1	*23/03-16/07/2021*	*Approved (A)*
Seminários D2	*23/03-16/07/2021*	*Approved (A)*
Métodos físico-químicos de caracterização de macromoléculas e coloides	*09/08-03/12/21*	*Approved (A)*
Espectrometria de massas	*05/10-23/11/21*	*Approved (B)*

APPENDIX II

Scientific production

TABLE A2– Scientific papers published in peer-reviewed journals as author or co-author.

Title	Journal	Situation	Submitted
Effect of pH and protein particle shape on the stability of amylopectin–xyloglucan water-in-water emulsions	Food Hydrocolloids	Published	07/10/2019
Effect of the Interfacial Tension on Droplet Association in Aqueous Multiphase Systems	Langmuir	Published	10/02/2021
Effect of adding a third polysaccharide on the adsorption of protein microgels at the interface of polysaccharide-based water in water emulsions	Journal of Colloid and Interface Science	Published	18/02/2021
Stabilization of Amylopectin-Pullulan Water in Water Emulsions by Interacting Protein Particles	Food hydrocolloids	Published	30/10/2021

APPENDIX III

Phase diagrams between binary mixtures

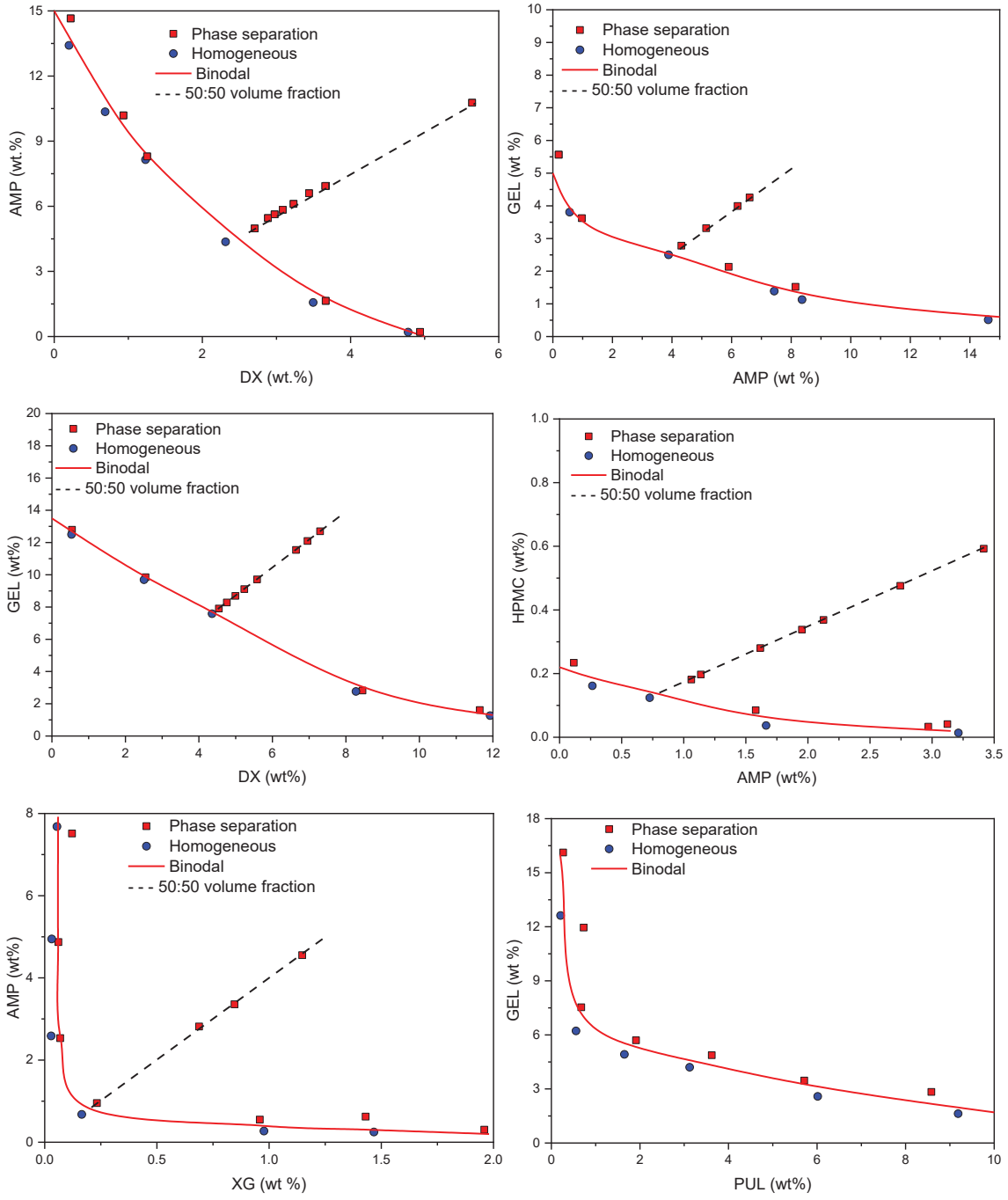

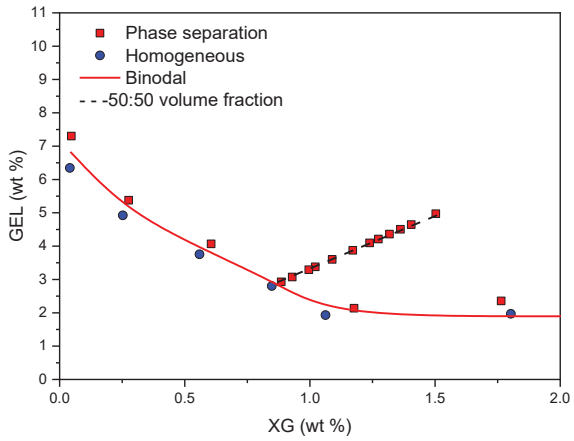
Phase separation
Homogeneous
Binodal
-50:50 volume fraction
GEL (wt %)
XG (wt %)

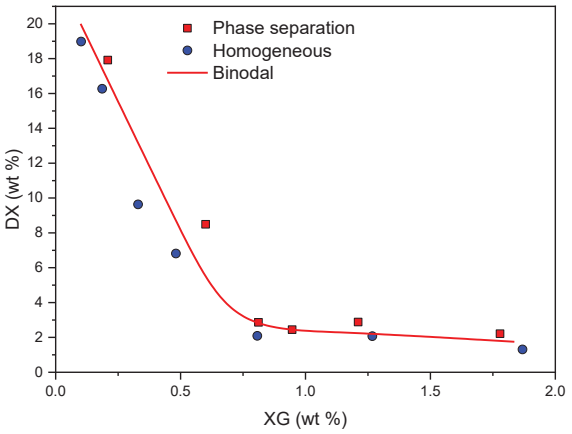
Phase separation
Homogeneous
Binodal
DX (wt %)
XG (wt %)

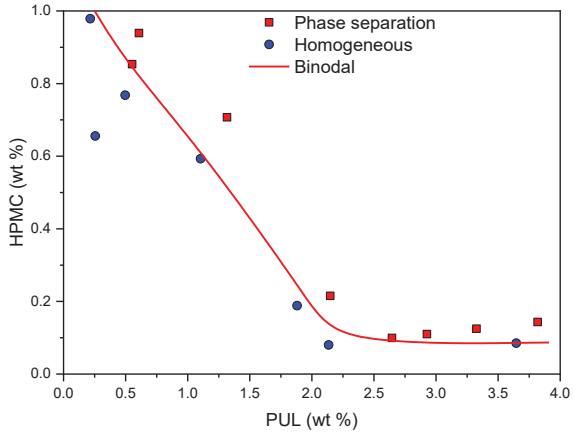
Phase separation
Homogeneous
Binodal
HPMC (wt %)
PUL (wt %)

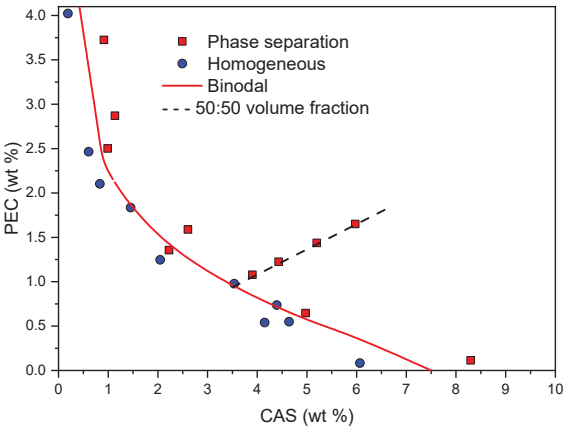
Phase separation
Homogeneous
Binodal
50:50 volume fraction
PEC (wt %)
CAS (wt %)

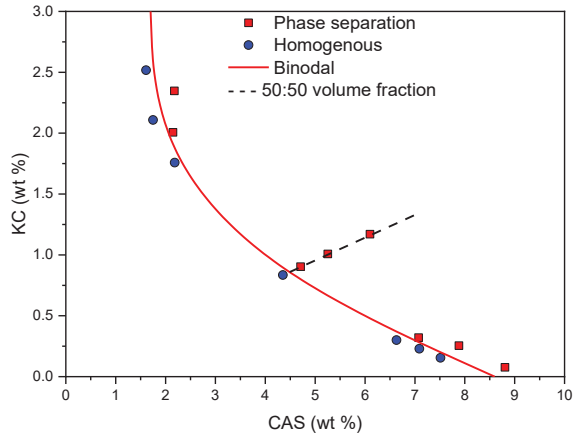
Phase separation
Homogenous
Binodal
50:50 volume fraction
KC (wt %)
CAS (wt %)

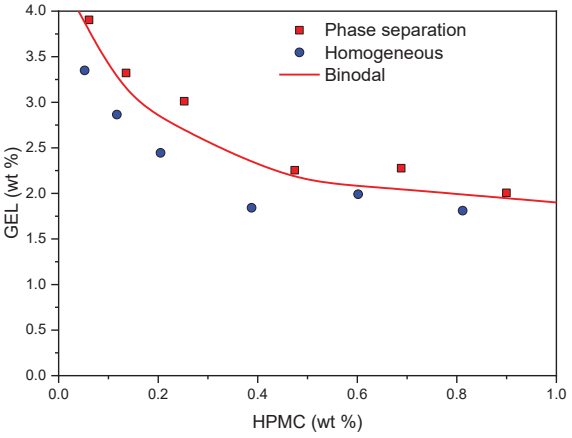
Phase separation
Homogeneous
Binodal
GEL (wt %)
HPMC (wt %)

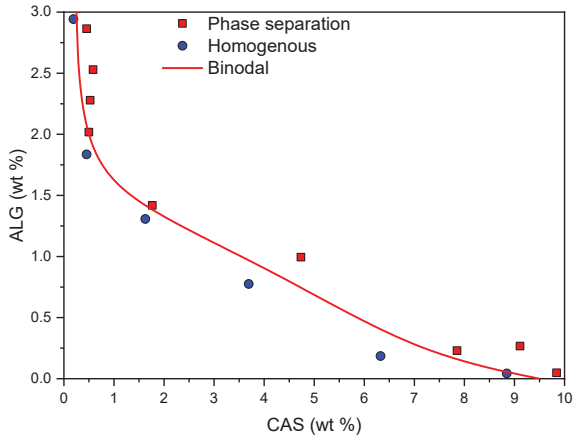
Phase separation
Homogenous
Binodal
ALG (wt %)
CAS (wt %)

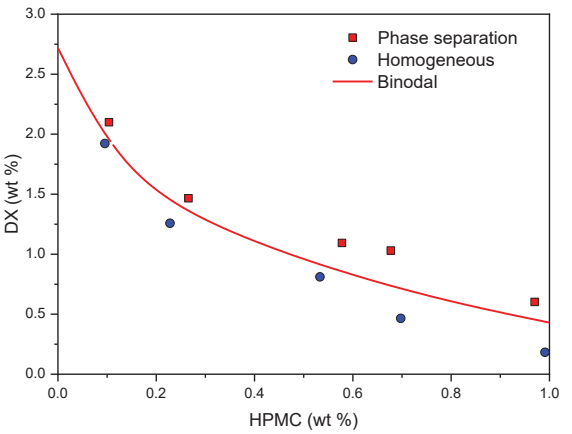
Phase separation
Homogeneous
Binodal
DX (wt %)
HPMC (wt %)

Appendix IV

CLSM images of AMPS of different compositions as indicated in each figure. The brightness of each phase depends on the partition of rhodamine B. The order of brightness increases as: XG < PUL < PEO < GEL < AMP. Notice that in the system of GEL + AMP in XG, MG particles were added to enhance the brightness of the GEL phase so it could be brighter than the AMP phase. The scale is presented in each image.

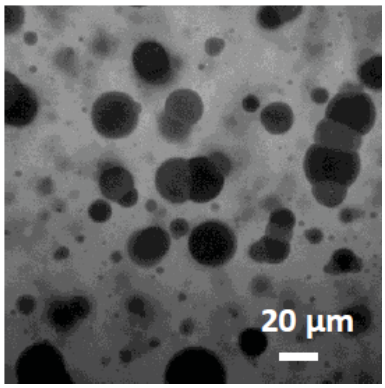

DX + PEO in GEL

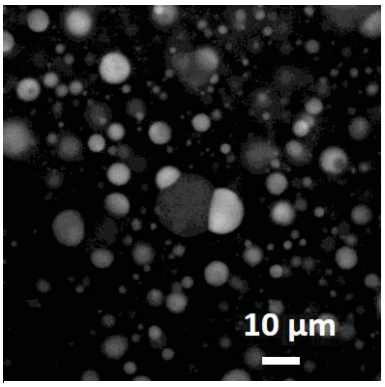

GEL + PEO in DX

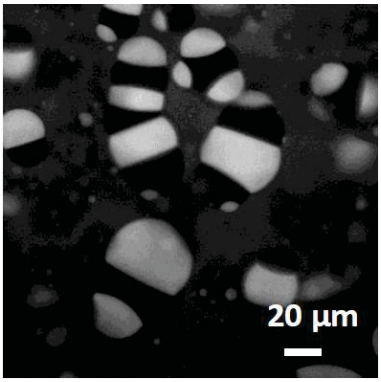

GEL + DX in PEO

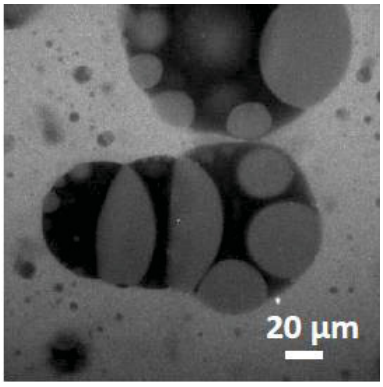

PUL + AMP in GEL

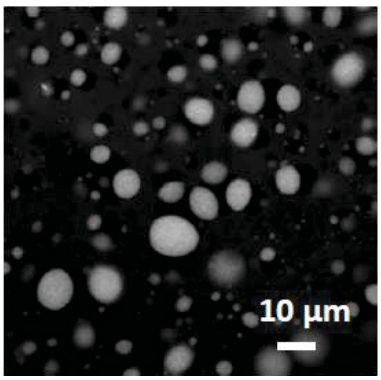

PUL + GEL in AMP

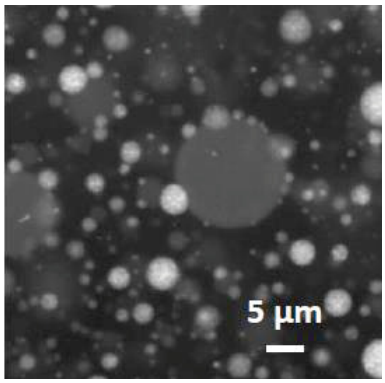

AMP + GEL in PUL

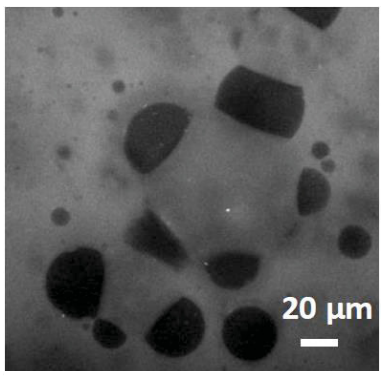

PEO + AMP in GEL

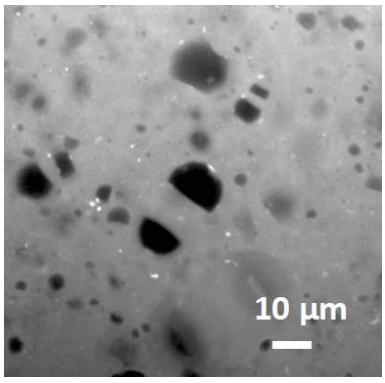

PEO + GEL in AMP

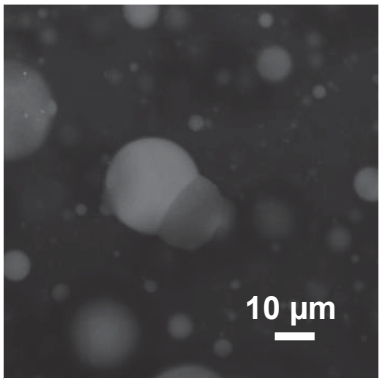

AMP + GEL in PEO

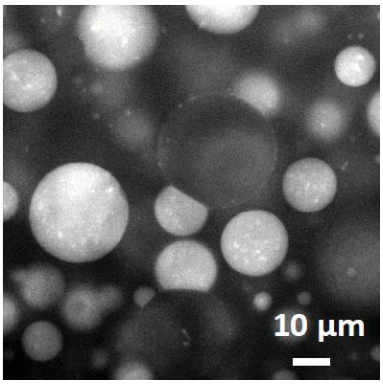

AMP + PEO in PUL

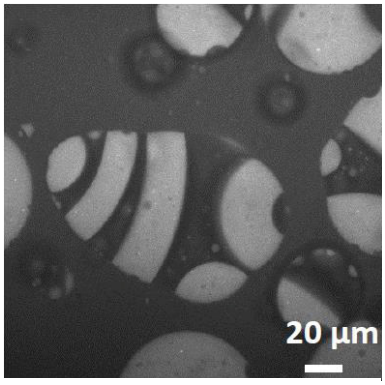

AMP + PUL in PEO

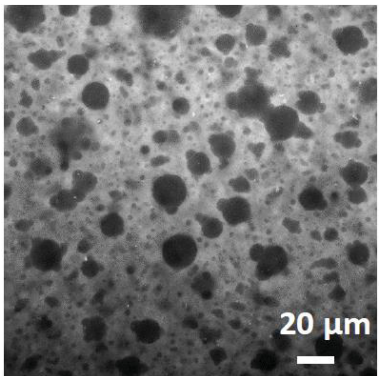

PEO + PUL in AMP

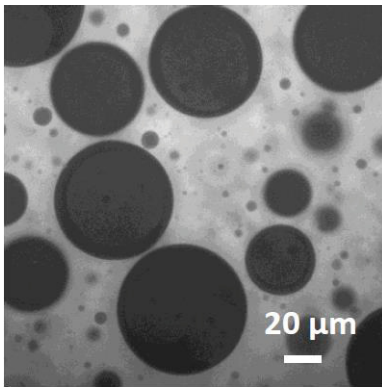

DX + PUL in GEL

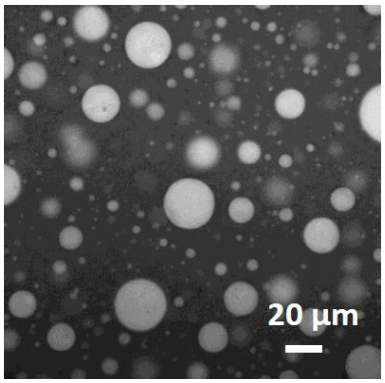

DX + GEL in PUL

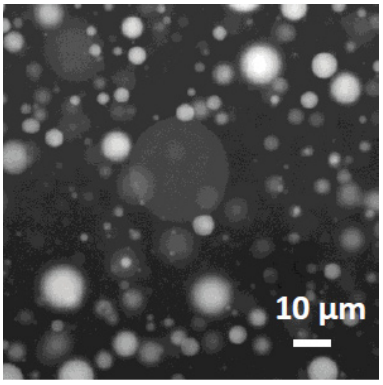

PUL + GEL in DX

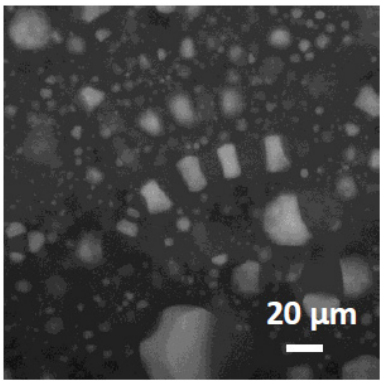

PEO + GEL in PUL

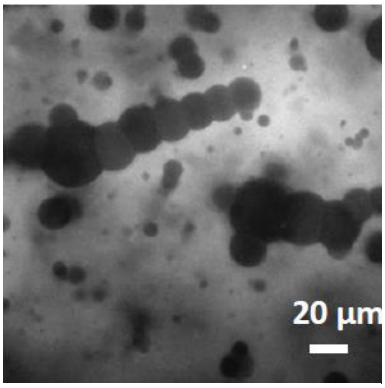

PEO + PUL in GEL

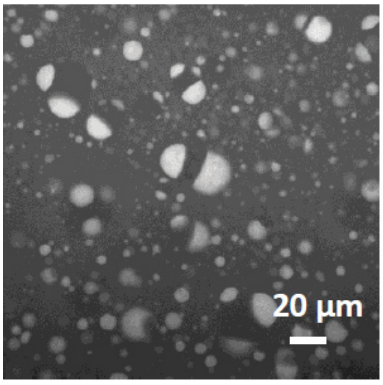

GEL + PUL in PEO

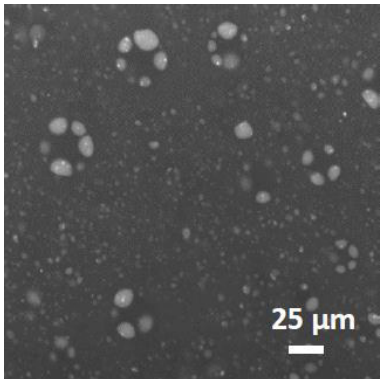

PEO + AMP in XG

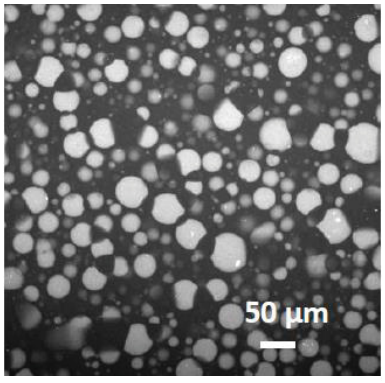

XG + AMP in PEO

Appendix V

Viscosity as a function of the shear rate for AMP and PUL at 9.03 and 5.75 wt%, which corresponds to the concentration of the separated phases in the tie-line investigated.